CHAPTER 3

# FUNDAMENTALS OF SOIL MECHANICS

## 3.1 INTRODUCTION

When designing a foundation, a geotechnical engineer is faced with three primary tasks: selection of the foundation type; computation of the load-carrying capacity; and computation of the movements of the foundation under the expected loading cases for both short-term and long-term time periods. Many factors that affect the selection of the type of foundation are discussed in Chapter 8, and the intervening chapters will present the methods recommended for design. All of these chapters assume knowledge of the fundamentals of soil mechanics. This chapter reviews the fundamentals of soil mechanics that must be mastered by any engineer who designs foundations.

## 3.2 DATA NEEDED FOR THE DESIGN OF FOUNDATIONS

In addition to having knowledge of soil mechanics and foundation engineering, the foundation engineer needs information on the soil profile supporting the foundation that is site specific in order to make the necessary computations of bearing capacity and settlement. The principal soil properties needed are the soil classification, the location of the water table, and the properties related to the shear strength and compressibility of the soil. In addition, the foundation engineer should anticipate events that might affect the performance of the foundation and consider them as warranted in the design process.

### 3.2.1 Soil and Rock Classification

The first information of interest to any designer of foundations is the soil and rock profile in which the foundations are to be constructed. This information often is the major factor that determines the type of foundation because foundations perform in different ways in different soil types and because the typical problems encountered during construction also vary in different types of soil and rock.

For purposes of foundation engineering, current design methods for determining the axial capacity of deep foundations generally classify soil and rock into five types (note that the following definitions are for foundation engineering, not for geology or other purposes). The five classifications for soil types are:

- Cohesive soils, including clays and cohesive silts.
- Cohesionless soils, including sand and gravels of moderate density.
- Cohesive intermediate geomaterials. This soil type consists of cohesive materials that are too strong to be classified as cohesive soils and too weak to be classified as rocks. It includes saprolites, partially weathered rocks, claystones, siltstones, sandstones, and other similar materials.
- Cohesionless intermediate geomaterials. This soil type consists of highly compacted granular materials, including very tight sand and gravel; naturally cemented sand and gravel; very tight mixtures of sand, gravel, and cobbles; and glacial till. Excavation in cohesionless intermediate geomaterials usually requires heavy equipment, specialized tools, and occasional blasting.
- Rock includes all cohesive materials that are too strong to be classified as cohesive materials. Rock types are further classified according to their mineralogy, fracture pattern, and uniformity.

The purpose of using these five classifications is to establish a system of soil descriptions covering the range of earth materials from the softest and most compressible to the hardest and most incompressible.

This same classification of soil types can be used for the design of foundations subjected to lateral loading. It is used to describe the soil types, but additional information on the position of the water table and the results of shear strength testing in the laboratory or field are also needed so that the proper load-transfer models can be selected by the foundation engineer.

### 3.2.2 Position of the Water Table

The soil and rock profile also includes information about the presence and elevation of the water table. The water table is the elevation in the soil profile

at which water will exist in an open excavation or borehole, given sufficient time for steady-state conditions to be reached. The presence of the water table is of interest to the foundation designer for two principal reasons. Firstly, the position of the water table is needed to establish the profile of effective stress in the soil versus depth. Secondly, the depth of the water table determines the depths below which special procedures must be used to control the groundwater during construction. This second point is important for the engineer to consider when selecting the foundation type and for the contractor to consider when selecting the method of construction.

### 3.2.3 Shear Strength and Density

The shear strength of soil or rocks is the most important soil and rock property used by the foundation designer. The foundation designer will often base the selection of the foundation type on the shear strength and use the values for shear strength in computations of axial and lateral capacity of the foundation.

The manner in which shear strength of soil or rock is measured and characterized often depends on the type of soil or rock. Typically, the shear strength of cohesive and cohesionless soils is expressed using the Mohr-Coulomb shearing parameters. Advanced constitutive models that are extensions and modification of the basic Mohr-Coulomb parameters are also used in major projects where additional soil investigations and laboratory tests are made.

Any implementation of the Mohr-Coulomb shearing parameters or any of the advanced models for shearing parameters will utilize the value of effective stress. Thus, the position of the water table must be known for their application.

The density, or unit weight, of the soil or rock is a soil property that is necessary for the computation of stresses due to gravity. The density of soil is computed using the weights of the solids in the soil and the weight of water in the soil. Any changes in soil density and volume that might arise from changes in the amount of water in the soil are computed if necessary.

### 3.2.4 Deformability Characteristics

Soils and rocks exhibit deformability in two modes that may occur independently or in combination. The two modes are deformation in shear at constant volume and deformation in volume change in either compression or dilation. Usually, the foundation engineer considers deformation by shearing at constant volume as a short-term behavior that occurs simultaneously with the application of loading to the foundation. Conversely, the foundation engineer may consider deformation by volume change to be a long-term behavior associated with the consolidation of the soil. Both of these modes of deformation will be discussed in the appropriate chapters of this book.

### 3.2.5 Prediction of Changes in Conditions and the Environment

The behavior of the soils supporting the foundation is influenced strongly by the stress and groundwater conditions present in the soil and rock profile. Thus, it is important to consider what conditions existed in the soil and rock profile when the soil investigation was conducted, what changes might occur in the future as a result of construction, and what changes might occur in the future due to additional nearby development or other causes. Often, this requires guesses about a possible worst-case scenario or a reasonable-case scenario for the future.

The principal factors of concern for changes in conditions that might occur during construction are any addition or reduction of overburden to the soil profile during the project and changes in the elevation of the water table. Any change in the overburden stress will directly affect the shearing properties of the soil and may affect its deformation properties as well. The position of the water table can be changed locally by the removal of some varieties of trees and by the amount (or lack) of irrigation or landscaping at a project.

The changes in soil conditions at a site are important factors to consider. History provides many examples of successful foundation designs rendered unsuccessful by changes in soil conditions. A few of the examples are well known, but many others are known only locally because the structure did not survive and was taken down or suffered minor or repairable damage. Foundation design engineers strive to provide trouble-free foundations because repair of defective foundations is very costly and inconvenient or the damage may be hidden and the structure sold to another party.

## 3.3 NATURE OF SOIL

In the geotechnical investigation, a sample of soil or rock can be retrieved from a geologic stratum to be examined, classified, and tested using a variety of laboratory tests. In addition, several types of field tests are performed when necessary. It is desirable to obtain the soil and rock samples with minimal disturbance by the sampling process so that the results of testing in the laboratory are representative of the true nature of the soils in the particular stratum.

### 3.3.1 Grain-Size Distribution

The methods used to design foundations do not consider the size of the soil particles (also called *grains*) as a primary factor. However, the terminology used to describe grain sizes is useful when describing the type of soil.

Soil consists of three main types—clays, silts, and sands or gravels—depending on the size of the grain. The commonly used separation sizes are 2 $\mu$m to separate clay and silt, and the #200 sieve (0.074 mm) to separate silt and sand. In general, grain sizes are measured in two ways. One way is

to pass the soils through a stack of wire sieves; the other way is to measure the rate of sedimentation in a hydrometer test and then infer the size of the soil grains. Measurements of grain size using sieves are used primarily for cohesionless soils such as sands and gravels. The hydrometer sedimentation test is used primarily for fine-grained soils such as silts and clays.

In a sieve analysis, the soil is passed through a stack of sieves progressing from large to small openings. The ranges in grain size are defined by the sizes of openings in testing sieves through which a soil particle can and cannot pass.

A hydrometer is a device for the measurement of fluid density. In the hydrometer sedimentation test, the density of a fluid is measured against time for a mixture of soil in water. As sedimentation occurs with the passage of time, the density of the fluid decreases because the suspended soils drop from suspension. The grain-size distribution is determined from Stokes' law[1] for the settling velocity of spherical bodies in a fluid of known density.

The types of soil with the smallest particles are *clays,* which may have particles smaller than 2 $\mu$m,[2] and the clay particles may have a variety of shapes. Usually, natural soils are composed of mixtures of several different minerals, though often one type of mineral is dominant. The behavior of clay is influenced significantly by the properties of the minerals present in the specimen, but the types of minerals are identified only in special circumstances using specialized tests.

In practice, various types of field and laboratory tests on soils from natural deposits are employed to define the soil properties used in design.

For comparison, here are the dimensions of various items:

- 0.4 to 0.66 $\mu$m—wavelength of visible light
- 1.55 $\mu$m—wavelength of light used in optical fiber
- 6 $\mu$m—anthrax spore
- 6 to 8 $\mu$m—diameter of a human red blood cell
- 7 $\mu$m—width of a strand of a spider web
- 1 to 10 $\mu$m—diameter of a typical bacterium
- $\sim$10 $\mu$m—the size of a water droplet in fog
- 0.05 $\mu$m—the maximum permissible deviation in curvature for an astronomical telescope mirror
- 17 to 181 $\mu$m—the range in diameter for human hair (flaxen to black)
- $>$2 $\mu$m—clay
- 2 $\mu$m to 74 $\mu$m—silt

[1] George G. Stokes (1819–1903), Fellow of the Royal Society and Lucasian Professor of Mathematics at Cambridge University.

[2] The identification of soil according to size has been proposed by a number of agencies; the sizes given here are from the American Society for Testing and Materials, D-2487-90 (1992).

### 3.3.2 Types of Soil and Rock

*Soil* and *rock* are descriptive terms that have different meanings, depending on their community of use. The following subsections present a few of the more common definitions.

***Soil*** To a farmer, soil is the earthen material that supports life.

To a geologist, soil is an ambiguous term.

To an engineer, soil is a granular material plus the intergranular gas and fluids. This includes clay, silt, sand, and gravel. It may also contain anything found in a landfill: household waste, cinders, ashes, bedsprings, tin cans, old papers, and so on.

***Rock*** To an engineer, rock is any individual material requiring blasting or another brute-force method to excavate. It is also classified as any material with a compressive strength greater than 725 psi (5.0 MPa). This definition is complicated by the presence of structures or defects that weaken the rock mass. The vagueness of the terms describing rock is due to the wide variety of materials encountered and the different information needs of those who use the descriptive terms.

Problems in geotechnical engineering involving the use of rock and many soils can seldom be solved by blind reliance on empirical data gathered from past projects or on sophisticated computerized analyses. Each situation is unique and requires

- Careful investigation
- Thorough analysis
- Engineering judgment based on varied experience
- Imagination to visualize the three-dimensional interplay of forces and reactions in complex systems
- Intuition to sense what cannot be deduced from scientific knowledge
- Initiative to devise new solutions for both old and new problems
- Courage to carry out the work to completion despite skeptics and the risk of the unknown

### 3.3.3 Mineralogy of Common Geologic Materials

*Clay minerals* are complex aluminum silicates formed from the weathering of feldspars, micas, and ferromagnesian minerals. The weathering reaction is

$$2KAlSi_3O_8 + 2CO_2 + 3H_2O \rightarrow 4SiO_2 + 2KHCO_3 + AlO_3 \cdot 2SiO_2 \cdot 2H_2O$$

The first product, silica, is a colloidal gel. The second product, potassium bicarbonate, is in solution. The third product, hydrous aluminum silicate, is

a simplified clay mineral. Their physical form is a wide, flat sheet many times wider and longer than thick.

The three most common clay minerals, in order from largest to smallest in size, are

- Kaolinite
- Illite
- Montmorillonite or smectite—very expansive, weak clays

Other somewhat less common clay minerals are

- Chlorite
- Attapulgite
- Vermiculite
- Sepiolite
- Halloysite, a special type of kaolin in which the structure is a tube rather than a flat sheet
- Many others

Clays are arbitrarily defined as particles less than 2 $\mu$m in the long dimension. Clay particles are very small. If clay is observed under an ordinary optical microscope, the individual particles would not be seen. If a 1-in. cube of clay is sliced one million times in each direction, the resulting pieces are approximately the size of clay particles. If the surface areas of a thimbleful of clay particles are added up, the total would be 6 million square inches, the same surface area from about five truckloads of gravel.

At the microscopic level, the clay fabric may have either a dispersed (parallel) or flocculated (edge-to-side) structure. The clay fabric may have a significant effect on engineering properties. Clay soils usually contain between 10% and 50% water by weight.

*Silt* is commonly found in flat floodplains or around lakes. Silt is usually deposited by flowing water or dust storms. Silt is composed of ground-up rock and is usually inorganic, that is, without plant material. A dry chunk of silt is easily broken by hand and is powdery.

***Clays*** The particles in clay soils may have two general types of structures, depending on the concentration of polyvalent ions present in the groundwater. If the particles are arranged in an edge-to-face arrangement, the clay has a *flocculated* structure, in which the individual plate-shaped particles are clustered, as shown in Figure 3.1. Particles of this type are known to have a positive charge at the edges of the particle and a negative charge on the face of the particle, as illustrated in Figure 3.1a. If the specimen of clay is remolded, thereby destroying its natural structure, the plates may become par-

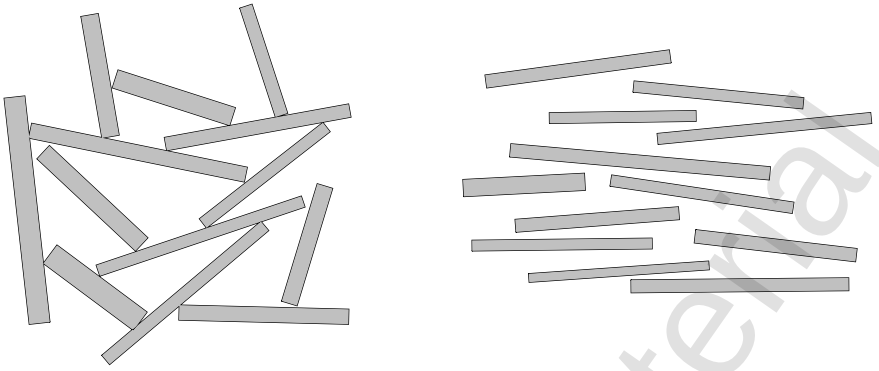

(a) Flocculated Structure (b) Dispersed Structure

**Figure 3.1** Clay structure.

allel to each other, as shown in Figure 3.1b. Frequently, remolding results in a loss of shear strength compared to the undisturbed specimen. If the particles are arranged in parallel, the clay has a *dispersed* structure.

In addition to its mineralogical composition, the strength of clay is strongly dependent on the amount of water in the specimen. The past stress history of a stratum of clay is also of great interest to the geotechnical engineer. If the stratum was deposited in water and attained considerable thickness over a long period of time, a specimen at a particular depth is *normally consolidated* if equilibrium exists, with no flow of water from the specimen due to the weight of the *overburden*. The specimen is *overconsolidated* if some of the overburden was removed by erosion or if the stratum was exposed to the atmosphere and later resubmerged. Consolidation may have occurred by *desiccation* if the stratum was uplifted and exposed to the air. Negative pore pressure develops due to *capillarity* and exposes the soil to positive compressive stress. The stratum will be overconsolidated; some formations of this sort have been resubmerged and exist in coastal areas in many parts of the world.

***Silts*** *Silt* is a single-grained soil, in contrast to clay, where the grains are bonded due to chemical attraction. Silt grains are too small to be seen with the naked eye, ranging in size from 2 $\mu$m to 0.074 mm. On drying, a lump of silt can be easily broken with the fingers. Deep deposits of silt present problems to the engineer in the design of foundations. Chapter 2 notes problems with foundations in loess, existing principally above the water table. Deposits of silt below the water table may be organic and compressible. Because of the small grains, water will flow slowly through the soil, and drainage due to a foundation load could be lengthy. Deep foundations penetrating the deposit of silt might be recommended in lieu of shallow foundations.

Silt can hold water and is usually soft when wet. A wet silt will flatten out when shaken, and the surface will appear wet. Silt is usually found in mixtures with sand or fine sand. A mixture of sand with a smaller amount of silt is often called a *dirty sand.*

Silt is usually a poor foundation material unless it has been compressed and hardened like siltstone. Many types of silt are compressible under low foundation loads, causing settlement. As a construction material, silt is difficult to work with. It is difficult to mix with water, is fluffy when dry, and pumps under compaction equipment if too wet. Silt particles can be flat, like clay particles, or blocky, like sand particles.

***Sands and Gravels*** *Sand* also is a single-grained soil that exists in a wide range of sizes, from fine (0.074 to 0.4 mm), to medium (0.4 to 2 mm), to coarse (2 to 4.76 mm). The grains of sand can have a variety of shapes, from subrounded to angular, and deposits of sand can have a variety of densities. Laboratory tests will reveal the effect of such variations on strength and stiffness. If the sand is loose, vibration from nearby motorized equipment can cause densification and settlement.

Sand is a granular material in which the individual particles can be seen by the naked eye. It is often classified by grain shape—for example, angular, subangular, or rounded. Sand is considered to be a favorable foundation material, but deposits are subject to erosion and scour, and need protection if they occur near a waterfront or a river.

Deposits of sand allow easy flow of water and do not hold water permanently. Water rising vertically through sand can cause quicksand. Any deposit of sand that holds water is a mixture containing finer material, either silt or clay. If a deposit of sand contains water and the deposit is surrounded by relatively impermeable deposits of clay or silt, a perched water table exists with a water table higher than exists outside the perched zone. Perched water sometimes results in construction difficulties if the perched water table is not recognized.

One problem with sand is that excavations often cave in. A slope in sand steeper than 1.5 horizontal to 1 vertical rarely occurs. The angle of the steepest natural slope is called the *angle of repose.*

The mineral composition of the grains of sand should receive careful attention. The predominant minerals in many sands are quartz and feldspar. These minerals are hard and do not crush under the range of stresses commonly encountered. However, other types of sand, such as calcareous sands, can be soft enough to crush. Calcareous sands are usually found between the Tropics of Cancer and Capricorn and present special problems for designers. One project for which the calcareous nature of a sand was of concern was an offshore oil production platform founded on piles driven into a deposit of lightly cemented calcareous soil off the coast of Western Australia. Open-ended steel pipe piles were driven to support the structure. Construction followed an intensive study to develop design parameters for axial loading. King and Lodge (1988) wrote that ''it was noted with some alarm that the 1.83 m

diameter piles not only drove to final penetration more easily than any of the pre-installation predictions but also that the piles free-fell under their own weight with little evidence of the expected frictional resistance." The calcareous sand was composed largely of the calcium carbonate skeletal remains of marine organisms (Apthorpe et al., 1988). During pile installation, the tips of the piles apparently crushed the grains of calcareous soil and destroyed the natural cementation. The cementation present in the sand was likely a natural consequence of the deposition and prevented development of the normal axial resistance along the length of the piles. The offshore project illustrates how the strength of sand grains and natural cementation can require special attention for designs of some foundations.

*Gravel,* as sand, also exists in many sizes from fine (4.76 to 19 mm) to coarse (19 to 75 mm).

Driving piles into deposits of sand and gravel may present difficulties. If the deposit is loose, vibration will cause a loss of volume and allow the pile to penetrate; otherwise, driving of a pile is impossible. The problem is especially severe for offshore platforms where a specific penetration is necessary to provide tensile resistance. Various techniques may be employed, but delays in construction may be very expensive.

*Cobbles* range in size from 75 to 1000 mm, and the size of *boulders* is above 1000 mm. A glacier can deposit a layer of cobbles and boulders with weaker soil above and below. Often, piles cannot be driven into such materials and drilling or coring for a drilled shaft foundation is the only practical alternative (see Chapters 5 and 11).

***Rock or Bedrock*** *Rock* or *bedrock* refers to deposits of hard, strong material that serves as an end-bearing foundation for piles or drilled shafts and, in some instances, as support for a shallow foundation. Characteristics of importance for rock are compressive strength and stress-strain characteristics of intact specimens. In some instances, the secondary structure of rock, referring to openings, joints, and cracks, is of primary importance. The secondary structure can be defined quantitatively by the *rock quality designation* (RQD), a number obtained by dividing the sum of the length of core fragments longer than 100 mm that were recovered by the overall depth that was cored (Chapter 4).

### 3.3.4 Water Content and Void Ratio

A soil sample is known to be saturated when it is weighed in the laboratory and its total weight is $W$. The sample is then placed in an oven at a temperature of 110°C and dried completely. The dry weight is measured as $W_d$. The loss in weight of the soil sample is the weight of water ($W_w = W - W_d$) that was in the original sample of soil. From this test, it is possible to compute the *water content* using

$$w = \frac{W_w}{W_d} \cdot 100\% \tag{3.1}$$

where water content is expressed as a percentage. Water contents are determined for almost every sample tested in a soils laboratory because soil properties are found to be sensitive to changes in water content.

The *void ratio* is defined as the volume of voids in a soil divided by the volume of the solid materials in a soil. The void ratio is convenient to use when calculating unit weights and strains due to consolidation. The symbol used for void ratio is $e$ and is computed as

$$e = \frac{V_v}{V_s} \tag{3.2}$$

where $V_v$ is the volume of voids ($V_v = V - V_s$) and $V_s$ is the volume of soils.

### 3.3.5 Saturation of Soil

A soil is composed of mineral solids and voids. The voids may be filled water, other liquids, or gas (air). If all voids are filled with liquids, the soil is *saturated.*

If a stratum of clay exists above the *water table,* the position in the earth where water will collect in an open excavation, then the soil will be subject to wetting and drying, presenting a difficult problem to the engineer. If the clay is *expansive,* shrinking on drying and swelling on wetting, the problem is even greater. The design of shallow foundations in expansive clay is discussed in Chapter 9. A lump of clay on drying will be difficult to break with the fingers.

The *degree of saturation* $S_r$ is defined as

$$S_r = \frac{V_w}{V_v} \cdot 100\% \tag{3.3}$$

### 3.3.6 Weight–Volume Relationships

Several relationships between weight and volume are frequently used by foundation engineers to compute the stresses in the soil due to gravity and the associated variation due to the location of the water table. This section presents the definitions of several weight–volume parameters, their interrelationships, and the equations in common use.

The *unit weight* of the soil is the weight of soil per unit volume. The most commonly used unit in the U.S. customary system is pounds per cubic foot

(pcf), and the most commonly used unit in the SI system is kilonewtons per cubic meter (kN/m$^3$). Other combinations of weight and volume units may be used in computations where consistent units are needed.

The unit weight, $\gamma$, can be computed using one of the following relationships:

$$\gamma = \frac{W}{V} = \frac{W_w + W_d}{V_s + V_v} = \frac{V_w\gamma_w + V_s\gamma_s}{V_s + eV_s} = \frac{V_w\gamma_w + V_s\gamma_s}{V_s(1 + e)} \tag{3.4}$$

where

$W$ = weight of the sample,
$W_w$ = weight of water in the sample,
$W_d$ = weight of soil after drying,
$V$ = total volume of the soil sample,
$V_s$ = volume of solids in the soil sample,
$V_v$ = volume of voids in the soil sample,
$\gamma_w$ = unit weight of fresh water (9.81 kN/m$^3$ or 62.4 pcf), and
$\gamma_s$ = unit weight of the solid mineral grains without any internal voids.

This expression for unit weight makes no assumption about the amount of water present in a sample of soil or rock, and is based simply on the weight and volume of the soil or rock.

The *saturated unit weight* is the unit weight of a fully saturated soil. In this case, no air or gas is present in the voids in the soil. An expression for the saturated unit, $\gamma_{sat}$, is obtained by dividing the volume terms in the numerator and denominator of Eq. 3.4 by $V_s$ and substituting the term for void ratio where appropriate:

$$\gamma_{sat} = \frac{e\gamma_w + \gamma_s}{1 + e} \tag{3.5}$$

The *specific gravity* of the mineral grains, $G_s$, is the ratio of the unit weight of solids divided by the unit weight of water:

$$G_s = \frac{\gamma_s}{\gamma_w} \tag{3.6}$$

The values for specific gravity are usually in such a narrow range (i.e., $2.60 \leq G_s \leq 2.85$) that an approximate value of 2.7 is usually assumed rather than performing the necessary laboratory tests for measurement.

It is convenient to rearrange the above relationship in the form

$$\gamma_s = G_s\,\gamma_w \tag{3.7}$$

and substitute Eq. 3.7 into Eq. 3.5 to obtain an expression for $\gamma_{sat}$ in terms of specific gravity, void ratio, and unit weight of water:

$$\boxed{\gamma_{sat} = \frac{G_s + e}{1 + e}\,\gamma_w} \tag{3.8}$$

Equation 3.8 is in the form usually used in practice.

A useful expression for void ratio can be derived from the expressions for degree of saturation, water content, and specific gravity. The derivation is

$$e = \frac{V_v}{V_s}$$

$$e = \frac{V_w}{V_s} \cdot \frac{1}{S_r}$$

$$e = \frac{W_w}{\gamma_w} \cdot \frac{\gamma_s}{W_s} \cdot \frac{1}{S_r}$$

$$e = \frac{W_w}{W_s} \cdot \frac{1}{S_r} \cdot \frac{\gamma_s}{\gamma_w}$$

$$e = w \cdot \frac{1}{G_s} \cdot S_r$$

$$\boxed{e = \frac{wG_s}{S_r}} \tag{3.9}$$

The *dry unit weight,* $\gamma_d$, is the unit weight for the special case where $S_r = 0$. The dry unit weight is computed using

$$\boxed{\gamma_d = \frac{\gamma}{1 + w}} \tag{3.10}$$

where the water content $w$ is expressed as a decimal fraction. The above expression for dry unit weight is valid for any value of $w$. Another useful relationship for dry unit weight in terms of specific gravity, void ratio, and unit weight of water is

$$\gamma_d = \frac{G_s}{1 + e}\,\gamma_w \tag{3.11}$$

Note that if $S_r$ is not 100% then Eq. 3.8 must be changed to

$$\gamma = \frac{G_s + eS_r}{1 + e}\,\gamma_w \tag{3.12}$$

This is a general expression that is valid for all values of degree of saturation. When $S_r$ is zero, this equation yields the dry unit weight, and when $S_r$ is 100%, this equation yields the saturated unit weight.

The *effective unit weight* $\gamma'$ (also called the *submerged unit weight*) is defined as

$$\gamma' = \gamma_{\text{sat}} - \gamma_w \tag{3.13}$$

where $\gamma_{\text{sat}}$ is the saturated unit weight.

Some instructors ask their students to memorize the six boxed equations above. All other weight–volume relationships can be derived from these equations.

### 3.3.7 Atterberg Limits and the Unified Soils Classification System

***Atterberg Limits*** The Swedish soil scientist A. Atterberg (1911) developed a method for describing quantitatively the effect of varying water content on the consistency of fine-grained soils like clays and silts. Atterberg described the stages of soil consistency and arbitrary limits shown in Table 3.1.

For many saturated clays, the relationship of volume and water content is similar to that shown in Figure 3.2. The volume of the soil sample will decrease if the water content is lowered from a high value to a lower value. At some value of water content, the solids become so tightly packed that the volume cannot decrease further and the volume remains constant. The shrinkage limit is defined as the water content below which the soil cannot shrink.

**TABLE 3.1 Atterberg Limits**

| Stage | Description | Limit |
|---|---|---|
| Liquid | Slurry, pea soup to soft butter, viscous liquid | Liquid limit, *LL* |
| Plastic | Soft butter to stiff putty, deforms without cracking | Plastic limit, *PL* |
| Semisolid | Cheese, deforms permanently, but cracks | Shrinkage limit, *SL* |
| Solid | Hard candy, breaks on deformation | |

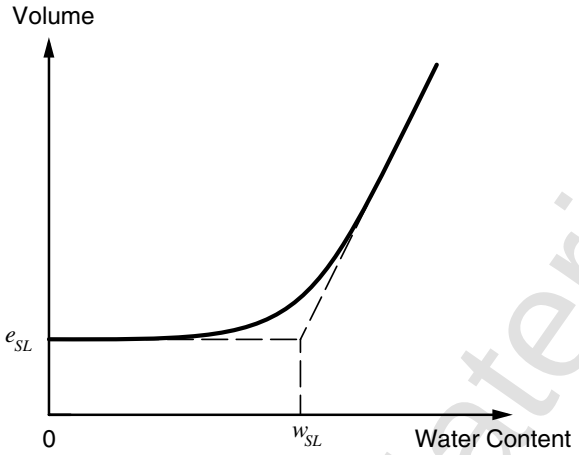


**Figure 3.2** Volume versus water content of saturated clay.

Professor Arthur Casagrande of Harvard University developed a testing device to standardize the test for liquid limit. The original device was not mounted on rubber feet, as are modern standardized devices, and the results varied, depending on whether the machine was operated directly over a table leg or not. Casagrande found that consistency was improved if the machine was placed on a copy of a telephone directory. The rubber feet were added to simulate the directory, and the consistency of readings from the liquid limit machines was improved to a satisfactory point. The modern version of the liquid limit testing machine, as standardized by the American Society for Testing and Materials (ASTM), is shown in Figure 3.3.

Atterberg limits are used to classify and describe soils in several useful ways. One widely used and extremely useful soil descriptor is the plasticity index ($PI$), which is defined as

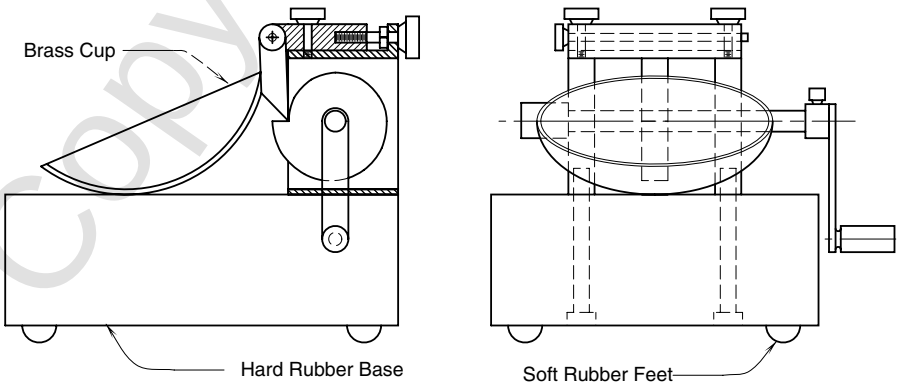


**Figure 3.3** Liquid limit machine.

$$PI = LL - PL \tag{3.14}$$

In addition, the liquidity index (*LI*), is used to indicate the level of the water content relative to the liquid limit (*LL*) and plastic limit (*PL*).

$$LI = \frac{w - PL}{LL - PL} = \frac{w - PL}{PI} \tag{3.15}$$

If the water content of a soil is higher than the *LL*, then *LI* is greater than 1. If a soil is drier than the *PL*, then *LI* is negative. A negative value of the *LI* usually indicates a problem condition where the potential for expansion on wetting is severe.

***Unified Soil Classification System*** This system was developed by the U.S. Army Corps of Engineers and the Bureau of Reclamation in 1952 and was subsequently adopted and standardized by the ASTM. Today, the Unified Soils Classification System is widely used in the English-speaking world.

The system uses a two-letter classification. The first letter is used to classify the grain size.

If more than 50% by weight is larger than the #200 sieve (0.074-mm openings), then a coarse-grained classification is used. If more than 50% is larger than a #4 sieve, then the letter *G* is used; otherwise, the letter *S* is used.

For sands and gravels, the second letter describes the gradation:

*W* = well graded
*P* = poorly graded
*M* = contains silt
*C* = contains clay

Examples of common classifications are *GP*, *GW*, *GC*, *GM*, *SP*, *SW*, *SM*, and *SC*.

If more than 50% by weight passes the #200 sieve, then the soil is fine-grained and the first letter is *M* for silt, *C* for clay, or *O* for organic soil.

The second letter for fine-grained soils describes their plasticity. The letter *L* is used for low plasticity ($LL < 50$), and the letter *H* for high plasticity ($LL > 50$). The Atterberg limits are tested on the fraction of soil passing the #40 sieve, not the full fraction of soil.

Examples of common classifications of fine-grained soils are *ML*, *CL*, *MH*, *CH*, *OL*, and *OH*.

If a soil is highly organic, with noticeable organic fibers, it is given a peat designation, *PT*.

***Relative Density*** The degree of compaction of granular soils is measured as relative density (Table 3.2), usually expressed as a percentage:

**TABLE 3.2 Classification of Cohesionless Soils by Relative Density**

| Designation | $D_r$, % | SPT $N$-Value |
|---|---|---|
| Very loose | 0–15 | 0–4 |
| Loose | 15–30 | 4–10 |
| Medium dense, firm | 35–70 | 10–30 |
| Dense | 70–85 | 30–50 |
| Very dense | 85–100 | 50+ |

$$D_r = \frac{e_{\max} - e}{e_{\max} - e_{\min}} \tag{3.16}$$

***Grain Size Distribution*** The uniformity coefficient $C_u$ and the coefficient of curvature (called the *coefficient of gradation*) $C_c$ were developed to help engineers evaluate and classify the gradations of granular materials. These coefficients are used to determine when different materials can be used effectively as filter materials in earth dams. Their definitions are

$$C_u = \frac{D_{60}}{D_{10}} \tag{3.17}$$

$$C_c = \frac{(D_{30})^2}{D_{60}D_{10}} \tag{3.18}$$

Well-graded soils have uniformity coefficients greater than 4 for gravels and 6 for sands, and a coefficient of curvature between 1 and 3. If the soil is not well graded, it is poorly graded.

A soil with a *gap-graded* distribution has ranges of soil particle sizes missing. In many applications, such as filter zones in earth dams used for drainage, gap-graded soils are avoided because they can be susceptible to subsurface erosion or piping.

Examples of gradation curves for well-graded and gap-graded soils are shown in Figure 3.4.

The results of the classification of the soils encountered in a borehole are of great importance to the foundation engineer because of the difference in the behavior of various soils on the imposition of loadings. The classification will guide the specification of laboratory tests, and possibly in situ tests, for acquisition of the data necessary for design.

## 3.4 CONCEPT OF EFFECTIVE STRESS

This chapter begins with the analysis of one-dimensional settlements, as shown in Figure 3.5. In this analysis, the stresses in the soils are uniform on

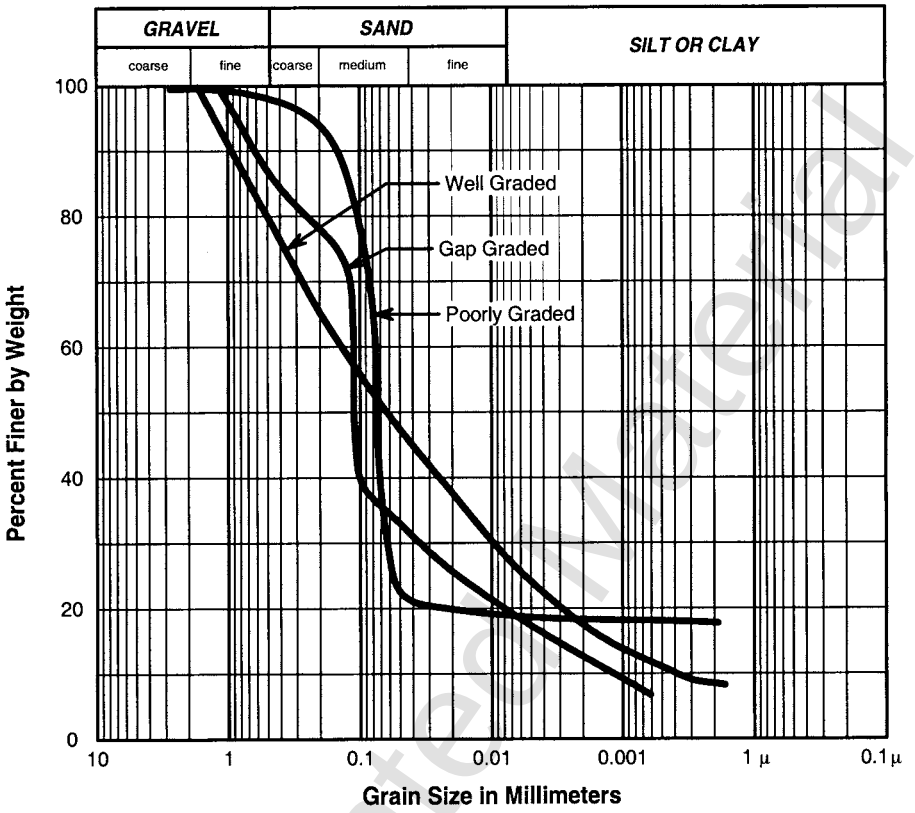


**Figure 3.4** Example of gradation curves for well-graded and gap-graded soils.

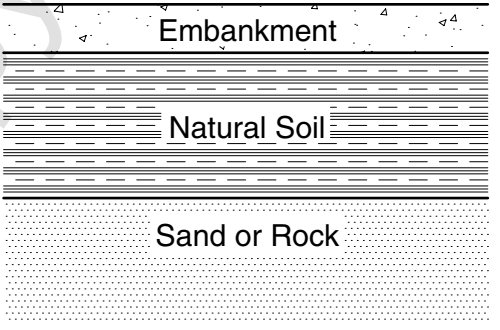


**Figure 3.5** A one-dimensional settlement problem.

horizontal planes. Under these conditions, the soil cannot deform laterally. In fact, in a one-dimensional consolidation problem, neither soil deformation nor water flow can occur in the horizontal direction, only in the vertical direction.

To simplify this problem, the following conditions are assumed:

- The subsoil is homogeneous, that is, it has the same properties everywhere in a layer.
- The subsoil is *saturated,* that is, all voids between the soil particles are filled with water, and no gas bubbles are present in the spaces between the soil particles.

### 3.4.1 Laboratory Tests for Consolidation of Soils

To determine what would happen in the field, foundation engineers obtain soil samples from the field and test the samples in the laboratory. Because the problem involves only one-dimensional deformation and one-dimensional water flow, a one-dimensional consolidation test in the laboratory is appropriate.

The laboratory apparatus used for this purpose is called a *one-dimensional consolidation cell* or *oedometer*. An example of a consolidation cell is shown in Figure 3.6. The soil sample that is tested is a circular disk with a diameter about two to four times its thickness. Diameters of testing specimens are typically between 2 and 4.5 in. (5 to 10 cm). Such small diameters are used to reduce the cost of drilling, sampling, and laboratory testing. However, samples with larger diameters are preferred so that the properties measured in the laboratory are more representative of the soil deposit in the field.

The soil is encased in a rigid metal ring to prevent deformations due to lateral squeezing of the soil and to force the flow of water in the vertical direction. The soil sample is covered with a loading cap, and vertical loads are applied to represent applied vertical stresses in the field. The original vertical load applied on the sample in the field depends on the depth from which the sample was retrieved and the weight of the soil and fill. Since the weight and thickness of the fill may not be known during the testing phase (and for other reasons as well), a wide range of stresses will be applied in the laboratory to obtain a stress-strain curve that can be used for a range of loads in the field.

The soil is assumed to be in equilibrium under an applied load in the laboratory and that an additional load is suddenly applied. Also, this additional load is assumed to represent the weight of the load in the field. Settlement of the top cap in the consolidation cell is measured using either a dial gauge or a linear transducer, with an accuracy of 0.0001 in. (0.0025 mm). When a compressive load is applied to saturated clay, the test operator discovers that the settlement is initially very small; in fact, the initial magnitude of the settlement approximately equals the settlement that would develop if


**Figure 3.6** Computer-controlled, one-dimensional consolidation testing equipment (photograph courtesy of Trautwein Soil Testing Equipment Company).

the soil sample was replaced with a rigid metal disc. This instantaneous settlement is caused by compression of the porous stones and other mechanical parts of the testing apparatus because the soil is nearly incompressible during the short interval after the application of stress.

If the applied load is sustained, the test specimen compresses and the amount of compression change with time in a manner similar to that shown in Figure 3.7. After a period of time, the compression essentially ceases and the soil is again in equilibrium. Similar settlement curves versus time are obtained for each level of loading, and the load is increased again. After the maximum consolidation stress of interest has been reached, the level of consolidation stress is lowered in stages, and the rebound of the specimen under each stage is measured, until the test specimen is unloaded completely.

For samples of usual dimensions in the laboratory, the time needed to achieve equilibrium varies from a few minutes for sands to several days for some clays. The delay is caused by the time needed for water to squeeze out of the specimen of soil. The more pervious soils come to equilibrium quickly, whereas relatively impervious clays are comparatively slow to equilibrate.

As in pipe-flow hydraulics, where the rate of water flow in a pipe depends on the diameter of the pipe, the rate at which water can be squeezed from a saturated specimen of soil depends on the sizes of the openings between the soil particles. Also, as in hydraulics, the rate of flow for a given pore (pipe) size decreases as the total flow distance increases, so the time required for equilibrium for a thick layer of soil in the field is much longer than for a

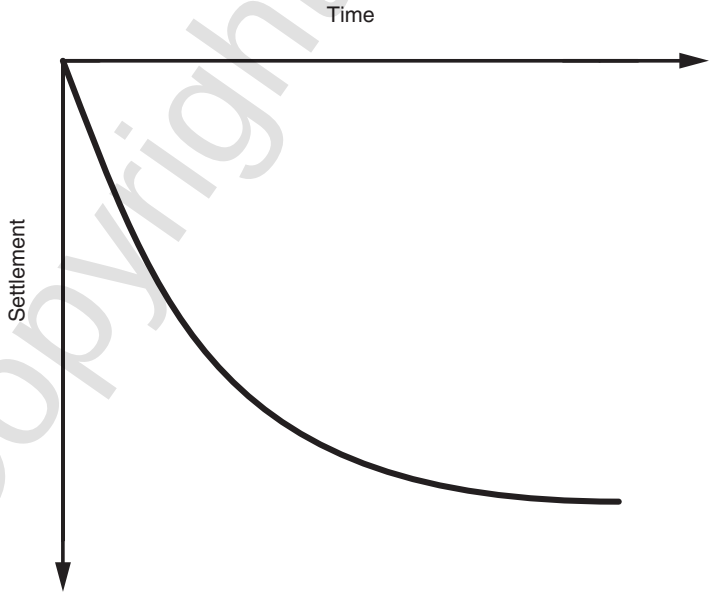


**Figure 3.7** Curve of settlement versus time for a saturated soil.

small specimen of the same soil in the laboratory. Delayed settlement can be a serious problem for the design engineer if the settlement is still continuing after a structure has been completed on a stratum of consolidating soil.

### 3.4.2 Spring and Piston Model of Consolidation

The mechanics of consolidation will be presented using a simple model of a spring and piston, shown in Figure 3.8, where a saturated soil is represented by a piston that moves up and down in a cylinder. The spring supporting the piston inside the cylinder represents the compression of the soil particles under an external applied load. To represent a saturated soil, the cylinder is also saturated; that is, it is filled with water without gas bubbles. Water can escape from the cylinder only through the valve, as shown. Included in this model is a pressure gage that can measure the pressure of the water at any time in the cylinder.

If an external load $P$ is applied to the piston with the valve closed, one would discover (just as in a laboratory consolidation test on a saturated soil sample) that immediately after loading, no settlement results. Instead, the force applied to the piston $P$ must be balanced by the force supporting the piston. The force supporting the piston is the combination of the force in the spring $P_s$ and the force in the water $P_w$. If the total area inside the cylinder is $A$, the area of the wire in the spring is $A_s$, and the area of the piston covered by water is $A_w$, then equilibrium of forces requires that

$$A = A_s + A_w \tag{3.19}$$

The spring constant $k$ is defined as

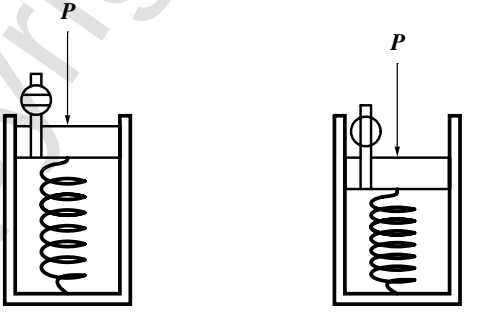


**Figure 3.8** Piston-spring model of consolidating soil.

$$k = \frac{P_s}{S} \tag{3.20}$$

where $S$ is the compression of the spring (equal to the settlement of the piston).

The bulk modulus of the water is defined as the change in volume of the water that results from the water pressure $u$ resulting from the application of the external force $P$

$$C_w = \frac{\Delta V_w / V_w}{u} \tag{3.21}$$

where $\Delta V_w$ is the change in volume of water, $V_w$ is the original volume of water, and $u$ is the pressure developed in the water. If the area of the cylinder is uniform, then the change in the volume of water is equal to the settlement times the area of the water:

$$\Delta V_w = S\, A_w \tag{3.22}$$

An expression for the water pressure due to the change in volume of the water under the applied external force is obtained by inserting Eq. 3.22 into Eq. 3.21 and rearranging:

$$u = \frac{S\, A_w}{C_w V_w} \tag{3.23}$$

The force carried by the water is equal to the water pressure acting over the area of the piston:

$$P_w = uA_w \tag{3.24}$$

Equilibrium of forces requires the externally applied force to equal the sum of forces carried in the spring and water. This is expressed as

$$P = P_s + P_w \tag{3.25a}$$

$$P = P_s + uA_w \tag{3.25b}$$

Stresses are found by dividing the forces by the area of the cylinder. Thus, total stress $\sigma$ applied to the cylinder is

$$\sigma = \frac{P}{A} \tag{3.26}$$

The stress carried by the spring is

$$\sigma' = \frac{P_s}{A} \tag{3.27}$$

The porewater pressure is

$$u_w = \frac{P_w}{A} = \frac{uA_w}{A} \approx u \tag{3.28}$$

because $A_s$ is much less than $A_w$. In this model, $A_s$ is much less than $A_w$ by choice, but studies of real soils have found that this is an excellent approximation. Thus, after dividing both sides by the area of the piston, Eq. 3.25b reduces to

$$\sigma = \sigma' + u \tag{3.29}$$

Usually this equation is written as

$$\boxed{\sigma' = \sigma - u} \tag{3.30}$$

Equation 3.30 is called *Terzaghi's effective stress equation,* and $\sigma'$ is called the *effective stress*. Other notations for effective stress in common use include the symbols $\overline{\sigma}$ and $\overline{p}$. This text will use $\sigma'$ to denote effective stress in most situations and use the prime ($'$) notation applied to other symbols to indicate conditions under which stresses are effective stresses.

When the spring and piston model is applied to real soils, the spring represents the compressible framework of soil particles and $P_s$ is the force carried by this framework. The effective stress is then the ratio of the force carried in the particle framework to the total area of the soil.

The settlement of the piston $S$ appears in both Eq. 3.20 and Eq. 3.23. Solving both equations for $S$, one obtains

$$S = \frac{P_s}{k} = \frac{C_w V_w u}{A_w} \tag{3.31}$$

Again, dividing both sides by the piston area $A$ and multiplying both sides by the spring constant $k$, one obtains an expression for effective stress:

$$\sigma' = \frac{P_s}{A} = \frac{k\, C_w\, V_w\, u}{A\, A_w} \tag{3.32}$$

If one inserts values of $k$ obtained by testing real soils and the appropriate values for the bulk modulus of water $C_w$, the volume of water $V_w$, the piston area $A$, and the water area $A_w$, one finds that

$$\sigma' \approx \left(\frac{1}{1000}\right)u \tag{3.33}$$

In other words, when the piston is loaded and the valve is closed, approximately 99.9% of the load goes into the water and none into the spring.

Laboratory measurement of the consolidation properties of saturated soils has found that if a pressure $\sigma$ is applied to the soil and drainage is not allowed, then the resulting porewater pressure $u$ equals the applied pressure $\sigma$. Insertion of typical values into Eq. 3.31 demonstrates why the settlement is essentially zero when a saturated soil is loaded without drainage.

If the valve is opened, the water in the cylinder escapes, settlement occurs, and the spring compresses under the external force. Settlement causes the spring (representing the soil particle framework) to compress and to take on an increasing fraction of the externally applied load. Eventually, enough water will escape so that the spring carries the full externally applied load and the porewater pressure is zero. The spring and piston model of consolidating soil is then in equilibrium. One can now calculate the spring constant of the model by dividing $P$ by the measured settlement $S$.

With the known value of the spring constant, piston settlements can be computed for any given applied load. In addition, measurement of the time rate of settlement in the laboratory and computing the soil property that characterizes the time rate of settlement (represented by the opening in the valve in the model) would allow the computation of the time rate of settlement in the field using an appropriate theory.

### 3.4.3 Determination of Initial Total Stresses

A homogeneous soil deposit with a horizontal ground surface is shown in Figure 3.9, and the vertical stress at depth $z$ is desired. A column of soil of area $A$ as shown may be considered. Static equilibrium in a vertical direction requires that the weight of the column $W$ plus any shear forces on the sides to equal the force on the bottom. Since the soil deposit is homogeneous and extends indefinitely in the horizontal direction, the stresses on all vertical planes are the same. Thus, if any shear exists on vertical planes, the shear on the outside of one face must be identical to the shear on the outside of the opposite face, so the shear forces are in equilibrium. Actually, if the soil

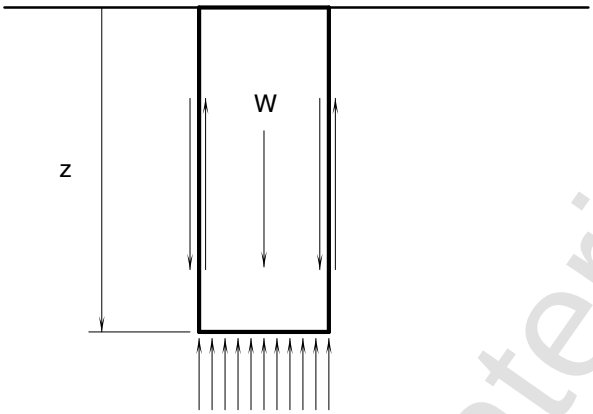


**Figure 3.9** Equilibrium of vertical forces for a vertical prism of soil.

deposit is formed by uniform deposition over the surface, no shearing stresses on vertical planes will occur. Thus, for force equilibrium in the vertical direction

$$W = \sigma A \tag{3.34}$$

where $\sigma$ is the total stress on the base. The stress is then

$$\sigma = \frac{W}{A} \tag{3.35}$$

As a matter of convenience, substitute

$$W = \gamma v = \gamma A z \tag{3.36}$$

where $v$ is the volume of the column of soils and $\gamma$ is the *total unit weight* (total weight per unit volume). After inserting Eq. 3.36 into Eq. 3.35, the following equation results

$$\sigma = \gamma z \tag{3.37}$$

Equation 3.37 is valid only if $\gamma$ is constant with depth. For real (nonhomogeneous) soils, the soil may be considered homogeneous on a microscopic scale, that is, in differential elements, so

$$d\sigma = \gamma \, dz \tag{3.38}$$

and

$$\sigma = \int_0^z \gamma dz \tag{3.39}$$

Equation 3.39 is valid for any soils with a horizontal ground surface.

The total unit weight $\gamma$ can be found for soil samples by measuring the weight and volume of the soil samples, but $\gamma$ is computed more conveniently from other parameters that are measured for other purposes.

### 3.4.4 Calculation of Total and Effective Stresses

The total vertical stress at a depth of 10 ft in a saturated clay that has an average water content of 22% will be calculated below as an example calculation of total and effective stresses:

$$e = \frac{wG_s}{S_r} = \frac{(0.22)(2.70)}{1.00} = 0.594$$

$$\gamma = \frac{G_s + eS_r}{1 + e}\gamma_w = \frac{2.70 + (0.594)\ (1.00)}{1 + 0.594}\ 62.4 \text{ pcf} = 129.0 \text{ pcf}$$

$$\sigma = \gamma z = (129.0 \text{ pcf})\ (10 \text{ ft}) = 1290 \text{ psf}$$

Previously, it was noted that compression of clay is controlled by changes in effective stress, not total stress. The effective stress is calculated using Eq. 3.30. When the water table is static (i.e., no flow of groundwater in the vertical direction), the water pressure increases linearly with depth, just as if no soil were present. The depth in the soil where the top of the equivalent free water surface exists is the *water table*. At the water table, the water pressure is zero gage pressure (1 atmosphere absolute). Below the water table the water pressure $u$ is equal to

$$u = z_w\ \gamma_w \tag{3.40}$$

where $z_w$ is the vertical distance below the water table. In a soil in the field, the water table is at a given depth and there is no sudden change in water content or any other property at the water table. In highly pervious soils, like sands and gravels, the water table is located by drilling an open hole in the soil and letting water flow into it from the soil until equilibrium occurs. The water level in the hole is then easily measured. For clays, the time needed to obtain equilibrium may be many days. To speed up equalization in clays, a *piezometer* may be used. A simple piezometer is formed in the field by drilling a hole, packing the bottom of the hole with sand, embedding a small-diameter tube with its bottom end in the sand and its top end at the surface, and then backfilling the rest of the hole with clay. The water level will equilibrate in

the small-diameter tube much faster than in a large borehole because less water is needed to fill the tube. Once the water table is located, the pore water pressures below the water table are calculated using Eq. 3.40.

In many practical problems the water table moves up and down with the seasons, so the level of the water table at the time of the soil exploration may indicate only one point within its range of fluctuation.

To simplify the initial calculation of water pressure, the water table in the sample problem was assumed to be at the surface. Then at a depth of 10 ft the water pressure would be

$$u = (10 \text{ ft})(62.4 \text{ pcf}) = 624 \text{ psf}$$

The effective stress is then computed using Eq. 3.30:

$$\sigma' = (1290 \text{ psf} - 624 \text{ psf} = 666 \text{ psf}$$

More generally, Eqs. 3.30 and 3.40 may be combined as follows:

$$\begin{aligned} \sigma' &= \sigma - u \\ &= \gamma z - \gamma_w z_w \\ &= \gamma(z - z_w) + \gamma z_w - \gamma_w z_w \end{aligned}$$

The term $\gamma (z - z_w)$ is clearly equal to the total stress and to the effective stress at the position of the water table (where $u_w = 0$). The terms $(\gamma z_w - \gamma_w z_w)$ may be combined to yield $\gamma' z_w$, where $\gamma'$ is the effective unit weight, as found according to Archimedes' principle.

The effective stress below the water table is then the sum of the effective stresses above and below the water table:

$$\sigma' = \gamma(z - z_w) + \gamma' z_w \tag{3.41}$$

The expression for submerged unit weight is obtained by subtracting $\gamma_w$ from $\gamma_{sat}$ using Eq. 3.8 (or Eq. 3.12 if $S_r$ is less than 100%) to derive an expression that does not use $w$ or $S_r$:

$$\begin{aligned} \gamma' &= \gamma - \gamma_w \\ &= \frac{G_s + e}{1 + e}\gamma_w - \gamma_w \\ &= \frac{G_s + e}{1 + e}\gamma_w - \frac{1 + e}{1 + e}\gamma_w \end{aligned}$$

$$\gamma' = \frac{G_s - 1}{1 + e}\,\gamma_w \tag{3.42}$$

The effective stresses in the soil prior to construction of the embankment are now known. Next, to determine the strains caused by the placement of the embankment fill, the effective stresses must be determined after settlement has been completed. This calculation is the same as the one used previously, except that now there is another layer of soil on the surface, so the depths are measured from the new surface.

The only question relates to the change in density that occurs during settlement. Since no solids are lost, the submerged weight of all the original soil above any depth remains the same (the loss of porewater during consolidation causes a decrease in void ratio and thus an increase in submerged unit weight, but this effect is exactly counterbalanced by the decreased thickness of the submerged soil above the depth in question).

However, if the elevation of the water table remains constant as the embankment settles, then some of the soil (including embankment soil) that was above the water table when the embankment was first placed will submerge below the water table after settlement has been completed. The amount of soil that is converted from total unit weight to submerged unit weight (Eq. 3.41) depends on the settlement that occurs but calculation of settlement is needed. Thus, a trial solution is sometimes needed where the effect of submergence is ignored in the first calculation of settlement. The first computed settlement is used to estimate a submergence correction, and another (better) settlement is calculated. The process may be repeated until a settlement of satisfactory precision has been calculated from a plot of computed settlement versus assumed settlement (usually only two trials).

### 3.4.5 The Role of Effective Stress in Soil Mechanics

The influence of effective stress is found throughout soil mechanics. Effective stress is an important factor in the consolidation of soil under the application of external loadings, as illustrated in the preceding discussion of the spring piston model, and it is an important factor in the development of the shearing strength of soils and rocks.

## 3.5 ANALYSIS OF CONSOLIDATION AND SETTLEMENT

### 3.5.1 Time Rates of Settlement

When a soil is subjected to an increase in effective stress, the porewater is squeezed out in a manner similar to water being squeezed from a sponge,

and the basic concepts presented above govern the time rate of settlement of the surface of a clay layer. The following sections describe the theory of one-dimensional consolidation for the case of instantaneous loading. In cases where the loading of the surface of the consolidating layer of soil varies over time, more advanced analytical techniques have been developed. These advanced theories of consolidation also may include more nonlinear soil properties than the simple theory that follows.

The theory to be presented herein is *Terzaghi's theory of one-dimensional consolidation,* first presented in 1923. It remains the most commonly used theory for computing the time rate of settlement, even though it contains simplifying assumptions that are not satisfied in reality. The theory yields results of satisfactory accuracy when applied to predicting time rates of settlement of embankments on soft, saturated, homogeneous clays.

***Primary Consolidation*** Water is forced out of a porous body like a sponge by the water pressure developed inside the sponge. However, in the case of thick layers of soil, the water pressure increases with depth, as in a quiet body of water, even though no flow is present in the water. Instead, water is forced to flow by applying an external pressure to the soil, but it is not the total water pressure that governs. In a soil where no water flow is occurring, the porewater pressure is termed the *static porewater pressure* $u_s$ and is equal to the product of the unit weight of water and the depth below the water table:

$$u_s = \gamma_w z_w \tag{3.43}$$

As discussed previously, the application of the load from an embankment increases the total porewater pressure and flow begins. The flow of water is caused by the part of the total pore pressure that is in excess of the static value. For convenience, the excess porewater pressure $u'$ is defined as

$$u' = u - u_s \tag{3.44}$$

where $u$ is the total porewater pressure and $u_s$ is the static water pressure. The rate of outflow of water is also controlled by how far the water must flow to exit and by the size of the openings in the soil. The average velocity of water flow in the soil $v$ varies directly with $u'$ and inversely with flow distance $L$:

$$v \propto \left(\frac{du'}{dL}\right) \tag{3.45}$$

The total rate of water flow (flow volume per unit of time), $q$, is

$$q = v\,A \tag{3.46}$$

where $v$ is the average flow velocity and $A$ is the cross-sectional area.

Actual experiments with soils show that the flow rate varies with the permeability of the soil and that the total rate of water flow is

$$q = \frac{k\,du'}{\gamma_w\,ds}\,A \tag{3.47}$$

where $k$ is a constant of proportionality termed the *coefficient of permeability* or the *coefficient of hydraulic conductivity,* and $s$ is now used to indicate distance in the direction of flow. Equation 3.47 is one form of *Darcy's law,* which states that water flows in response to an energy gradient in the soil. Those familiar with fluid mechanics may also know this, as flow will occur in response to a differential in hydraulic head.

Darcy's law is applied to the one-dimensional consolidation problem first in a qualitative sense. A clay layer is underlain by a freely draining sand (Figure 3.10). The water table is at the surface. An embankment is put into place in a very short period of time, and the total pore pressure increases by an amount $\gamma H$, where $\gamma$ is the unit weight of the embankment material and $H$ is the thickness of the embankment. Excess pore pressures are developed in the sand layers too, but the sand consolidates so fast that the excess porewater pressure in the sand is dissipated by the time the construction of the embankment is complete, even though very little consolidation has occurred in the clay at this stage. Thus, the sand is *freely draining* compared with the clay, and $u'$ is set equal to zero in the sand. The initial excess porewater pressure in the clay, $u'_0$, equals $\gamma H$ and is independent of depth. Because only the excess porewater pressure causes water flow, the value of $u'$ is plotted

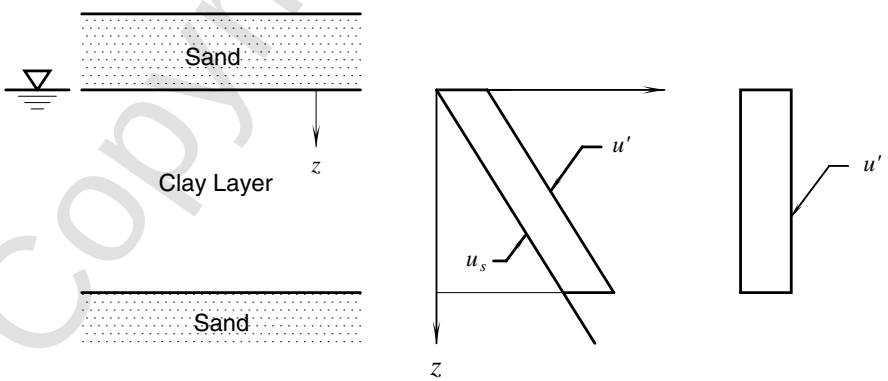


**Figure 3.10** Pore pressures in a clay layer loaded instantaneously.

versus depth, as in Figure 3.10, and the total porewater pressure, $u$, and the static porewater pressure, $u_s$ are ignored.

At the upper and lower boundaries of the clay layer (Figure 3.10) where drainage occurs, the original excess porewater pressure transitions between $u_0'$ in the clay layer and zero at the boundary with the sand over a very small distance. Thus, at time zero, just after the embankment has been put in place, the excess porewater pressure gradient, $du'/dz$, at both drainage boundaries approaches infinity, and thus the rate of outflow of porewater is also nearly infinite (Eq. 3.47). The total outflow volume of water $Q$ is

$$Q = \int_0^t q \, dt \tag{3.48}$$

where $t$ is time. Clearly, an infinite value of $q$ can exist only instantaneously; then the flow rate drops and finally becomes zero when equilibrium is again established. The flow rate of water from the soil $q$ decreases because the excess porewater pressure dissipates, thereby decreasing the gradient, $du'/dz$, and the resulting flow (Eq. 3.47). The shapes of the curves of $q$ and $Q$ versus time must be as shown in Figure 3.11. The settlement of the surface is found by dividing $Q$ by $A$, the horizontal area of the soil deposit from which the flow $Q$ emanates. The excess porewater pressures must vary as indicated in Figure 3.12, where time increases in the order $t_0$, $t_1$, $t_2$, . . . , $t_\infty$.

Development of a mathematical theory to yield numerical values for these curves requires mathematics for solution of differential equations using Fourier series. Solutions may be developed for a variety of different initial excess porewater pressure distributions. The following solution is for the case of a uniform distribution of excess porewater pressure versus depth with drainage from the upper and lower boundaries.

The settlement at any time $S$ is equal to the average degree of consolidation $U$ times the ultimate settlement $S_u$:

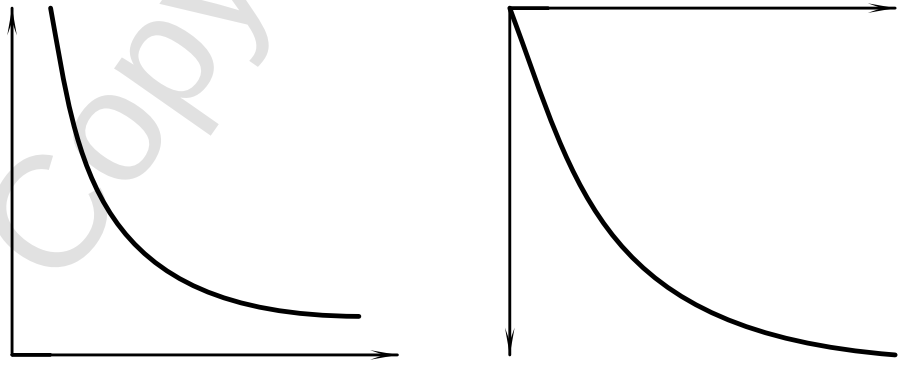

**Figure 3.11** Shapes of $q$-$t$ and $Q$-$t$ diagrams derived intuitively.

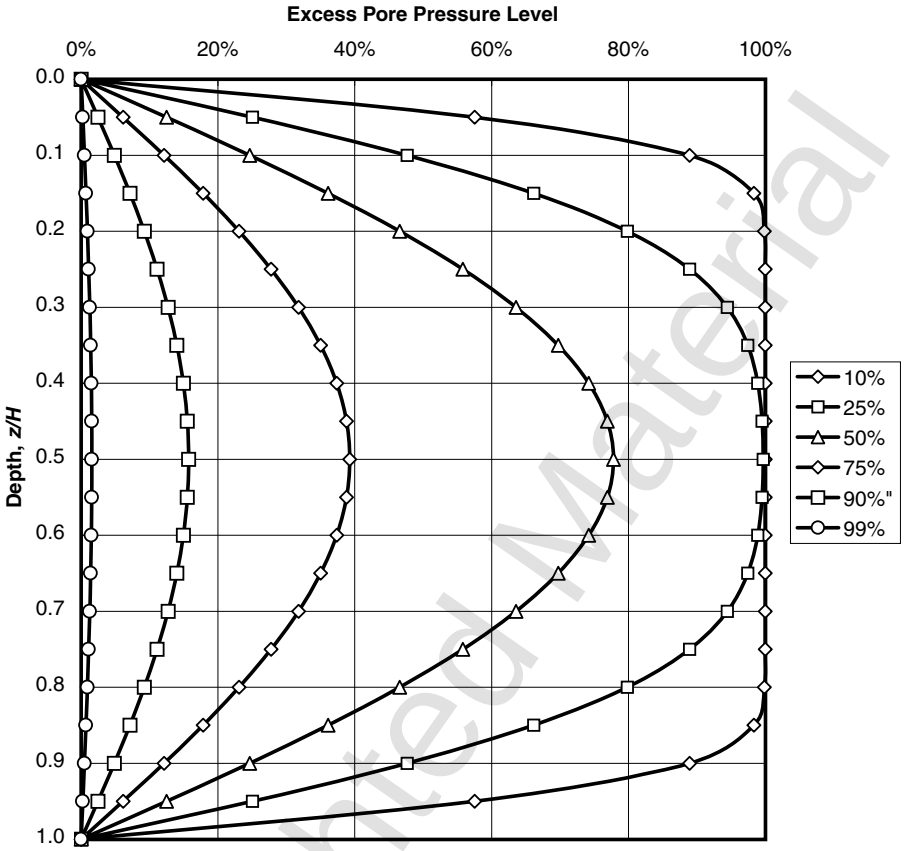


**Figure 3.12** Curves of excess pore pressure versus depth for instantaneous loading.

$$S = US_u \tag{3.49}$$

In this equation, $S_u$ is the settlement calculated previously and $U$ has a value between zero and unity. $U$ is given by

$$U = 1 - \sum_{m=0,1,2\ldots}^{\infty} \frac{2}{M^2} e^{-M^2 T} \tag{3.50}$$

where $M$ is

$$M = \frac{\pi}{2}(2m + 1) \tag{3.51}$$

$e$ is the base of Napierian (natural) logarithms, and $T$ is a dimensionless *time factor* given by

$$T = \frac{c_v\, t}{(H/n)^2} \tag{3.52}$$

where

$c_v$ = *coefficient of consolidation,*
$t$ = time (equal to zero at the instant the embankment is put in place),
$H$ = total thickness of the clay layer, and
$n$ = number of drainage boundaries.

The coefficient of consolidation has units of length$^2$/time and is given by the equation

$$c_v = \frac{k(1 + e)}{a_v \gamma_w} \tag{3.53}$$

where

$k$ = coefficient of permeability,
$e$ = void ratio,
$a_v$ = *coefficient of compressibility,* and
$\gamma_w$ = unit weight of water.

The coefficient of compressibility is the slope of the curve of void ratio versus effective stress and is given by

$$a_v = -\frac{de}{d\sigma'} \tag{3.54}$$

The profile of excess porewater pressure versus depth is calculated using

$$u' = \sum_{m=0,1,2\ldots}^{\infty} \frac{2u_0'}{M} \sin\left(\frac{Mz}{H/n}\right) e^{-M^2 T} \tag{3.55}$$

The following is a sample calculation of the settlement–time curve. The soil profile in this problem is a homogeneous layer of saturated clay with a thickness of 10 ft. The compressible stratum is overlain and underlain by freely draining sand layers, and the water table is at the upper surface of the clay and is assumed to remain at the interface of the compressible layer and the upper sand layer. The upper sand layer has a submerged unit weight of 70 pcf. The clay is normally consolidated and has an average water content of 40%, a compression index of 0.35, and a coefficient of consolidation of

0.05 ft²/day. A 15-ft-thick wide embankment is rapidly put in place. Its unit weight is 125 pcf. In this problem, the clay layer will not be subdivided into sublayers.

The solution begins with the computation of the initial void ratio, effective unit weight, and initial effective stress at the middle of the clay layer:

$$e_0 = \frac{w_0 G_s}{S_r} = \frac{(0.40)(2.70)}{1.00} = 1.08$$

$$\gamma' = \frac{G_s - 1}{1 + e_0}\,\gamma_w = \frac{2.70 - 1}{1 + 1.08}\,62.4 \text{ pcf} = 51 \text{ pcf}$$

$$\sigma_0' = \sum_{j=1}^{\text{layers}} H_j \gamma_j' = (10 \text{ ft})(70 \text{ pcf}) + (5 \text{ ft})(51 \text{ pcf}) = 955 \text{ psf}$$

The change in vertical effective stress due to the construction of the wide embankment is

$$\Delta\sigma' = (15 \text{ ft})(125 \text{ pcf}) = 1875 \text{ psf}$$

The final vertical settlement is

$$S_u = C_c \frac{H}{1 + e_0} \log\left|\frac{\sigma_f'}{\sigma_0'}\right|$$

$$= \frac{(0.35)(120 \text{ in.})}{1 + 1.08} \log\left|\frac{955 \text{ psf} + 1{,}875 \text{ psf}}{955}\right| = 9.5 \text{ in.}$$

Values of $T$ as a function of $U$ are given in Table 3.3.

**TABLE 3.3 Dimensionless Time Factors**

| $U$, % | $T$ | $U$, % | $T$ |
|---|---|---|---|
| 0% | 0 | 55% | 0.238909 |
| 1% | 7.85E-05 | 60% | 0.286399 |
| 5% | 0.001964 | 65% | 0.340414 |
| 10% | 0.007854 | 70% | 0.402851 |
| 15% | 0.017672 | 75% | 0.47673 |
| 20% | 0.031416 | 80% | 0.567164 |
| 25% | 0.049087 | 85% | 0.683757 |
| 30% | 0.070686 | 90% | 0.848085 |
| 35% | 0.096212 | 95% | 1.129007 |
| 40% | 0.125673 | 99% | 1.781288 |
| 45% | 0.159121 | 99.9% | 2.714491 |
| 50% | 0.196731 | 99.99% | 3.647693 |

In lieu of using the values of $T$ versus $U$ in Table 3.3, values for $T$ can be approximated for selected values of $U$ by the following equations:

For values of $U$ less than 60%:

$$T = \frac{\pi}{4} U^2 \tag{3.56}$$

For values of $U$ between 60% and 99%:

$$T = 1.781 - 0.933 \log(100 - U\%) \tag{3.57}$$

The easiest way to calculate a complete $S$-$t$ curve is to use Table 3.3 to calculate values of $S$ and $t$ for given values of $U$. For example, if $U = 50\%$, then $T = 0.197$ and the settlement is (from Eq. 3.49)

$$S = US_u = (0.50)(9.5 \text{ in.}) = 4.75 \text{ in.}$$

and the corresponding time is (from Eq. 3.52)

$$t = \frac{TH^2}{c_v n} = \frac{(0.197)(10 \text{ ft})^2}{(0.05 \text{ ft}^2/\text{day})(2)^2} = 98.5 \text{ days}$$

Other points on the $S$-$t$ curve corresponding to different values of $U$ are calculated in a similar way.

Calculations like those shown above are often made in engineering practice, but many settlement problems are more complex than the case with instantaneous loading that was considered. Some of the more common factors that require the application of computer-based solutions for problems of time rate of settlement occur when fill is placed and/or removed versus time, consolidation properties exhibit significant nonlinear properties, artesian conditions are affected by construction activities, and consolidation in the field is accelerated using wick drains.

***Secondary Compression*** After sufficient time has elapsed, the curve of settlement versus logarithm of time flattens. Theoretically, the curve should become asymptotically flat, but observations both in laboratory tests and in the field find a curve with a definite downward slope. This range of settlement with time is called *secondary compression* and includes all settlements beyond primary consolidation.

The slope of the secondary compression line is expressed as the coefficient of secondary compression $C_\alpha$:

$$C_\alpha = \frac{\Delta e}{\log\left|\frac{t_2}{t_1}\right|} \tag{3.58}$$

The coefficient of secondary compression is used in settlement computations in a manner similar to that of the compression, reloading, and rebound indices, except that time is used in place of effective stress when computing the settlement:

$$S = C_\alpha \frac{H}{1 + e} \log\left|\frac{t_2}{t_1}\right| \tag{3.59}$$

The terms *consolidation* and *compression* are used carefully in this book. *Compression* includes any type of settlement due to a decrease in the volume of soil. *Consolidation* refers to settlement due to the squeezing of water from the soil and the associated dissipation of excess pore water pressures.

### 3.5.2 One-Dimensional Consolidation Testing

It is not realistic to measure the consolidation characteristics of many soils in the field because the time necessary to do so is usually many years. Instead, soil samples are obtained as part of the field investigation program and representative samples are tested in the laboratory. The time required to measure soil properties in the laboratory is usually a few days or a few weeks. The testing procedures used in the laboratory are usually varied, depending on the type of soil, the nature of the problem in the field, the type of equipment available in the laboratory, and other factors.

In the following discussion, a soil sample to be tested is assumed to be a saturated clay contained in a thin-walled steel tube used for sampling. The sampling tube is typically 3 in. (75 mm) in diameter. The consolidation cell to be used is shown in Figure 3.6. The usual steps in preparing a consolidation test are as follows:

- The cell is dismantled and cleaned prior to testing.
- The inside surface of the confining ring is given a thin coating of silicone grease to minimize friction between the ring and soil and to seal the interface from seepage in order to force the fluid flow to be in the vertical direction.
- The ring is weighed and has a weight of 77.81 g.
- The soil is trimmed into the ring so that it fills the ring as exactly as possible (volume = 60.3 cc), and the ring and soil are weighed together (176.50 g).

- The soil is covered, at the top and bottom, with a single layer of filter paper to keep the soil from migrating into the porous stones, and the consolidation cell is assembled.
- The cell is placed in a loading frame, and a small seating pressure (60 psf or 3 kPa) is applied. A dial indicator or displacement transducer, capable of reading to 0.0001 in., is mounted to record the settlement of the loading cap.
- The tank around the ring is filled with water and the test begins.

The usual steps taken during the consolidation test are as follows:

- If the soil swells under the seating load, then the seating load is increased until equilibrium is established.
- The applied pressure is then increased in increments, usually with the stress doubled each time.
- Settlement observations are recorded at various times after the application of each load level. A set of settlement readings obtained for a pressure of 16,000 psf (766 kPa) are shown in Figure 3.13 as an example. When testing most clay soils are tested, each load is left in place for 24 hours.
- After the maximum pressure has been applied, the load acting on the soil specimen is unloaded in four decrements (e.g., down from 64,000 psf to 16,000 psf to 4000 psf).
- When a suitably low pressure is reached, the rest of the remaining load is removed in a single step and the apparatus is dismantled rapidly to minimize any additional moisture taken in by the soil.

The steps taken after the consolidation test is completed are as follows:

- The confining ring is dried on the outside, and then the ring and the soil are weighed together (156.66 g in Figure 3.14).
- The ring and soil are then oven-dried for 24 hours, and their combined dry weight is measured (137.44 g in Figure 3.14). In the example shown in Figure 3.14, the dry weight of the solids ($137.44 - 77.81 = 59.63$ g) is calculated, as are the volume of solids ($59.63/2.80 = 21.3$ cc), volume of voids at the beginning ($60.3 - 21.3 = 39.0$ cc), and original void ratio ($39.0/21.3 = 1.83$).

Because the settlements under each pressure were measured, the change in void ratio from the beginning of the test to that pressure is calculated using Eq. 3.60:

## ONE-DIMENSIONAL CONSOLIDATION TEST

### Loading Test Data

| | |
|---|---|
| Load Number | 10 |
| Total Load on Sample | 16,000 psf |
| Date Load Applied | 3/26/04 |
| Load Applied by | JDC |

| Time | | Dial Readings | |
|---|---|---|---|
| Clock | Elapsed, min. | Original | Adjusted |
| 10:08 a.m. | 0 | 2199 | 2301 |
| | 0.1 | 2163 | 2337 |
| | 0.25 | 2150 | 2350 |
| | 0.5 | 2135 | 2365 |
| 10:09 | 1 | 2113 | 2387 |
| 10:10 | 2 | 2083 | 2417 |
| 10:12 | 4 | 2050 | 2450 |
| 10:16 | 8 | 2019 | 2481 |
| 10:23 | 15 | 2000 | 2500 |
| 10:38 | 30 | 1985 | 2515 |
| 11:08 | 60 | 1972 | 2528 |
| 12:08 p.m. | 120 | 1961 | 2539 |
| 2:08 | 240 | 1951 | 2549 |
| 6:08 | 480 | 1943 | 2557 |
| Tues. 7:57 a.m. | 1309 | 1933 | 2567 |

**Figure 3.13** Example data form for recording the time-settlement data during a one-dimensional consolidation test.

$$S_j = \left(\frac{\Delta e}{1 + e_0} H\right)_j \tag{3.60}$$

$$\Delta e = \frac{1 + e}{H} S \tag{3.61}$$

The total settlement $S_t$ measured in the laboratory is the sum of the settlement of the soil $S$ and the settlement in the apparatus $S_a$, so $S$ is calculated as

## ONE DIMENSIONAL CONSOLIDATION TEST

Project _____ Boring No. _____ Sample No. _____

| Sample Description: *Norwegian Quick Clay from Aserum* | | | |
|---|---|---|---|
| Consolidation Frame No. | 1 | Consolidation Ring No. | 1 |
| Diameter of Ring | 2.500 in. | Operator: | class |
| Height of Ring | 0.748 in. | Specific Gravity | 2.80 |

| | Before | After | Trimmings |
|---|---|---|---|
| Weight, wet soil plus tare, gm | 176.50 | 156.66 | 73.42 |
| Weight, dry soil plus tare, gm | 137.44 | 137.44 | 67.97 |
| Weight, moisture, gm | 39.06 | 19.22 | 5.45 |
| Weight, tare, gm | 77.81 | 77.81 | 59.62 |
| Weight, dry soil, gm | 59.63 | 59.63 | 8.35 |
| Water Content, *w*, % | 65.8% | 32.3% | 65.2% |

| **Initial Conditions** | |
|---|---|
| Volume of Ring | 60.3 cc |
| Volume of Solids = $W_d/\gamma_s$ | 21.3 cc |
| Volume of Voids | 39.0 cc |
| Void Ratio | 1.830 |
| Volume of Water | 39.0 cc |
| Initial $S_r$ | 100% |

**Figure 3.14** Sample data form for a one-dimensional consolidation test.

$$S = S_t - S_a \tag{3.62}$$

The apparatus settlement is caused by compression of the porous stones above and below the specimen (Figure 3.6) and the filter paper, and to a trivial extent by compression of other parts of the apparatus. Numerical values for $S_a$ are usually obtained by literally performing a full consolidation test with no soil in the ring. Either a metal block is used in place of the sample or the

loading cap bears directly on the lower drainage stone. The void ratios are then calculated for each consolidation pressure by subtracting $\Delta e$ from $e_0$. A laboratory report form and data for the test specified in Figure 3.14, are shown in Figure 3.15.

In principle, calculation of the coefficient of consolidation should be simple. For any given pressure in the laboratory, say the $n$th pressure, the settlement at the end of the $n - 1$ load is $S_{u,n-1} = S_{0,n}$, where $u$ again means ultimate and 0 now means time zero under the $n$th load. The settlement at the end of consolidation under the $n$th load is $S_{u,n}$. At $U = 50\%$,

**ONE-DIMENSIONAL CONSOLIDATION TEST - Calculation Sheet**
Height of Solids = 0.2655 inch
Initial Void Ratio = 1.830

| Load No. (1) | Beam Load, lb (2) | Stress psf (3) | Decrease in Height of Voids (0.0001's) (4) | Machine Deflection (0.0001's) (5) | Net Dec. in Height of Voids $\Sigma\Delta H$ (6) | $\frac{\Sigma\Delta H}{H_s}$ (7) | Void Ratio, $e$ (8) |
|---|---|---|---|---|---|---|---|
| 1 | | 31 | 8 | 0 | 8 | 0.003 | 1.827 |
| 2 | | 62 | 12 | 3 | 9 | 0.003 | 1.827 |
| 3 | | 125 | 42 | 5 | 37 | 0.014 | 1.816 |
| 4 | | 250 | 88 | 11 | 77 | 0.029 | 1.801 |
| 5 | | 500 | 286 | 18 | 268 | 0.101 | 1.729 |
| 6 | | 1,000 | 1079 | 29 | 1050 | 0.396 | 1.424 |
| 7 | | 2,000 | 1571 | 44 | 1527 | 0.576 | 1.254 |
| 8 | | 4,000 | 1911 | 60 | 1851 | 0.697 | 1.133 |
| 9 | | 8,000 | 2214 | 78 | 2136 | 0.805 | 1.025 |
| 10 | | 16,000 | 2497 | 100 | 2397 | 0.903 | 0.927 |
| 11 | | 32,000 | 2764 | 127 | 2637 | 0.994 | 0.836 |
| 12 | | 64,000 | 3033 | 159 | 2874 | 1.082 | 0.748 |
| 12a | | 64,000 | 3098 | 159 | 2939 | 1.107 | 7.723 |
| 13 | | 16,000 | 3011 | 118 | 2893 | 1.089 | 0.741 |
| 14 | | 4,000 | 2950 | 92 | 2858 | 1.077 | 0.753 |
| 15 | | 1,000 | 2849 | 69 | 2780 | 1.047 | 0.783 |
| 16 | | 250 | 2723 | 56 | 2667 | 1.004 | 0.826 |
| 17 | | 31 | 2548 | 48 | 2500 | 0.942 | 0.888 |

**Figure 3.15** Sample data form for calculation of the void ratios at various consolidation pressures.

$$S = S_{0,n} + 0.50\ (S_{u,n} - S_{0,n}) = 1/2(S_{0,n} + S_{u,n}).$$

The engineer reads the time needed to achieve 50% consolidation, $t_{50,n}$, from the laboratory *S-t* curve. At $U = 50\%$, $T = 0.197$ (from Table 3.3), so from Eq. 3.52

$$t = \frac{T(H/n)^2}{c_v} = \frac{0.197(H/n)^2}{c_v} \tag{3.63}$$

Once $c_v$ has been calculated, the entire theoretical *S-t* curve can be calculated by successively entering the appropriate values of $T$ into Eq. 3.63 and plotting the theoretical curve on the same graph for comparison with the measured curve. If the theory is correct, then the theoretical and experimental curves should be identical. The theoretical curve is calculated as follows using the symbols defined previously. A table is prepared with values of $U$ and $T$ (from Table 3.3) in the first two columns. For each value of $U$, the settlement $S$ is calculated at time $t$ using

$$S = S_0 + U\ (S_u - S_0)$$

The corresponding values of $t$ are computed using Eq. 3.63, where $H$ is the average thickness of the specimen for consolidation under the given load. The *S-t* data from Figure 3.13 are plotted in 3.16. For this load, $S_0 = 2301$ dial divisions (each equal to 0.0001 in.) and $S_u = 2567$ divisions. Thus, $S_{50} = 2434$ and $H = 0.750$ in. $-$ $(2434 - 100) \times 10^{-4} = 0.517$ in. (100 is the machine deflection from Figure 3.13). From Figure 3.16, $t_{50} = 2.9$ minutes. Thus,

$$c_v = \frac{T(H/n)^2}{t} = \frac{(0.197)(0.517\text{ in.}/2)^2}{2.9\text{ min}} = 0.00455\text{ in.}^2/\text{min}$$

The dimensionless time factors needed to calculate a theoretical curve of settlement versus time are presented in Table 3.3

The theoretical curve is shown in Figure 3.16, and it clearly does not fit the measured curve very well. The only points in common are at time zero, where both curves must start at $S = 2301$ divisions; at $U = 50\%$ where the calculations force the two curves to be identical; and at times indefinitely.

To examine the discrepancies in more detail, the data are redrawn to a semi-log scale in Figure 3.17. The most obvious discrepancy is found over long time period where the experimental curve continues sloping downward, whereas the theoretical curve should level off. Apparently, the Terzaghi model is not quite correct over long times. Apparently, the soil compresses, perhaps like a spring, but then it *creeps,* causing continued settlement at large times.

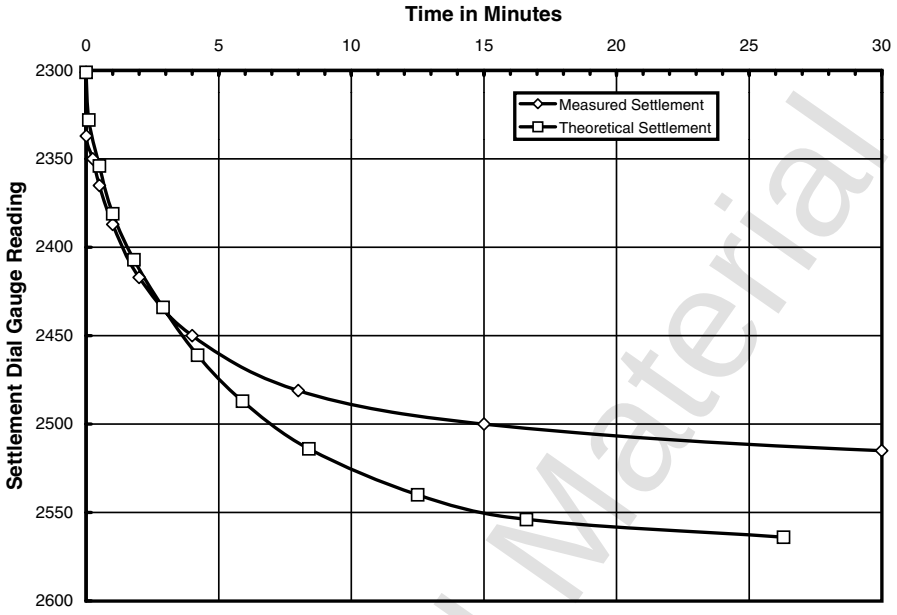


**Figure 3.16** Measured and theoretical time settlement curves.

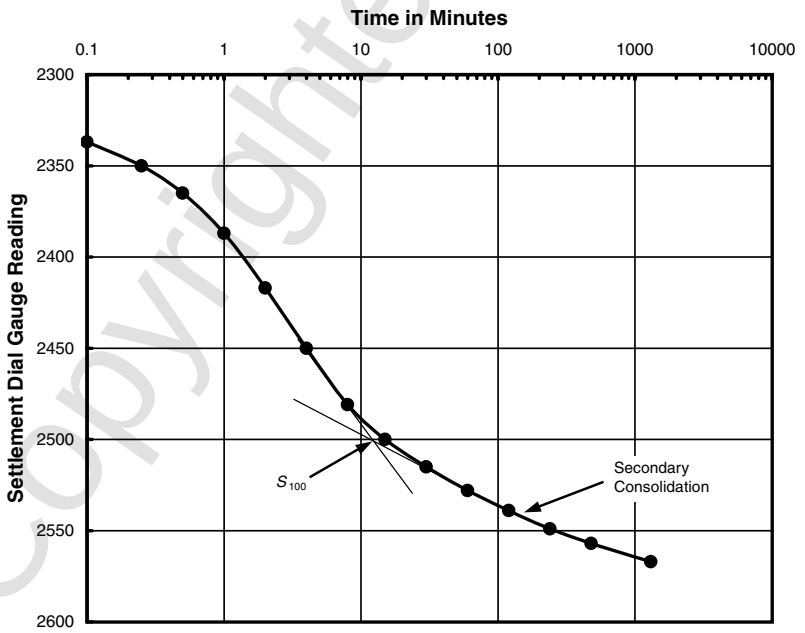


**Figure 3.17** Measured and theoretical settlement versus logarithm of time.

Terzaghi recognized this effect. He termed the part of consolidation (settlement) that obeys his theory the *primary consolidation* and the postprimary creep the *secondary compression*. Casagrande and Fadum (1940) proposed a simple construction to separate primary from secondary settlements. They drew one tangent line to the secondary settlement curve and another to the primary curve at the point of inflection (where the direction of curvature reverses), as shown in Figure 3.17, and found that the intersection of these two lines defines approximately the settlement at the end of primary consolidation. This settlement is defined as $S_{100,n}$ where 100 indicated the point of 100% primary consolidation.

Further studies indicate some non-Terzaghian consolidation right at the beginning too. The correction is based on Eq. 3.56. The correction, also originated by Casagrande and Fadum (1940), is performed as follows: a point is selected on the laboratory $S$-log($t$) curve near $U = 50\%$ (Figure 3.17), and the time is recorded as $4t$ and the settlement as $S_{4t}$. The point on the curve is now located corresponding to $t$ and settlement $S_t$ (this symbol was used previously for a different variable) is recorded. The corrected settlement at the beginning of primary settlement $S_0$ is

$$S_0 = S_t - (S_{4t} - S_t) \tag{3.64}$$

where the subscript $n$'s have been left off for simplicity.

The coefficient of consolidation $c_v$ is now calculated as before, but the $U = 50\%$ point is defined at $S_{50}$ where

$$S_{50} = \frac{S_0 + S_{100}}{2} \tag{3.65}$$

and $S_0$ and $S_{100}$ are the settlements at the beginning and end of primary consolidation. The theoretical curve calculated using this value of $c_v$ is compared with the measured curve in Figure 3.17, and the curves compare very well for the range $20 \leq U \leq 90\%$. More complicated theories exist that fit the experimental curves better, but the mathematics associated with their use is formidable and the theories have not been used successfully in engineering practice.

### 3.5.3 The Consolidation Curve

Several parts of the analysis must be altered to conform to the methods normally used in engineering practice. First, the $\sigma'$-$\varepsilon$ curve is not plotted in the conventional manner but rather is rotated, as shown in Figure 3.18, because then the strain scale reads in the same direction in which settlement occurs. Furthermore, it is common practice to plot $\sigma'$ on a logarithmic scale as shown in Figure 3.19.

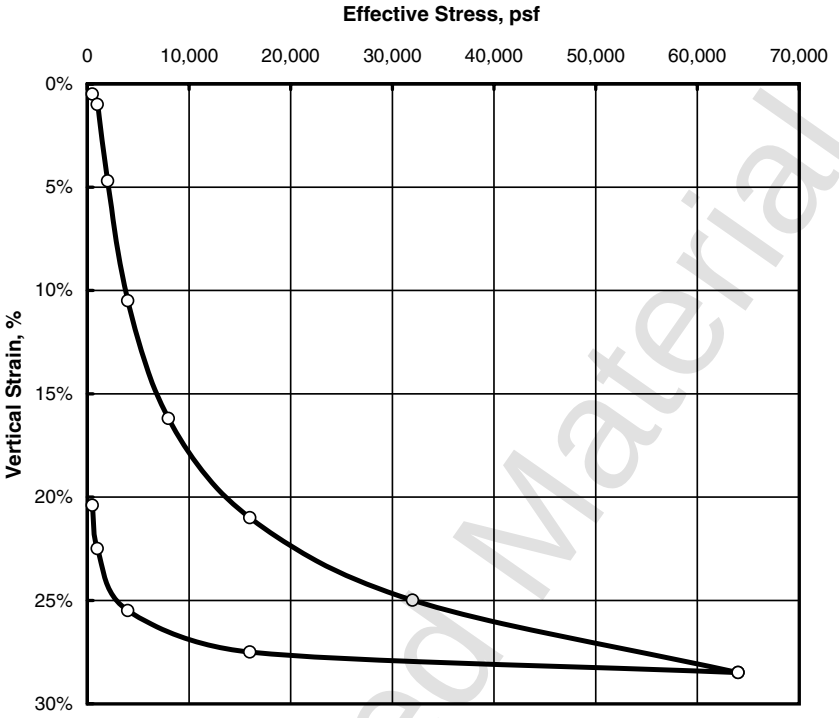


**Figure 3.18** Consolidation curve on a natural scale.

Determining the vertical strain analytically rather than by reading it from a curve is sometimes convenient. If a one-dimensional consolidation test is performed on a specimen of very soft clay, one will obtain a curve such as that shown in Figure 3.20. If the soil is in equilibrium in nature at a stress such as $\sigma_0'$ and the stress is increased, by placement of an embankment to $\sigma_f'$, the curve between $\sigma_0'$ and $\sigma_f'$ can be approximated by a straight line. The slope of the line is $C_\varepsilon$, termed the *strain index*. It is defined as

$$C_\varepsilon = \frac{\varepsilon_f - \varepsilon_0}{\log \sigma_f' - \log \sigma_0'} = \frac{\varepsilon_f - \varepsilon_0}{\log \dfrac{\sigma_f'}{\sigma_0'}} \tag{3.66}$$

The strain caused by the loading is $\varepsilon = \varepsilon_f - \varepsilon_0$, so equations from Eqs. 3.68 and 3.66 on the settlement of a layer $j$ with thickness $H$ can be computed using

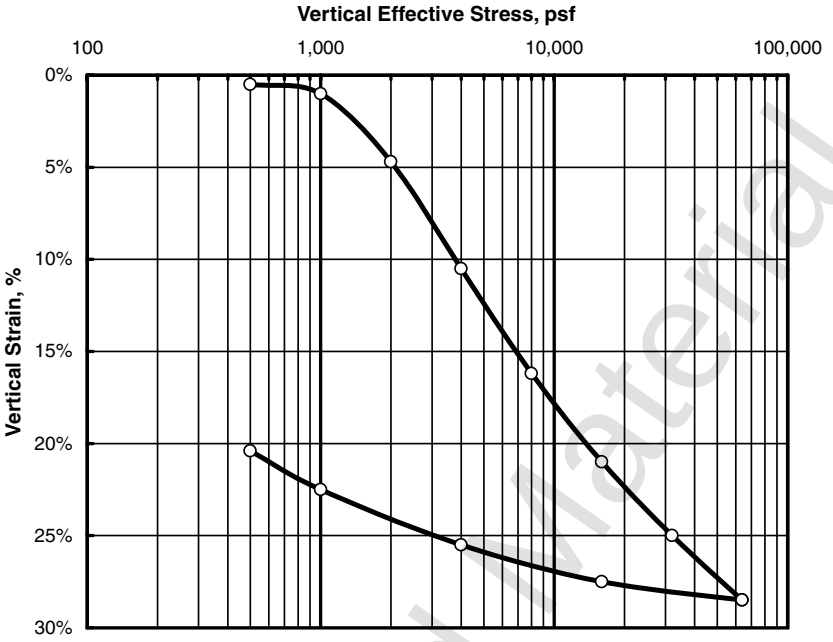


**Figure 3.19** Consolidation curve on a semilog scale.

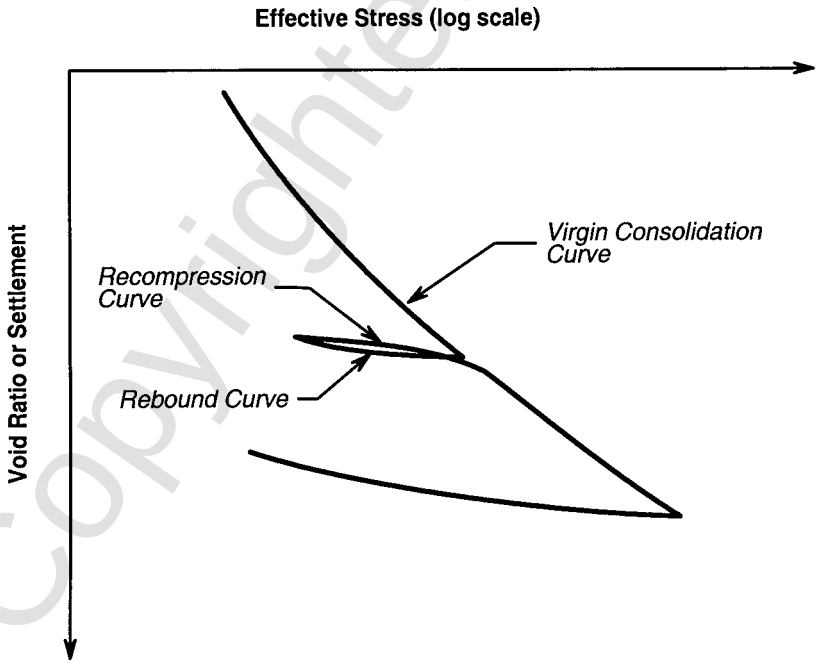


**Figure 3.20** Virgin consolidation curve for vertical strain versus logarithm of vertical effective stress.

$$S_j = \left( C_\varepsilon H \log \frac{\sigma'_f}{\sigma'_0} \right)_j \tag{3.67}$$

A soil that has been deposited from suspension and consolidated to some stress, clearly the maximum stress to which the soil has ever been subjected, is said to be *normally consolidated,* and the associated $\sigma$–$\varepsilon$ relationship is termed the *virgin consolidation curve*.

Compression of a soil causes largely irreversible movements between particles, so if the soil is unloaded, the resulting *rebound curve,* or *swelling curve,* has a flatter slope than the virgin curve and the *recompression curve* (also called the *reloading curve*) forms a hysteresis loop with the rebound curve. Soils now existing under effective stresses smaller than the maximum effective stress at some time in the past are said to be *overconsolidated*.

If the soil is undergoing consolidation down the virgin curve, it is *underconsolidated*. Obviously, this is a transient condition unless deposition of sediment is occurring at a fast enough rate that the excess porewater pressures cannot be dissipated.

The samples tested for Figure 3.20 started as a slurry, and the strain is calculated using the initial height of the unconsolidated slurry.

### 3.5.4 Calculation of Total Settlement

Among the first problems is to investigate the *spring constant* of the soil. A soil sample of height $H$ is placed in an apparatus such as the one shown in Figure 3.6. A series of loads are applied, and for each load the settlement and the elapsed time are measured when equilibrium is established. For convenience, $S$ is divided by $H$ to obtain strain $\varepsilon$ and a stress-strain curve is plotted. The curve is likely to have the shape shown in Figure 3.21. The spring representing the model must be nonlinear to fit measured soil properties.

If the stress-strain curve is really representative of the soil in the field, the curve should be useful for analysis. A thin stratum of soil at depth $z_j$ in the soil deposit is considered. The stratum has a thickness $H_j$, and before placement of the embankment, it is in equilibrium under a vertical stress, $\sigma'_j$. The condition of the soils is indicated by point $j$ in Figure 3.21. If a stress $\Delta\sigma'$ from the embankment is added, the strain $\Delta\varepsilon$ results. The settlement of the surface caused by the compression of the $j$th layer is then

$$S_j = (\Delta\varepsilon)_j H_j \tag{3.68}$$

The settlement of the surface caused by compression of the entire subsoil is then

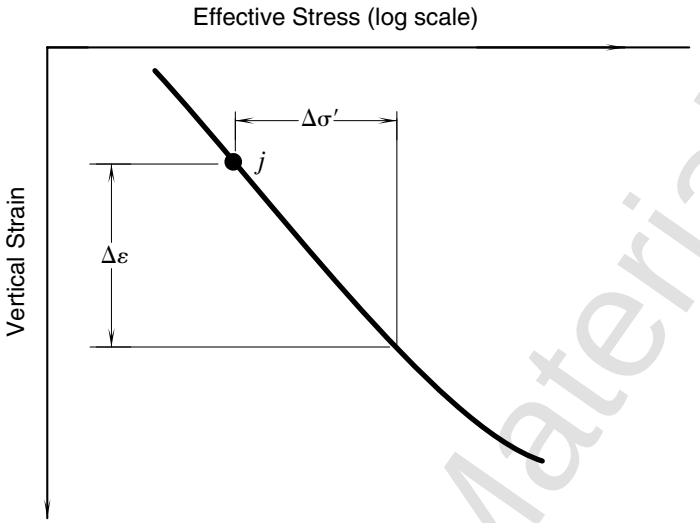


**Figure 3.21** One-dimensional stress-strain curve for soil.

$$S = \sum_{j=1}^{\text{layers}} S_j \tag{3.69}$$

where

$$H = \sum_{j=1}^{\text{layers}} H_j \tag{3.70}$$

Although the foregoing analysis is simple, many necessary quantities remain undefined. For example, how is the added effective stress $\Delta\sigma'$ calculated with depth below a foundation? How is the initial effective stress calculated? How are the proper $\sigma'$-$\varepsilon$ curves obtained? These quantities and many others must be determined before any realistic field problems can be analyzed.

### 3.5.5 Calculation of Settlement Due to Consolidation

Sufficient data have now been presented so that the total settlement under a wide embankment can be calculated. To review, the settlement is computed as follows:

1. The subsoil is divided into a series of layers.
2. The quantities $\gamma$, $\gamma'$ value and the $\sigma'$-$\varepsilon$ curve are measured for each layer.

3. The initial effective stresses are calculated at the center of each layer (the stress at the center may be considered an average stress for the layer).
4. The stress added by the embankment is determined.
5. The strain resulting in each layer from the applied stress is read from the appropriate $\sigma'$-$\varepsilon$ curve.
6. The settlement of each layer is then calculated using Eq. 3.68.
7. The settlement of the original ground surface is calculated from Eq. 3.69.
8. If the settlement is large enough so that submergence effects are important, then successive trials of Steps 4 through 7 are used until a settlement of desired accuracy has been determined.

### 3.5.6 Reconstruction of the Field Consolidation Curve

The consolidation curve measured in the testing laboratory is not used directly for computation of total settlement because it represents the behavior of soil in the laboratory, not in the field. Instead, the laboratory curve must be corrected to obtain the *field consolidation curve*. This procedure is called *reconstruction of the field consolidation curve.* The reasons for this correction are as follows.

A soil in the field is assumed to have been consolidated to $\sigma'_{\max}$ and then rebounded to point $A$, and an embankment is assumed to be placed so that the effective stress will increase again. In calculating the settlement (Eq. 3.68), the strains must be calculated in terms of the height of the sample (or stratum $j$ in the field) at point $A$, not the original height, so the slopes of the reloading are virgin curves that must be suitably corrected. Similar corrections are required if a soil sample is to be used as representative of a stratum, but does not come from the center of the stratum, and for various other applications. The occasional inconveniences due to changed total heights are minor, and some engineers use the types of graphs shown in Figure 3.19, but most geotechnical engineers prefer to avoid confusion by calculating strains in terms of a constant height. The height selected is the *height of solids* $H_s$, a fictitious height defined as

$$H_s = \frac{V_s}{A} \tag{3.71}$$

where $V_s$ is the volume of solid mineral grains and $A$ is the cross-sectional area of the test specimen. The vertical strains are calculated in terms of $H_s$ and are

$$\begin{aligned}\frac{\Delta H}{H_s} &= \frac{(\Delta H)A}{H_s A} \\ &= \frac{\Delta V}{V_s} \\ &= \frac{\Delta(V_v + V_s)}{V_s} \\ &= \frac{\Delta V_v + \Delta V_s}{V_s} \\ &= \frac{\Delta V_v}{V_s} = \Delta e\end{aligned} \tag{3.72}$$

because $\Delta V_s = 0$. Thus, void ratios are plotted instead of strains, and the change in void ratio is a strain expressed in terms of the constant height of solids. The settlement equation (Eq. 3.68) becomes

$$\begin{aligned}S &= \frac{\Delta V}{A} \\ &= \frac{\Delta V_v}{V_s} \cdot \frac{V_s}{A} \\ &= \Delta e \frac{V_s}{A} \cdot \frac{H}{H} \\ &= \Delta e \frac{HV_s}{V} \\ &= \Delta e \frac{HV_s}{V_s + V_v} \\ &= \Delta e H \frac{1}{1 + \dfrac{V_v}{V_s}}\end{aligned}$$

Thus

$$S_j = \left(\frac{\Delta e}{1 + e} H\right)_j \tag{3.73}$$

The $e$-log $\sigma'$ curve for an overconsolidated clay may have the appearance of the curve shown in Figure 3.22. If a structure is placed on the soil deposit so that $\sigma'_0$ increases to $\sigma'_f$, the settlement is then

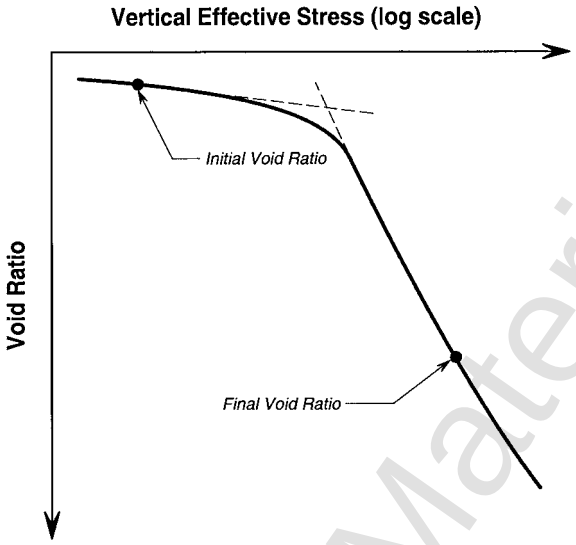


**Figure 3.22** Consolidation curve for overconsolidated clay.

$$S_j = \left( \frac{e_0 - e_f}{1 + e_0} H_0 \right)_j \tag{3.74}$$

If the soil is normally consolidated and the virgin curve is approximately linear on the log scale, then the slope of the virgin curve on the $e$-log $\sigma'$ plot $C_c$ is defined as follows:

$$\boxed{C_c = \frac{e_1 - e_2}{\log \sigma'_2 - \log \sigma'_1} = \frac{e_1 - e_2}{\log \left| \frac{\sigma'_2}{\sigma'_1} \right|}} \tag{3.75}$$

where points 1 and 2 are both on the virgin curve. The slope, $C_c$, is termed the *compression index* and is defined in such a way that it is positive even though the curve slopes downward.

The change in void ratio $\Delta e$ can be computed from $C_c$ by rearranging Eq. 3.75:

$$\Delta e = e_1 - e_2 = C_c \log \left| \frac{\sigma'_2}{\sigma'_1} \right| \tag{3.76}$$

The settlement $S$ that results from increasing the loading from $\sigma'_1$ to $\sigma'_2$ is computed by combining Eqs. 3.74 and 3.75 using

$$S = \frac{e_1 - e_2}{1 + e_1} H_1 = C_c \frac{H_1}{1 + e_1} \log \left| \frac{\sigma'_2}{\sigma'_1} \right| \tag{3.77}$$

In the usual notation, the initial condition of the normally consolidated soil is denoted by the subscript 0 and the final condition by the subscript $f$. The settlement for layer $j$ is then

$$S_j = \left( C_c \frac{H_0}{1 + e_0} \log \left| \frac{\sigma'_f}{\sigma'_0} \right| \right)_j \tag{3.78}$$

If the soil is overconsolidated in the field and the applied loads will make $\sigma'_f < \sigma'_{max}$, then the settlement can be calculated analytically using an equation of the same form as Eq. 3.78, but with $C_c$ replaced by the slope of a reloading curve $C_r$ so that

$$S_j = \left( C_r \frac{H_0}{1 + e_0} \log \left| \frac{\sigma'_f}{\sigma'_0} \right| \right)_j \tag{3.79}$$

If $\sigma'_f > \sigma'_{\max}$, then the settlement can be calculated from point 0 to point $i$ (Figure 3.22) and then from $i$ to $f$:

$$\boxed{S_j = \left( C_r \frac{H_0}{1 + e_0} \log \left| \frac{\sigma'_i}{\sigma'_0} \right| \right)_j + \left( C_c \frac{H_0}{1 + e_0} \log \left| \frac{\sigma'_f}{\sigma'_i} \right| \right)_j} \tag{3.80}$$

The constant height of solids $H_s$ is

$$H_s = \frac{H_0}{1 + e_0} \tag{3.81}$$

and

$$\frac{H_0}{1 + e_0} = \frac{H_i}{1 + e_i} = \frac{H_f}{1 + e_f} = H_s \tag{3.82}$$

Equation 3.79 is often used for inexpensive projects where no laboratory measurements can be afforded and a value for $C_r$ is assumed based on previous experience from other projects in the area for which laboratory testing has been performed. Equation 3.80 is used where experience (or laboratory tests) shows that a soil has been overconsolidated by a fixed amount independent of depth—for example, by erosion of a known thickness of surface soil—so the stress, $\sigma'_i - \sigma'_0$, is known.

### 3.5.7 Effects of Sample Disturbance on Consolidation Properties

One problem remains: whether or not the laboratory tests give properties that can be used directly in the field. More explicitly, does taking a soil sample from the ground and putting it into the consolidation cell in the laboratory cause a change in properties? Field sampling of soils will be discussed with respect to the effects of disturbance on the results of tests in the laboratory.

The most extreme disturbance would be obtained by physically remolding a soil. An $e$-log $\sigma$ curve for a hand-carved sample (minimum sampling disturbance) is shown in Figure 3.23 for a sample of Leda clay from Toronto, Canada, and also is a curve is shown for a sample that was completely remolded prior to testing. Clearly, using a seriously disturbed sample of this soil for a field design would lead to large errors in predicting total settlement. As a simple example, a clay is considered that is 40 ft thick in the field. To simplify the calculations (with some loss of accuracy), the layer will not be subdivided. An average initial effective stress of 1000 psf is assumed along

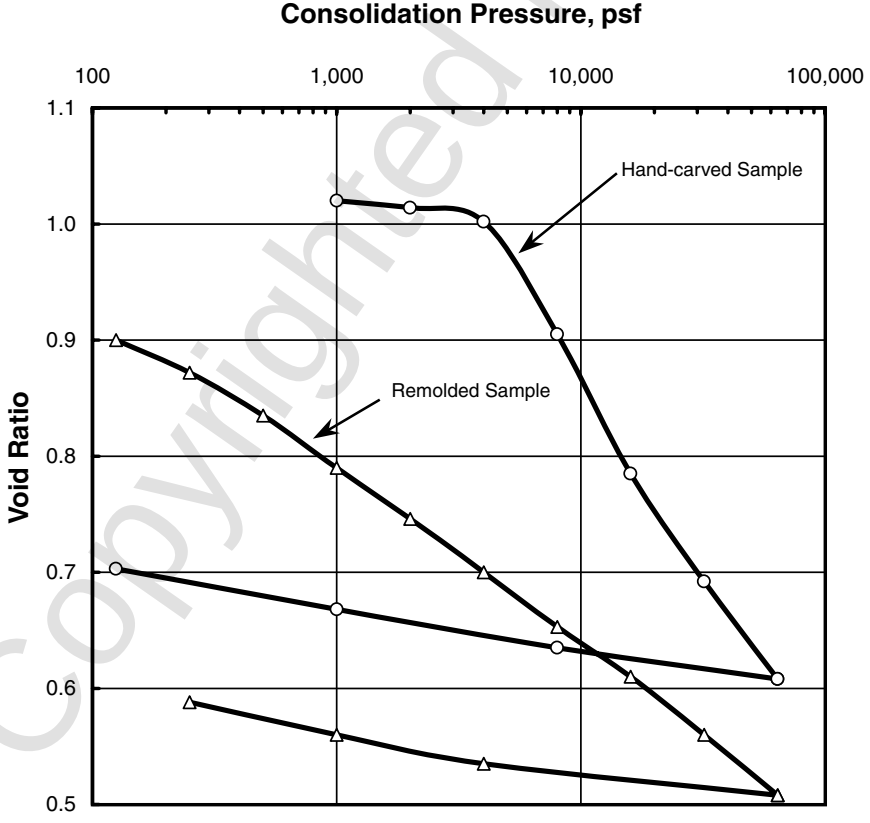


**Figure 3.23** Consolidation curves for undisturbed and remolded clay.

with an increase in effective stress of 3000 psf. Eq. 3.60 will be used to calculate settlements. The calculated settlement for the hand-carved specimen is

$$S = \frac{1.020 - 1.002}{1 + 1.020} 480 \text{ in.} = 4.3 \text{ in.}$$

If the curve for the remolded sample is used (which started at the same $e_0$ but settled under the first applied load), the settlement is

$$S = \frac{1.020 - 0.707}{1 + 1.020} 480 \text{ in.} = 74 \text{ in.}$$

Gross errors in settlement predictions are clearly possible with some soils if disturbance is severe. Most soils are less sensitive to disturbance, and careful sampling and handling will reduce the effects of disturbance further.

It would be useful if the position of the ''undisturbed'' consolidation curve ($e$-log $\sigma'$) could be estimated from a test on a disturbed sample, but it seems obvious that there is no way of reconstructing the curve of the hand-carved sample, shown in Figure 3.23, from the curve of the remolded sample. A less severe example of disturbance is shown in Figure 3.24. The soil here was a red-colored plastic clay from Fond du Lac, Wisconsin. Samples were taken alternately with 3-in.- and 2-in.-diameter thin-walled samplers. The 3-in. sampler apparently caused less disturbance than the 2-in. sampler. If the sample is only slightly disturbed, it might be possible to reconstruct an approximate undisturbed (field) curve. Figure 3.25 shows the results of a one-dimensional consolidation test on clay that started as a suspension. After consolidating at 1000 psf (point 1), the sample was allowed to swell in steps back to 20 psf and was then reloaded. Note that the reloading curve makes its sharpest curvature near the maximum previous consolidation pressure ($\sigma'_{\max} = 1000$ psf). Based on this fact, Casagrande (1936) recommended a construction for finding $\sigma'_{\max}$ (a first step in reconstructing a field curve). His construction is shown in Figure 3.26. Casagrande located the point of sharpest curvature on the $e$-log $\sigma'$ laboratory curve and drew three lines at that point: a horizontal line, a tangent line, and a line bisecting the angle between the first two lines. Another line is drawn tangent to the virgin consolidation curve, and the intersection of this line and the bisecting line is taken as the best estimate of $\sigma'_{\max}$. The method clearly does not work for badly disturbed samples, such as, the remolded samples in Figure 3.23, and the application of the Casagrande construction to undisturbed samples where the curve bends sharply down at $\sigma'_{\max}$ (Figure 3.23) is uncertain, so many engineers prefer to estimate the value of $\sigma'_{\max}$ by eye.

The next step is to calculate $\sigma'_0$ in the field. The void ratio in the field $e_0$ is the same as the initial void ratio in the laboratory because no change in water content is allowed during sampling or storage, and none is allowed

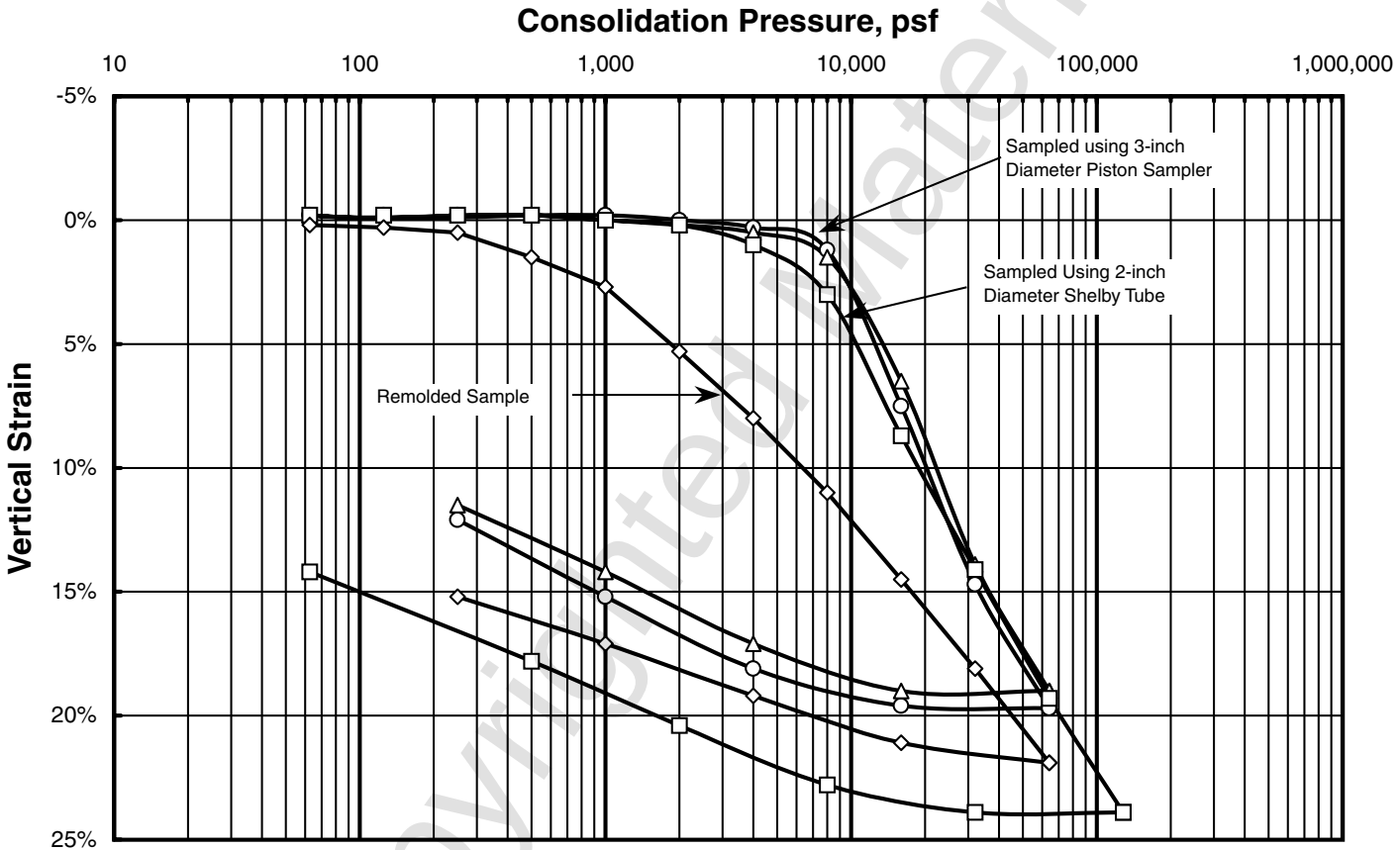


**Figure 3.24** One-dimensional consolidation curves on tube samples and a remolded sample of clay.

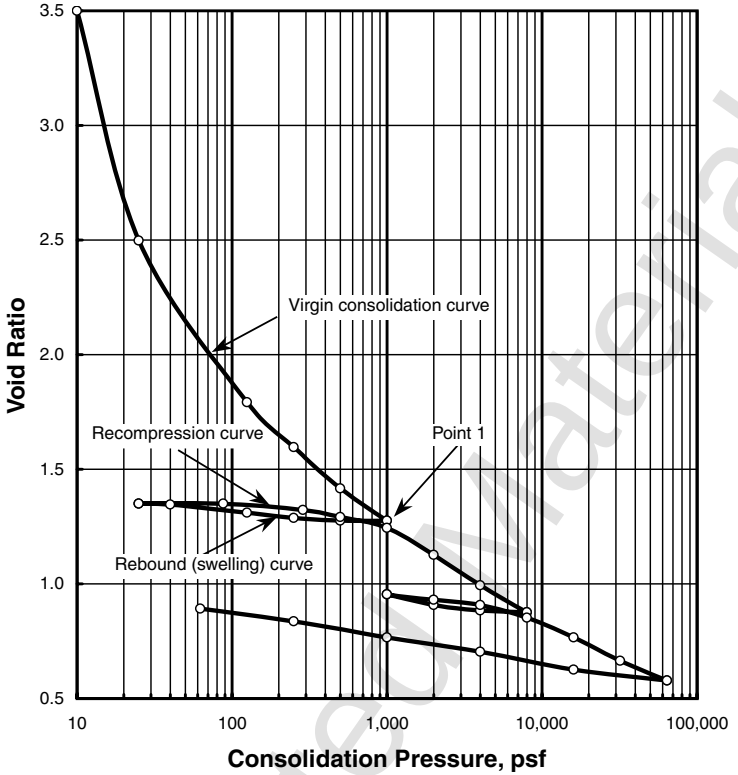


**Figure 3.25** One-dimensional consolidation curve for a specimen of clay that was sedimented from suspension.

when the soil is equilibrating under the first load in the laboratory. If $\sigma'_{max}$, determined from the laboratory curve, is equal to $\sigma'_0$, the soil is normally consolidated. The field curve must then pass through the point ($e_0$, $\sigma'_0$) and will merge smoothly with the laboratory virgin curve.

A question arises as to how close $\sigma'_0$ and $\sigma'_{max}$ are likely to be, considering the difficulty of estimating $\sigma'_{max}$ from a laboratory curve and considering that the value of $\sigma'_0$ depends on the elevation of the water table, which may be difficult or (or uneconomical) to locate in the field. As one example of a relevant study, Skempton (1948) found a soil deposit known to be normally consolidated by geological evidence. He took samples, performed laboratory one-dimensional consolidation tests, and compared $\sigma'_0$ with $\sigma'_{max}$. His data are summarized in Table 3.4. Samples were taken with a 4 1/8-in.-diameter sampler with an area ratio of 23%.

If $\sigma_0$ is substantially less than $\sigma'_{max}$, then the soil is clearly overconsolidated. For example, Figure 3.27 shows the consolidation curve for stiff clay where $\sigma_0$ is about 230 psf and $\sigma'_{max}$ is about 5300 psf. In this figure, the laboratory

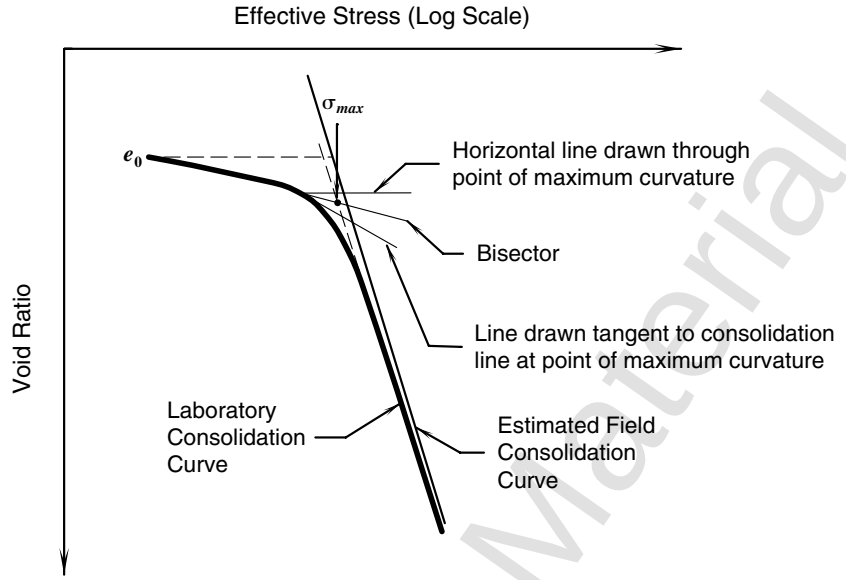


**Figure 3.26** Casagrande's construction to find the maximum previous consolidation pressure.

curve passes below the $(e_0, \sigma'_0)$ point, so the sample is disturbed. The procedure to use in estimating the location of the field curves is the following: the soil in the field was assumed to be consolidated to $\sigma'_{\max}$ and then rebounded directly to $\sigma'_0$. The slopes of the swelling curves in the field and in the laboratory are also assumed to be the same. The location of the field swelling curve is then estimated by passing a curved line, parallel to the laboratory swelling (rebound) curve, from a point on the $\sigma'_{\max}$ line (Figure 3.27) back to $(e_0, \sigma'_0)$. The field reloading curve then starts at $(e_0, \sigma'_0)$, forms a hysteresis loop with the swelling curve, passes below the point on the virgin curve corresponding to the original consolidation at $\sigma'_{\max}$, and merges with the laboratory virgin curve or its extension. This construction, originated by

**TABLE 3.4 Comparison of $\sigma'_0$ and $\sigma'_{\max}$ for a Normally Consolidated Estuarine Clay from Grosport, England**

| Boring | Sample | Depth, ft | $\sigma'_0$, psf | $\sigma'_{\max}$, psf | $\frac{\sigma'_0 - \sigma'_{\max}}{\sigma'_0}$ |
|---|---|---|---|---|---|
| 1 | 2 | 21 | 740 | 560 | +18 |
| 1 | 6 | 61 | 2480 | 2440 | +2 |
| 3 | 2 | 19 | 680 | 600 | +12 |
| 3 | 7 | 56 | 2100 | 1680 | +20 |
| 4 | 2 | 17 | 640 | 880 | −38 |

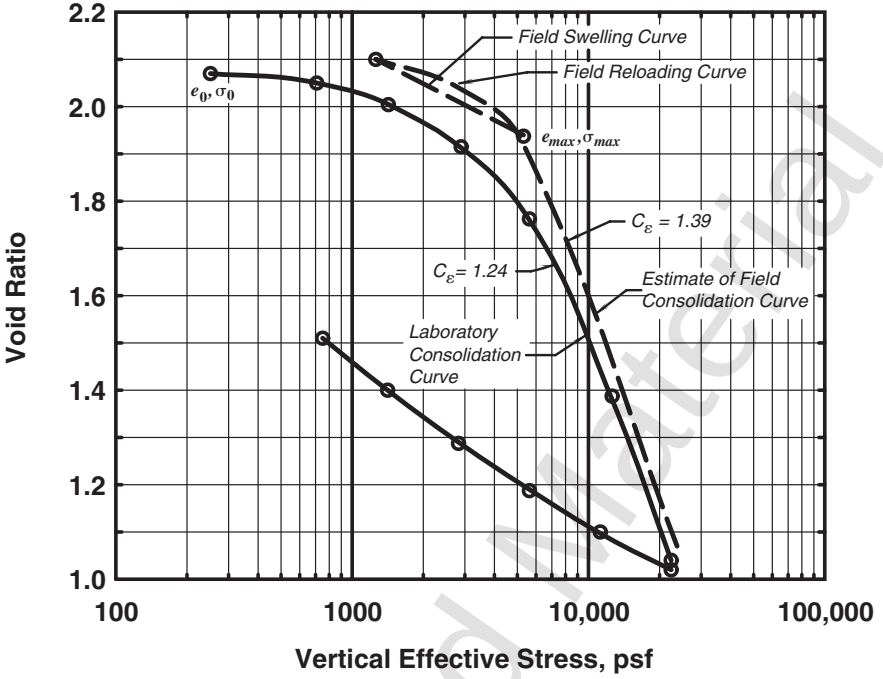


**Figure 3.27** One-dimensional consolidation curve for an overconsolidated clay.

Schmertmann (1955), was used to estimate the location of the field curves in Figures 3.24 and 3.27.

The time rate of settlement is controlled by the estimated value of the coefficient of consolidation in the same way that the total settlement is controlled by the consolidation curve. The effect of complete remolding on the $c_v$ of a sensitive clay is shown in Figure 3.28 (the same test as for Figure 3.23). At low confining pressure, remolding caused a severe reduction in $c_v$. If time rate or settlement calculations are important on a project, then high-quality undisturbed samples should be used for testing.

### 3.5.8 Correlation of Consolidation Indices with Index Tests

On small projects, it may not be economically possible to perform laboratory tests. Consequently, geotechnical design computations are carried out using estimated values for soil properties. On other projects, the cost of the structure is such that a few laboratory tests can be performed but the soils under the structure are so highly variable that no reasonable number of consolidation tests would provide the needed information. In such cases, it would be desirable if the slope of the consolidation curve could be correlated with some soil property that is simpler to measure (and less expensive). These correla-

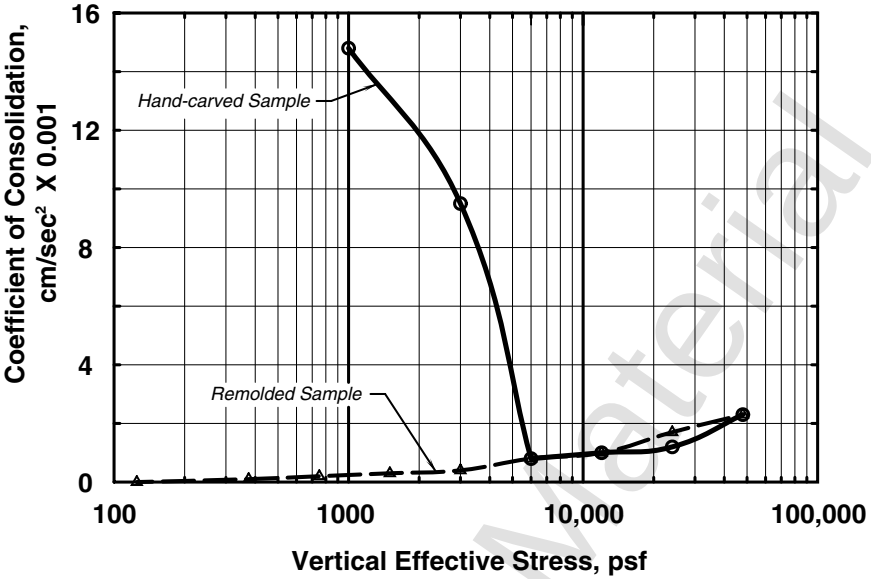


**Figure 3.28** Coefficients of consolidation of leda clay.

tions may be made by an individual firm for soil deposits encountered in their locale, or correlations may be developed that apply to soils with a common geologic origin. Several examples will be cited.

Peck and Reed (1954) reported that

$$C_c = 0.18\, e_0 \quad \text{for soft clays in Chicago} \tag{3.83}$$

Moran et al. (1958) showed that

$$C_c = 0.01\, w_0 \quad \text{for highly organic clays} \tag{3.84}$$

where $w_0$ is the field water content in percent. Terzaghi and Peck (1967), based on a paper by Skempton (1944), showed that

$$C_c = 0.009\,(LL - 10) \tag{3.85}$$

where $LL$ is the liquid limit.

None of these correlations are exact, but when used with the soils for which the correlation was developed, they are often accurate within $\pm 30\%$. Considering that soil properties sometimes change by more than 30% within a few feet or meters or less, such correlations may be sufficiently accurate and may yield far more accurate estimates than would be obtained by investing the same money in a few consolidation tests.

A major source of uncertainty in using such correlations is the issue of whether or not the soil is normally consolidated in the field. Since the reloading index is usually four to six times less than the compression index, it is important to know whether to use the reloading index or the compression index. If no laboratory consolidation test results are available, the best estimate of whether a soil is normally consolidated or overconsolidated is obtained by comparing the strength of the soil in the field with the strength expected for a normally consolidated soil.

### 3.5.9 Comments on Accuracy of Settlement Computations

***Accuracy of Predictions of Total Settlement*** One-dimensional settlement analyses are used in estimating total settlements, and the rates at which they occur, under the central parts of loads that are wide compared to the depth of the compressible layer. For soft, normally consolidated clays, the accuracy of the prediction of total settlement is mainly limited by the natural variability in soil properties coupled with a limited number of tests, as dictated by economic constraints. The accuracy of prediction is adequate for real design work.

For stiff, overconsolidated clays, the accuracy of the prediction of total settlement seems to be affected by sampling disturbance, which increases the slopes of reload curves in the laboratory. Although the predicted settlements are likely to be too large, the total settlements are small enough that they are often not a serious problem. The only serious problems are with lightly overconsolidated clays, where the engineer may be uncertain whether the loading will be entirely on a reloading curve or partially on a virgin curve.

***Prediction of Time Rate of Settlement During Secondary Compression*** Predictions of time rates of settlement are relatively inaccurate in most cases. In the special case of saturated, homogeneous, normally consolidated clays, the prediction of the rate of primary consolidation is based on Terzaghi's theory and appears to be reasonably accurate. Further, field studies suggest that the slope of the secondary settlement curve ($S$-log $t$) in the field is about the same as in the laboratory, so the secondary settlement in the field is estimated just by plotting the primary field $S$-log $t$ curve and then drawing in the secondary curve tangent to the laboratory curve, as suggested in Figure 3.29.

In most field problems, the simplifying assumptions of Terzaghi's theory are not satisfied. Estimates of the times required for consolidation in such cases are usually based on previous experience in the area, although more advanced analytical techniques than those considered here have shown much promise.

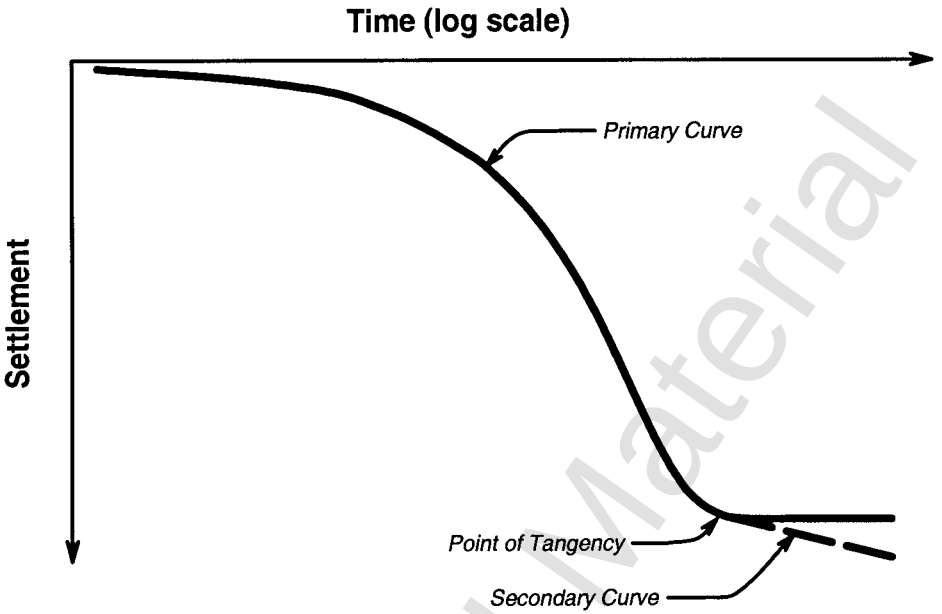


**Figure 3.29** Method for predicting secondary settlements.

## 3.6 SHEAR STRENGTH OF SOILS

### 3.6.1 Introduction

The following discussion is an introduction to the shear strength of soils, a topic requiring a book to discuss thoroughly. Throughout this discussion, shear strength will be discussed in terms of the Mohr-Coulomb failure criteria: cohesion and friction. Different methods of shear testing are introduced in this discussion. The reader should learn when various shear tests may be unsuitable for characterization of shear strength for an engineering design because the particular design methodology was developed originally using a single, specific form of shear testing.

### 3.6.2 Friction Between Two Surfaces in Contact

This discussion of the mechanics involved in the shear strength of soils begins with fundamental concepts based on Amonton's law of friction. A block resting on a horizontal plane is shown in Figure 3.30. A vertical force $N$ and a shearing force $F$ are applied to the block. If the shearing force $F$ is gradually increased until sliding occurs, then $F$ exceeds the friction force holding the block in place. The magnitude of $F$ is

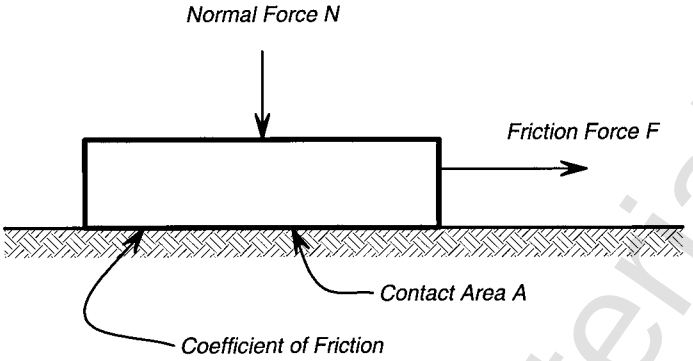


**Figure 3.30** Block sliding on a plane.

$$F = \mu N \tag{3.86}$$

where $\mu$ is the coefficient of friction between the block and the plane. Dividing both sides of Eq. 3.86 by the area of the block, $A$, we obtain

$$\frac{F}{A} = \frac{N}{A}\mu \tag{3.87}$$

or, in terms of the shear and normal stresses, $\tau$ and $\sigma$,

$$\tau = \sigma\ \mu \tag{3.88}$$

The angle of the resultant force or stress acting on the plane is denoted by the Greek letter $\phi$, shown in Figure 3.31. Eq. 3.88 can be written in the form

$$\tau = \sigma_n \tan(\phi) \tag{3.89}$$

The above equation shows that the shear stress at failure is proportional to the applied normal stress and that the relationship between these stresses is a straight line inclined at the angle $\phi$, as shown in Figure 3.32.

*Relationship Between Principal Stresses at Failure.* The relationship between the principal stresses at failure when the failure envelope has a cohesion intercept is obtained by solving Eq. 3.94 for the desired principal stress and then using the trigonometric identity

$$\frac{1 + \sin\phi}{1 - \sin\phi} = \tan^2\left(45° + \frac{\phi}{2}\right) \tag{3.90}$$

The resulting equations are

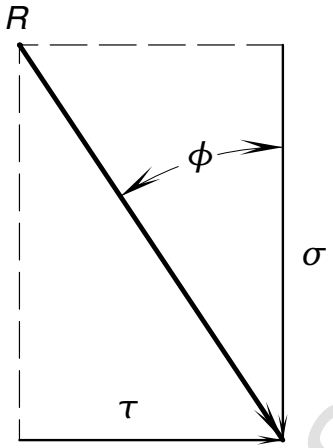


**Figure 3.31** Definition of the friction angle.

$$\sigma_1 = \sigma_3 \tan^2\left(45° + \frac{\phi}{2}\right) + 2c \tan\left(45° + \frac{\phi}{2}\right) \tag{3.91}$$

$$\sigma_3 = \sigma_1 \tan^2\left(45° - \frac{\phi}{2}\right) + 2c \tan\left(45° - \frac{\phi}{2}\right) \tag{3.92}$$

Equations 3.99 and 3.100 apply to circles tangent to linear failure envelopes whether the envelopes are expressed in terms of total stresses or effective stresses, provided, of course, that the symbols are adjusted for the type of stress used and for the type of test.

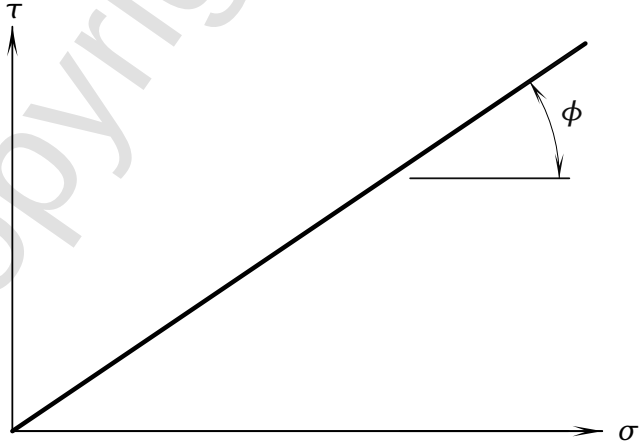


**Figure 3.32** Stress diagram for a block sliding on a plane.

### 3.6.3 Direct Shear Testing

A method for testing soils that is similar to the sliding block test is the direct shear test. A cross-sectional view through a direct shear apparatus is shown in Figure 3.33. In this test, the soil is placed in a box that is split horizontally in a manner that allows the upper and lower halves to be displaced relative to one another while a vertical stress is applied to the upper surface of the test specimen. The shape of the shear box may be square or circular in plan. The soil may be consolidated prior to shearing if the soil being tested is clay. During the test, the horizontal displacement of the shear box is increased and the shear force is measured until failure occurs or until maximum displacement is reached.

If a series of direct shear tests are performed on a dry sand using various vertical pressures, the shear stress at failure can be plotted versus the vertical normal stress in a diagram like that shown in Figure 3.34. By analogy with the block sliding on the plane, the slope of the line in this diagram is designated by the Greek letter $\phi$, and the angle is called the *angle of internal friction*.

The typical results for a direct shear test series on stiff clay are shown in Figure 3.35. In this diagram, the shear strength of the soil consists of two parts. The first part is indicated by the intercept of the vertical axis, labeled $c$, called the *cohesion.* The second part is indicated by the slope of the line


**Figure 3.33** Direct shear test.

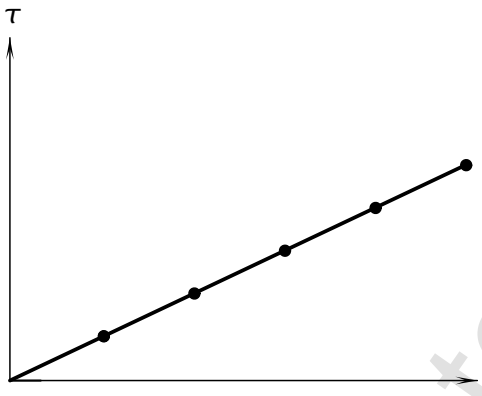


**Figure 3.34** Failure envelope for direct shear tests.

and is called the *internal friction.* The shear strength of the soil is then given by the equation

$$\tau = c + \sigma_n \tan(\phi) \tag{3.93}$$

The lines in Figures 3.34 and 3.35 represent the relationship between shearing stress and normal stress at failure. It is not possible to have a stable state of stress if values plot above these lines. Because these lines envelop all stable states of stress, they are called the *failure envelope*.

### 3.6.4 Triaxial Shear Testing

Triaxial shear tests are performed on solid cylindrical specimens of soil. The height of the test specimen is usually about twice its diameter. The diameter varies from about 1.3 in. or (33 mm) to 4 in. (100 mm) for more common specimens. In a typical *triaxial cell,* the soil specimen is held between the

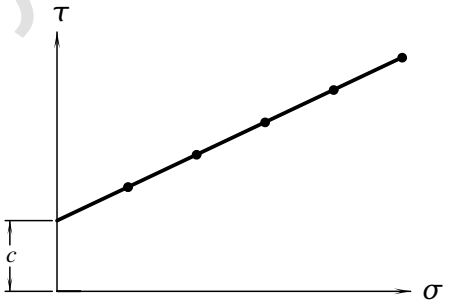


**Figure 3.35** Direct shear envelope on clay.

*base pedestal* and the *top cap* of the triaxial cell and is laterally confined in a thin, impervious rubber membrane. The membrane is sealed to the top cap and base pedestal using silicone grease and rubber O-rings. A photograph of a modern triaxial cell is shown in Figure 3.36. A more detailed discussion of the design and construction of triaxial cells and associated equipment is presented by Bishop and Henkel (1957) and by Andersen and Symons (1960).

The pressure in the triaxial cell confines the specimen under a hydrostatic stress. It is not possible to develop a shear stress on the rubber membrane

**Figure 3.36** Photograph of a triaxial cell.

covering the sides of the specimen because it is flexible; thus, the exterior vertical surface of the specimen is a principal surface. If the vertical surfaces of the specimen are principal surfaces, then any horizontal plane through the specimen is also a principal surface. When a compressive load is applied through the loading piston, the vertical stress acting on horizontal planes is the maximum principal stress ($\sigma_1$) and the horizontal stress acting on vertical planes is the minimum principal stress ($\sigma_3$). In the triaxial test, the intermediate principal stress ($\sigma_2$) is equal to the minor principal stress. The axial stress applied to the soil specimen by the loading piston is ($\sigma_1 - \sigma_3$), and this quantity is called the *principal stress difference*.

If the loading piston is attached to the top cap, it is possible to apply a tensile load to the specimen and make the horizontal stress the major principal stress. This makes all vertical planes the major principal planes, with the intermediate principal stress equal to the major principal stress. Tests performed in this manner are called *extension tests*. In extension tests, the stress on horizontal planes is still compressive; an extension test is not a tensile test.

Triaxial tests are performed in two or more stages. In the first stage, the specimen is subjected to an initial state of stress. This stress may be hydrostatic (also called *isotropic*) or may be made to simulate the in situ state of stress by using different values for the vertical and radial stresses (this state is called *anisotropic*). For simplicity in the following discussion, the assumption is made that the initial state of stress is hydrostatic.

The triaxial test specimen may be allowed to consolidate after the confining stress is applied. If consolidation is permitted, multiple stages of consolidation pressures may be used. The specimen is sheared in the final stage and may or may not be allowed to drain during shearing. If the specimen is allowed to drain, it is possible to measure any volume change in the test specimen during the shearing stage.

There are three possible types of triaxial tests, depending on the combination of drainage conditions during the application of confining stresses and during shear. The three types of tests are consolidated-drained, consolidated-undrained, and unconsolidated-undrained. Short descriptions of these types of triaxial tests follow.

***Consolidated-Drained Triaxial Tests*** In this type of test, the soil specimen is allowed to consolidate completely under the initial state of stress prior to initiating shear. During shearing, either the axial deformation is applied so slowly that the porewater pressures have time to dissipate (the drains are left open) or else the axial stress is increased in small increments and each increment of pressure is maintained constant until the porewater pressure has dissipated. The amount of time required to shear the soil while allowing for dissipation of porewater pressures is determined from the consolidation properties of the test specimen. Common names for this type of test include *consolidated-drained* (*CD-test*), *drained* (*D-test*), and *slow* (*S-test*).

The amount of time required to complete a consolidated-drained test is long compared to that of the other two types of triaxial tests.

***Consolidated-Undrained Triaxial Tests*** In this type of test, the soil specimen is again allowed to consolidate fully under the initial state of stress in manner similar to that used in the consolidated-drained test. During shear, however, the drainage lines are closed and the specimen is sheared to failure under undrained conditions. This test is commonly referred to as a *consolidated-undrained test* (*CU-test*), a *consolidated-quick test* (*CQ-test*), or an *R-test.*

There are two varieties of consolidated-undrained tests. In one type, the specimen is sheared quickly in about 10 to 15 minutes. In the second type, the porewater pressures developed in the soil specimen are measured using porewater pressure transducers connected to drainage lines from the specimen. When the porewater pressures are measured, it is necessary to shear the specimen slowly enough for the porewater pressures to equilibrate throughout the test specimen. The additional time required for shearing is determined from the time needed to complete consolidation of the test specimen prior to shearing. While the time required for porewater pressure equalization in the specimen is often on the order of several hours, the testing time is usually much shorter than the time required to complete shearing in the consolidated-drained test.

***Unconsolidated-Undrained Triaxial Tests*** In this type of test, the soil specimen is not allowed to consolidate under the initial state of stress or to drain during shear. This test is commonly called an *unconsolidated-undrained test* (*UU-test*) or a *quick test* (*Q-test*).

Unconsolidated-drained tests cannot be performed because consolidation would occur whenever the drained specimens were opened during the shearing stage.

*Test Nomenclature.* The above notations were developed at various institutions at various times. The *quick* versus *slow* type designation was developed at Harvard University during the 1930s, when quick tests meant that the specimen was sheared too quickly for the porewater to get out even though the drainage lines were open throughout the test. Drained test were performed slowly, so they were called *slow tests.* Actually, drained tests can be performed quite rapidly if the soil has high permeability (hydraulic conductivity), and undrained tests can be performed very slowly—for example, to study the creep-deformation properties at constant water content—so the quick versus slow designation soon became meaningless, though still widely used. Between World War II and the early 1960s, much of the important research on the shearing properties of soils was performed at the Imperial College of Science and Technology and at the Norwegian Geotechnical Institute, where the more descriptive terms—*drained* versus *undrained* and *consolidated* versus *unconsolidated*—were developed. These latter terms have a disadvantage in conversation since the prefix *un-* may be either slurred, and thus missed, or else emphasized so much that the sentence is disrupted. Confusion in spoken discussion can be avoided by using the terms proposed by Casagrande (1960):

- $Q$-test = unconsolidated-undrained (does not mean quick)
- $R$-test = consolidated-undrained.
- $S$-test = consolidated-drained (does not mean slow)

The letter $R$ was selected by Professor Arthur Casagrande of Harvard University for consolidated-undrained tests because it is between the letters $Q$ and $S$ in the alphabet. Casagrande's terminology has not been accepted by all geotechnical engineers for a variety of reasons. The reader should be aware of the terms that are commonly used to refer to the different types of tests and to understand the procedures employed in the testing.

In this text, $Q$, $R$, and $S$ will be used with symbols representing various soil parameters to designate the type of test used to define the parameter. A bar over the symbol or an apostrophe will designate that effective stresses were used. Thus, $\phi'_R$ and $c'_R$ are the effective stress angle of internal friction and cohesion obtained using $R$-type triaxial tests.

### 3.6.5 Drained Triaxial Tests on Sand

The changes in stress conditions in a sand specimen during shearing may be understood by plotting the states of stress on a Mohr-Coulomb diagram. During Stage 1, a hydrostatic pressure is applied and the specimen is allowed to consolidate completely. The three principal stresses are all equal to $\sigma_3$, and Mohr's circle plots as a single point in Figure 3.37a.

In Stage 2a (Figure 3.37b) a stress difference is applied representing an intermediate state in loading where the applied stress difference is not large enough to cause failure. Shear stresses exist on all inclined planes through the specimen. In Stage 2b (Figure 3.37b), the axial stress has been increased to its maximum value and the soil specimen fails.

If such tests are performed on a series of identical specimens under various cell pressures and all failure circles are plotted on a single diagram, a single

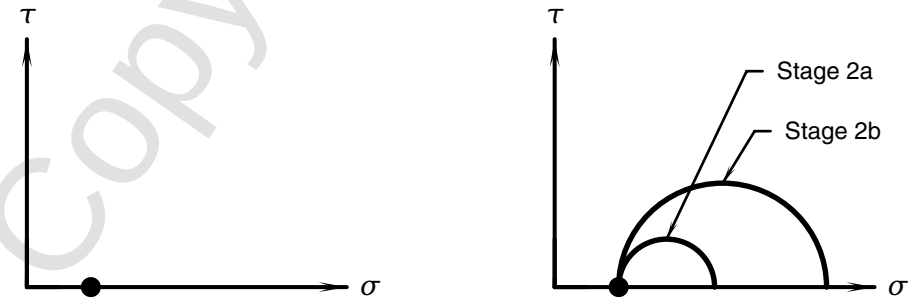


(a) Initial Isotropic State of Stress (b) Application of Stress Difference

**Figure 3.37** Mohr diagram for isotropic state of stress.

line can be drawn from the origin that is tangent to each circle. Such a series of circles is shown in Figure 3.38. Specimens of sand do not fail until some part of the stress circle touches this line. Therefore, this line is called a *failure envelope.* By analogy with the direct shear tests and, more exactly, by consideration of the stresses on the planes of failure, the slope of this line represents the obliquity of the resultant stress on the failure plane. As before, the slope of this line is called the *angle of internal friction* of the sand.

The relationships between stresses, strains, and the angle of internal friction vary from one sand to another and with the density of an individual sand. At the levels of confining stress usually encountered in foundation engineering, angular sands tend to have higher angles of internal friction than sands with rounded grains. Dense sands have higher angles of internal friction than loose sands.

A classic study of the shearing behavior of fine sands was reported by Bjerrum et al. (1961). The study concerned both the drained and undrained behavior of a fine sand that is widely found in Norwegian fjords. It was found that when a dense sand is sheared under drained conditions, it usually undergoes a small decrease in volume at small strains, but the denseness of the packing prevents significant volume decreases. As the sand is strained further, the grains in the zone of failure must roll up and over one another. As a result, the sand expands with further strain. The relationship between volumetric and axial strain for different densities of sand is shown in the lower half of Figure 3.39. Loose sands undergo a decrease in volume throughout the shear test.

The expansion of dense sand with increasing strain has a weakening effect and the specimens fail at relatively low strains, as seen in Figure 3.40. The densification of initially loose specimens with increasing strain makes such sands *strain-hardening* materials, and failure occurs at larger strains.

The relationship between angle of internal friction and initial porosity for fine quartz sand is shown in Figure 3.41. For this sand, the angle of internal

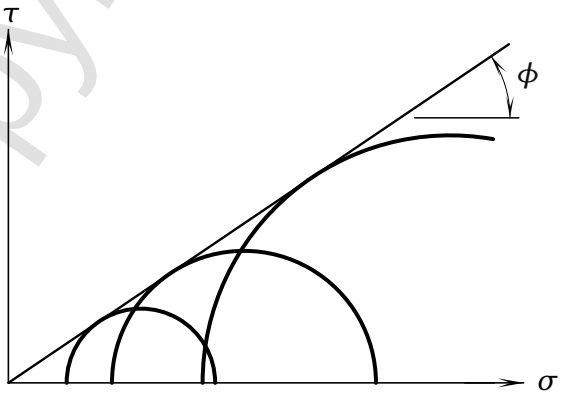


**Figure 3.38** Mohr circles for *S*-tests on cohesionless soil.

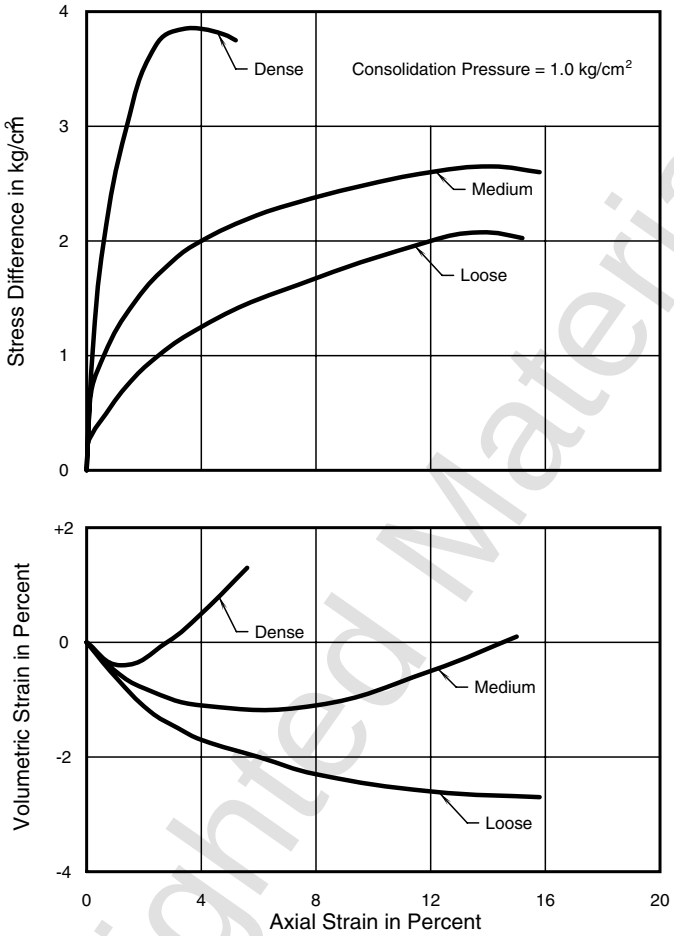


**Figure 3.39** Typical volume change versus axial strain curves for fine sand (from Bjerrum et al., 1961).

friction decreases gradually until the initial porosity is about 46 or 47% and then decreases rapidly. Sand with such high initial porosities is not common, but the occasional catastrophic landslides in deposits of loose sand suggest that low angles of internal friction can occur in nature.

The data for porosity shown in Figure 3.41 were converted to void ratios and redrawn in Figure 3.42. Also drawn in this figure are vertical lines denoting the ranges of relative density for the sand that was tested. The maximum and minimum void ratios for relative density were evaluated on dry samples of sand and the shear tests were performed on saturated sand. For these data, the angle of friction is found to drop when the void ratio is larger than the maximum value measured on dry sand for relative density evaluations. These extremely low friction angles were possible because the test

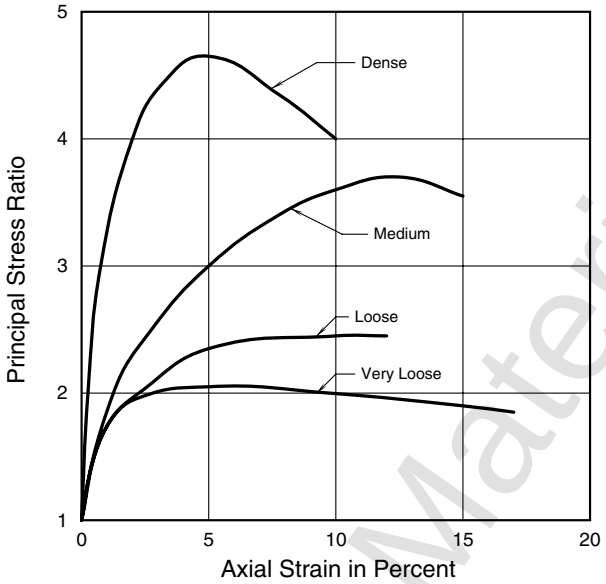


**Figure 3.40** Typical axial stress difference versus axial strain curves for fine sand (from Bjerrum et al., 1961).

specimens were formed by deposition in water. Thus, the loosest sand specimens were normally consolidated and never subjected to the higher stresses than can exist in dry sand. The lesson to be learned from this study is that the range of friction angles that may exist for saturated sands in nature can be both larger and smaller than the values measured in the laboratory if the sand is permitted to dry.

The application of shearing deformation results in densification of loose sands and expansion of dense sands. Available data suggest that, for a given sand and given confining pressure, the density at high strains is the same for all specimens. Analysis of the stress-strain curves suggests that loose sands get stronger with strain (because of an increase in density) and approach a given strength. The data suggest that the strength of a dense specimen of the same sand peaks at low strains where interlocking of grains is maximum and then decreases and approaches the same limiting level of strength as for the loose sands. The strength of dense sands decreases toward the limiting level and the strength of loose sands increases toward the limiting level. The strength of a soil at large strains, where neither volume nor strength is changing with strain, is termed the *ultimate strength.*

### 3.6.6 Triaxial Shear Testing of Saturated Clays

#### *Triaxial Compression Tests on Normally Consolidated Specimens*

*Drained Tests.* Drained (*S*-type) triaxial compression tests on saturated specimens are performed in the same manner in which they are performed for

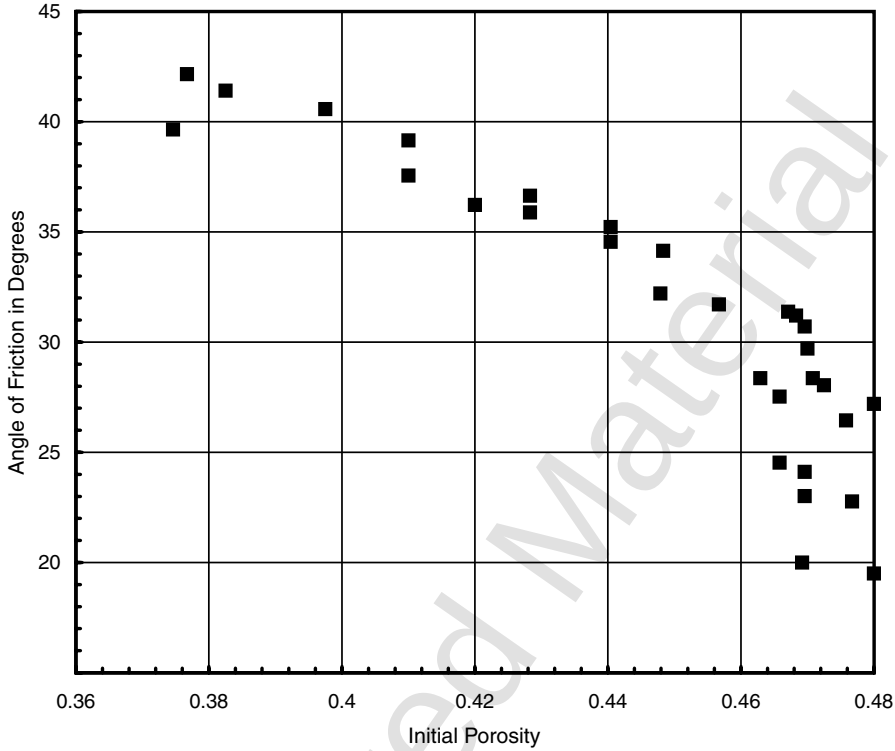


**Figure 3.41** Angle of friction versus initial porosity for fine sand (from Bjerrum et al., 1961).

sand, with the allowance of greater durations of time that allow adequate dissipation of the excess porewater pressures generated during shear. For tests performed using a constant rate of deformation, the time to failure may vary from a minimum of about 6 hours to over 6 months, depending on the coefficient of permeability of the clay.

The type of Mohr-Coulomb diagram obtained from such tests is shown in Figure 3.43. Normally consolidated clays are consolidated from dilute suspensions that have essentially zero shear strength. Hence, the application of a very small confining pressure results in the development of a very small strength, and the failure envelope passes through the origin. The slope of the failure envelope is denoted by $\phi'_S$—the effective stress angle of internal friction determined using *S*-type tests.

The curves for compressive stress–axial strain and for volumetric strain–axial strain for drained tests on specimens of saturated, normally consolidated clay are similar to the curves for sand shown in Figure 3.39, except that the specimens of clay may undergo volume decreases of more than 10% during shear. The decrease in volume during shear means that the relatively loose soil structure is breaking down under the action of shearing deformation.

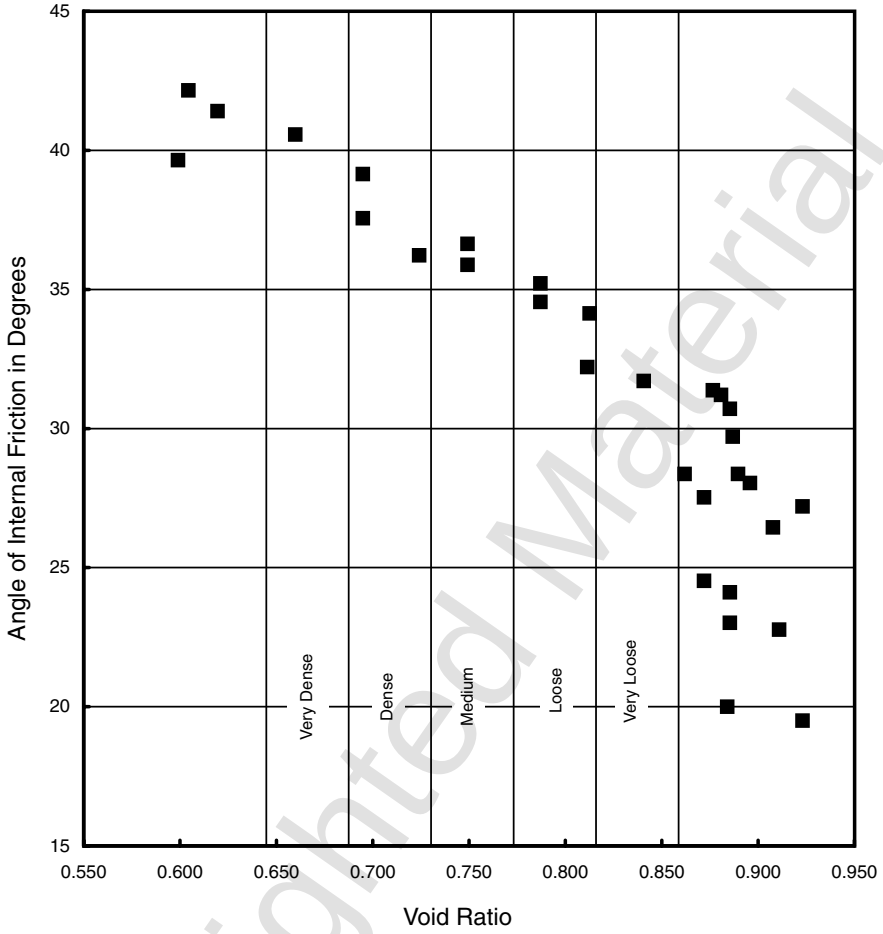


**Figure 3.42** Angle of friction versus initial void ratio for fine sand (from Bjerrum et al., 1961).

*Unconsolidated-Undrained Tests, $\phi = 0$ Case.* If a saturated specimen of soil is subjected to a change in hydrostatic total stress under undrained conditions, such as by increasing the pressure in a triaxial cell without allowing the specimen to drain, the porewater pressure changes by an amount equal to the change in hydrostatic pressure. Direct observations of this behavior are possible. A soil specimen is assumed to be taken from the field and placed in a triaxial cell. An initial cell pressure in the specimen is measured. The difference between the cell pressure and the porewater pressure is the effective stress. If the cell pressure is increased, the porewater pressure will increase by an equal amount, and no change in effective stress will occur if both the specimen and the measuring system are saturated. Thus, according to the

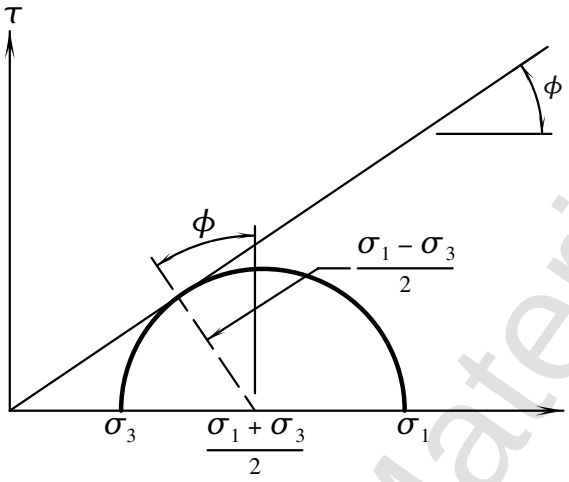


$$\sin \phi = \frac{\sigma_1 - \sigma_3}{\sigma_1 + \sigma_3}$$

$$\frac{\sigma_1}{\sigma_3} = \frac{1 + \sin \phi}{1 - \sin \phi} = \tan^2\left(45° + \frac{\phi}{2}\right)$$

**Figure 3.43** Mohr's circles for *S*-tests.

principal of effective stress, no change in shearing strength is possible. The confining pressure in the triaxial cell, therefore, has no effect on the shearing strength of the soil. A total stress failure diagram for a saturated soil is shown in Figure 3.44. The dashed circle is the Mohr's circle for effective stress at failure. The circles shown with solid lines are the total stress circles of stress. The shear strength is independent of the cell pressure, all these circles of stress have the same diameter, and the tangent to the failure envelope is horizontal; thus, $\phi = 0$. Actual experimental data have been published for both sands and clays showing that the angle of internal friction is zero experimentally as well as theoretically (Bishop and Eldin, 1950).

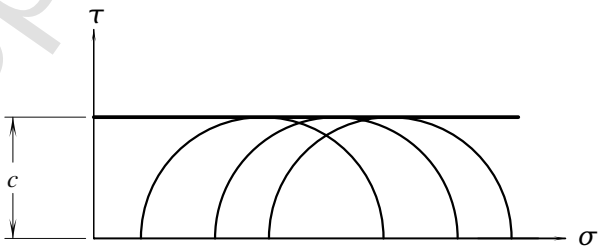


**Figure 3.44** Failure diagram for *UU*-tests on saturated soil.

If an undisturbed sample of a saturated soil can be obtained, the strength of the soil in situ can be obtained by performing a *Q*-type triaxial test. If the test specimen remains saturated under zero gage pressure, the shear strength of the soil may be measured using an unconfined compression test because the diameter of the circle of stress passing through the origin is the same as the diameter of all other circles of stress. Thus, the $\phi = 0$ concept is the justification for using unconfined compression tests to measure the shear strength of a sample of saturated clay. The unconfined compression test is justified only if the samples remain saturated.

In practice, samples of soil often become slightly unsaturated under conditions of zero total stress and are subject to some sampling disturbance. Both factors cause a loss of strength that cannot be estimated without more detailed investigations.

*Consolidated-Undrained* (R-*Type*) *Tests.* For consolidated-undrained (*R*-type) triaxial compression tests on samples of saturated clay, the testing procedure differs, depending on whether or not porewater pressures are to be measured. If porewater pressures are not measured, the specimen is consolidated under the desired initial state of stress, the drainage connections are closed, and the specimen is sheared to failure over a time period that varies from a few minutes to perhaps half an hour. The time to failure varies, depending on whether or not complete stress-strain data are recorded.

If porewater pressures are to be measured, it is absolutely necessary that the porewater pressure connections be saturated and free of air bubbles. The presence of a small amount of free air in the drainage lines or fittings will usually have a negligible effect on shearing strength but will cause the measured porewater pressure to be considerably smaller than the actual porewater pressure in the specimen. Two approaches are used in practice to saturate the drainage system. The preferred method is to consolidate the specimen first, then simultaneously increase the confining pressure and porewater back pressure by the same amount. No change in effective confining stress and no change in strength ($\phi = 0$ condition) occur because the porewater pressure and cell pressure are increased by the same amount.

The second method used is to apply back pressure to the specimen first under a low effective confining stress, usually around 1 psi, then consolidate the specimen to the final effective confining pressure under the back pressure. The two methods work equally well for saturated clays of low plasticity. The first method usually requires back pressures in the range of 20 to 40 psi and works best on specimens that are initially partly saturated and on clays of high plasticity that are expansive. The second method may require back pressures of up to 100 psi to be effective in saturating the test specimen. In no case does the second method work better than the first method for common geotechnical applications. The increased pressure in the porewater pressure system dissolves any air bubbles that might be present and ensures saturation. When the system is properly saturated, the application of an increment of

hydrostatic cell pressure results in the immediate development of an equal porewater pressure. Thus, the measurement of the excess porewater pressure resulting from an increment of cell pressure is a sensitive check on whether the specimen and the measuring system are properly saturated.

After ensuring that the specimen and the system are saturated, the specimen is loaded to failure with simultaneous measurements of the porewater pressure. The time to failure varies from about an hour for pervious clays to over a month for relatively impervious clays. The steps in the three-stage *R*-test are depicted in Figure 3.45, where additional symbols have been used to clarify the stresses. In Stage 1, the specimen is consolidated under a hydrostatic stress ($\sigma_{3c}$), the excess porewater pressure is zero, and the initial effective stress is $\sigma'_{3i}$. In Stage 2, an increment of hydrostatic pressure ($\Delta\sigma_3$) is applied, and if the specimen is saturated, the porewater pressure increases by the same amount. In Stage 3, the specimen is subjected to a compressive stress ($\sigma_1 - \sigma_3$) and an additional increment of porewater pressure ($u_2$) is generated. The resulting state of stress is found by adding the stresses from Stages 1, 2, and 3.

The three-stage *R*-test depicted in Figure 3.45 is the most common type of *R*-test, but several modifications are possible. For example, initial consolidation may be performed under conditions of no lateral deformation to approximate in situ conditions. During the consolidation stage of such a test, axial and volumetric strains are measured. Lateral strain is zero when the volumetric strain and axial strain are equal, so a stress difference is applied during consolidation that is just sufficient to produce zero lateral strain. The common assumption is that such specimens are consolidated under $K_0$ conditions.

As an example, a specimen is consolidated to 500 psf ($\sigma_{3c}$) during Stage 1, subjected to an increase of cell pressure and porewater pressure of $\sigma_3 = \Delta u = u_1 = 600$ psf (Stage 2), and then subjected to a stress difference of

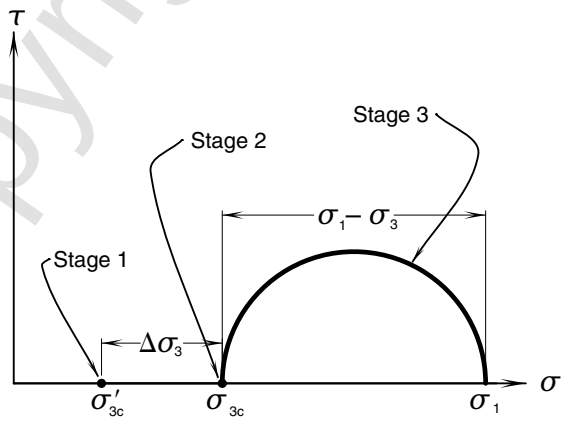


**Figure 3.45** States of stress during the *R*-test.

($\sigma_1 - \sigma_3$) of 200 psf that generates a porewater pressure ($u_2$) of 150 psf (Stage 3). The resulting stresses are

$\sigma_1 - \sigma_3 = 200$ psf
$u = 600 + 150 = 750$ psf
$\sigma_3 = 500 + 600 = 1100$ psf
$\sigma_3' = 1100 - 750 = 350$ psf
$\sigma_1' = 350 + 200 = 550$ psf

In another modification, either the lateral stress is increased with a constant axial stress until failure occurs or the lateral stress is maintained constant and the axial stress is decreased until failure occurs. Such tests are called *extension tests*. All stresses must be compressive in an extension test. An extension test is not a tensile test, it is a compressive test, with the lateral stress exceeding the axial stress.

For normally consolidated clay, the tendency of the soil structure to break down during shear leads to a transfer of part of the effective stress to the porewater; thus, positive porewater pressures are developed. A typical stress-strain curve for an *R*-type test is shown in Figure 3.46. The strain at the peak stress difference (often defined as the point of failure) may vary from less than 1% to 20%.

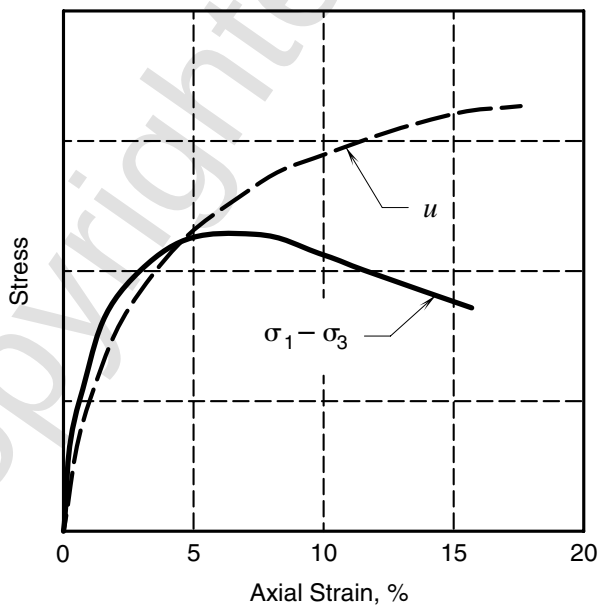


**Figure 3.46** Stress-strain curve for the *R*-test with positive pore water pressure.

A comparison of the stress-strain properties of clays under drained and undrained conditions is of interest. Under drained conditions, the soil structure is broken down during shear and the volume decreases, that is, the density increases during shear. The continuously decreasing volume (increasing density) causes the soil to gain strength as it is deformed. Thus, the soil may be considered a strain-hardening material under these conditions of drainage. Eventually, the applied stress exceeds the strength and the specimen fails. The large strains at failure result from the continuous increase of strain.

In an undrained test on a normally consolidated specimen, the total confining pressure is constant. Thus, the continuously increasing porewater pressure (Figure 3.46) causes a reduction of the effective confining pressure ($\sigma_3'$). The strength of the soil is controlled by the effective stress, not the total stress; thus, continuous reduction in effective confining pressure causes the soil to lose strength as shearing deformations are applied. Hence, the soil in an undrained test is strain weakening, and the strains at failure (at peak stress difference) are considerably smaller than those obtained from drained tests on initially identical specimens (this argument is restricted to specimens that decrease in volume during drained shear and have positive porewater pressures during undrained shear, which is generally true for normally or lightly overconsolidated clays).

Mohr-Coulomb failure envelopes cannot be plotted in terms of total stresses because the strength is not a function of the state of total stress (see the discussion of *Q*-type tests). Failure envelopes may be plotted in terms of effective stresses at failure or, for tests in which porewater pressures are not measured, in terms of the consolidation pressure. In the first case, $\sigma_1'$ and $\sigma_3'$ are calculated at failure, and the failure circle is plotted in a Mohr-Coulomb diagram like that shown in Figure 3.47. The effective stress failure envelope usually passes through the origin for normally consolidated clays.

For many field problems, it is not possible to determine the change in porewater pressure in situ during loading. Thus, it may be expedient to assume that the porewater pressures generated in situ are equal to those generated in an undisturbed specimen of soil during laboratory shear testing. Applying this assumption, it is unnecessary to measure porewater pressures in the laboratory, thus substantially reducing the cost of laboratory tests. The Mohr-Coulomb diagram is then plotted using $\sigma_3 = \sigma_{3i}'$ and $\sigma_1 = \sigma_{3i}' + (\sigma_1 - \sigma_3)_{\max}$. This circle is a total-stress circle if the cell pressure is not increased after final consolidation (to check saturation). If the cell pressure is increased after consolidation, then the circle is not a total-stress circle. No problem will develop if $\sigma_3$ is always taken as $\sigma_{3i}'$, where $\sigma_{3i}'$ is the minor principal effective stress at the moment that shearing begins. The slope of the failure envelope expressed in terms of $\sigma_{3i}'$ is designated as $\phi_R$.

As typical calculations, a specimen is assumed to be consolidated under a stress $\sigma_{3c} = 1000$ psf, the cell pressure is increased by 750 psf with a simultaneous increase of porewater pressure of 750 psf, and, at failure, ($\sigma_1 -$

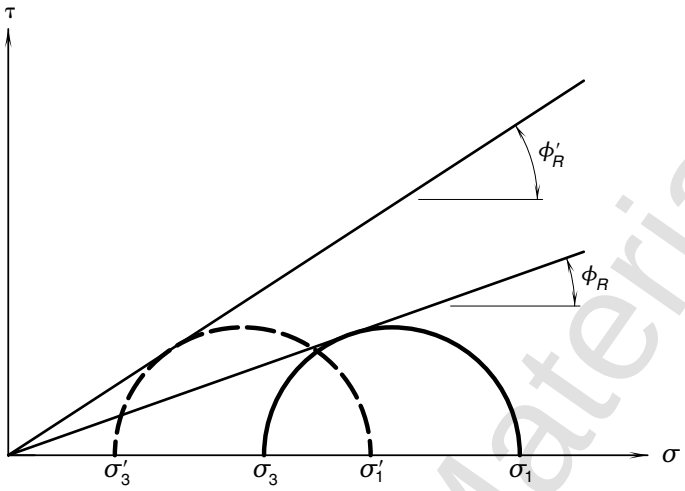


**Figure 3.47** Effective stress failure envelope for the *R*-test.

$\sigma_3$) = 600 psf and $u_2$ = 700 psf. The computation of $\phi'_R$ and $\phi_R$ is shown below.

$\sigma_1 = 1000 + 600 = 1600$ psf
$\sigma'_3 = 1000 - 700 = 300$ psf
$\sigma'_1 = 300 + 600 = 900$ psf

Applying $\sigma_1 = \sigma_3 \tan^2(45° + \phi'/2) = \sigma_3 = 1 + \sin\phi'/1 - \sin\phi'$

$\tan^2 (45 + \phi_R/2) = 1600/1000 = 1.60$
$\phi_R = 13.3°$
$\tan^2(45 + \phi'_R/2) = 900/300 = 3.00$
$\phi'_R = 30.0°$

Whether the failure envelopes are defined in terms of the initial effective stress or the effective stress at failure, the diameter of Mohr's circle is the same. The horizontal distance between the two circles for a single test is equal to the porewater pressure ($u_2$) generated during shear.

The ratio between the slopes of the envelopes defined in terms of initial effective stress and effective stress at failure can be obtained by solving for sin $\phi$ and sin $\phi'$, dividing one equation by the other, and substituting $A(\sigma_1 - \sigma_3)$ for $u_2$, where $A$ is an experimentally determined parameter. Solving for sin $\phi'$,

$$\sin \phi' = \frac{\sin \phi}{1 - 2A \sin \phi} \tag{3.94}$$

If the $A$-coefficient has a value of 1, then the $R'$-envelope has a slope about two times the slope of the $R$-envelope for the range in $\phi$ usually encountered.

Attempts to correlate the effective-stress angle of internal friction with one of the index parameters have not been successful. The relationship between $\phi'$ and the plasticity index is suggested by the points plotted in Figure 3.48. Most soils represented in this diagram are from Norway because much of the available knowledge about the shearing properties of undisturbed clay has come from the Norwegian Geotechnical Institute in Oslo. Apparently most of these soils have effective-stress angles of internal friction between about 23° and 36°. Correlations between the effective-stress angle of internal friction of undisturbed clay and any of the common index properties are not likely to be very satisfactory because the index properties are determined using completely remolded soil. Any structural effects in the soil or effects related to natural cementation would influence the undisturbed properties but not the index properties. Further, there are serious difficulties associated with the measurement of porewater pressures in clays of low permeability, and these difficulties influence the evaluation of $\phi'$. Errors associated with sampling

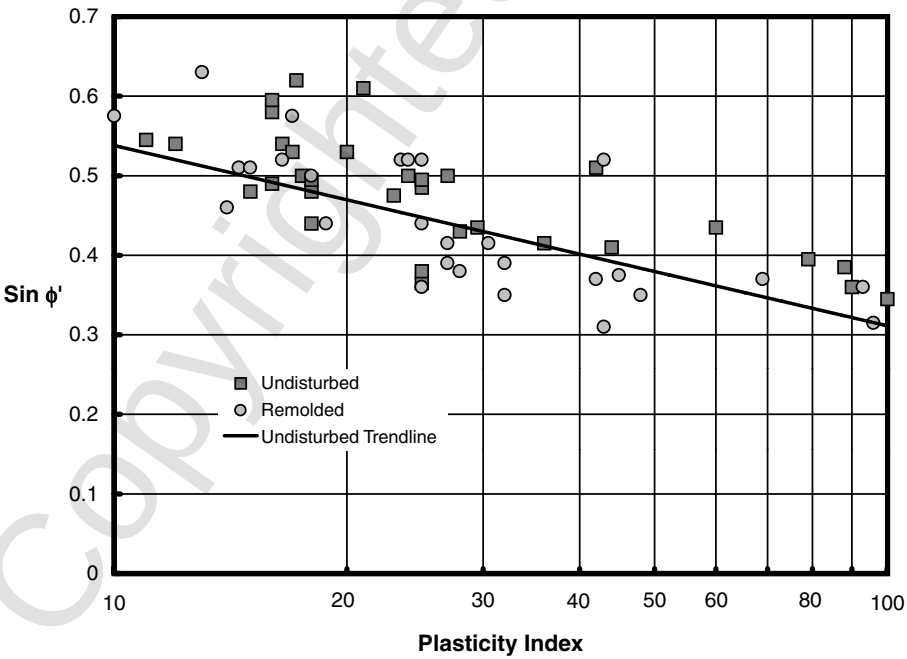


**Figure 3.48** Angle of friction versus plasticity index (from Kenney, 1959).

disturbance, nonuniform stress and strain conditions in the triaxial cell, and other experimental problems also influence the results of these shear tests. Investigations into the shearing characteristics of undisturbed cohesive soils are in progress, but the problems are so complex that a simple solution of the problem is unlikely.

*Drained versus Undrained Values of $\phi'$.* In performing drained triaxial compression tests, there is little ambiguity regarding the method of defining failure; the several failure criteria maximize at the same point. For undrained tests, however, the two common failure criteria of peak $(\sigma_1 - \sigma_3)$ and peak $(\sigma_1'/\sigma_3')$ result in a higher value of $\phi'$. Available data suggest that the effective stress angles of internal friction of drained $(\phi_S')$ and undrained $(\phi_R')$ soil samples correlate better when the peak $(\sigma_1'/\sigma_3')$ failure criterion is used with the undrained tests. Field data are insufficient to judge which failure criterion correlates best with field conditions.

*$c/p$ Ratios.* The previous discussion of the shearing properties of normally consolidated, saturated clay has described how the shear strength of the soil increases linearly with the logarithm of consolidation pressure. In a normally consolidated soil deposit, the consolidation pressure increases almost linearly with depth. Thus, the shear strength of the soil will also increase almost linearly with depth.

Early investigations of the increase of shear strength with depth were based on unconfined compression tests or $Q$-type triaxial tests. The soils studied were saturated in all cases, causing $\phi = 0$. If the strength of the soil increased linearly with overburden pressure in the field, then the shear strength profile versus depth could be defined with a single parameter, $c/p$. The strength $c$ is actually the undrained shear strength, and $p$ is the vertical effective overburden pressure. Occasionally, the notation $s_u/\sigma_v'$ is used in place of $c/p$.

Early studies of the variation of strength with depth, using the unconfined compression test, were complicated by the problem of sampling disturbance. Disturbance of the soil samples during sampling operations and transport to the laboratory resulted in a decrease in the strength of the samples, and laboratory strength values were significantly less than field strength values. To avoid the problem of sampling disturbance, attempts were made to develop techniques for measuring the strength of the soil in situ under undrained conditions. Probably the most common way of measuring in situ strength is to use the field vane device, of which is shown in Figure 3.49. The vane is made of two thin steel fins set at right angles to each other and attached to a thin rod. The vane is pressed into the soil to the desired depth, and then a torque is applied to the rod to rotate the vane about its vertical axis. The soil fails on a vertical cylindrical surface. The area of this surface is calculated from the dimensions of the vane. Knowledge of the torque required to cause failure, the area of the failure surface, and the radius of the vane makes it possible to calculate the undrained shear strength. The variation of undrained

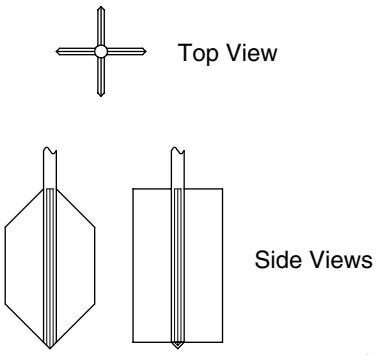


**Figure 3.49** Field vane apparatus.

shear strength with depth for a uniform deposit of clay in Drammen, Norway, is shown in Figure 3.50, where the undrained shear strength is shown to increase linearly with depth for depths greater than about 7 m. For shallower depths, the soil has been desiccated and has thus been strengthened. The remolded strengths plotted in Figure 3.50 were obtained by rotating the vane several times and then measuring the strength again.

In the early investigations, the vane strength was always greater than the strength determined using unconfined compression tests because all samples taken into the laboratory were disturbed by the sampling operation. As specialized sampling techniques were developed, the laboratory strengths became higher (due to less disturbance); recent studies have shown that the laboratory strengths exceed the vane strengths. As a result of variations of soil properties with depth, it is difficult to make accurate comparisons of vane and unconfined compression strengths, but one recent study suggested that the unconfined compression tests yielded strengths about 30% higher than the vane strengths. The cause of this discrepancy is not fully understood, but part of it may result from the vane device measuring shear strength on vertical planes (the area of the end of the vane is small), the high rate of shearing in the zone of failure, and the degree of plasticity of the soil. The normal effective stress on a vertical plane is $K_0$ times the normal effective stress on the horizontal plane, where $K_0$ is termed the *coefficient of earth pressure at rest* and typically has a value of about 0.5 for a normally consolidated clay. If the strength is a function of the normal effective stress, then the vane strength should be lower than the strength on diagonal planes as measured using the unconfined compression apparatus.

In situ shear strengths may also be determined by pushing a cone down into the soil and measuring the resistance. Most of the research had been done for the Dutch cone penetrometer. Beginning in the early 1980s, pore pressure measuring equipment was added to Dutch cone equipment and was used to identify changes in stratigraphy in the soil profile. The cone penetrometer test

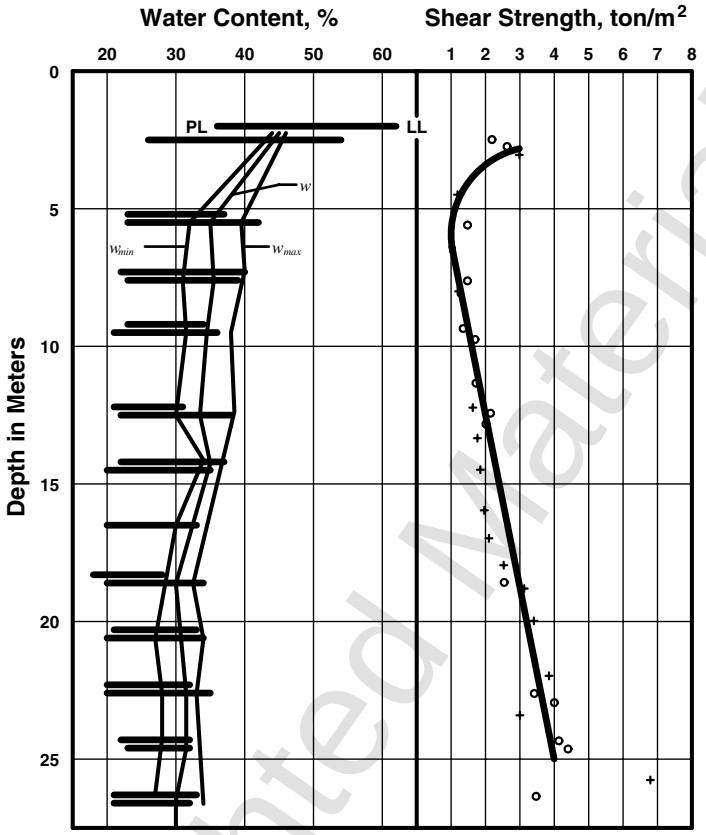


**Figure 3.50** Strength profile from Drammen, Norway.

is favorable in that each cone sounding is a model pile load test. However, the use of shear strengths determined from cone soundings for other applications, such as slope stability, should be done with caution.

The $c/p$ ratio has proved to be a useful parameter in foundation engineering in areas where deep deposits of soft clays are encountered. Correlations between the $c/p$ ratio of normally consolidated soils and the plasticity index have been developed (Figure 3.51). Additional research has established the relationship between $c/p$ ratio and overconsolidation ratio for a variety of soils (Figure 3.52).

Use of the $c/p$ ratio for design purposes was formalized by Ladd and Foott (1974) in the SHANSEP (Stress History And Normalized Soil Engineering Properties) method. This method is a synthesis of the observations and methods of several researchers into a relatively straightforward approach that can be used if one has the benefit of a complete field investigation and high-

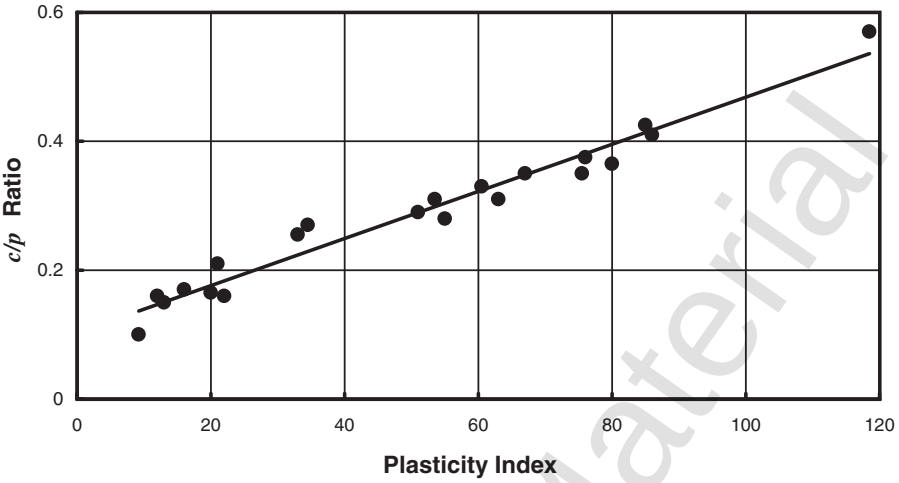


**Figure 3.51** The $c/p$ ratio versus the plasticity index.

quality laboratory tests. The difficulty in using the SHANSEP method is in establishing the stress history, consolidation characteristics, and overconsolidation ratio of the soil. The SHANSEP method is expensive, but its use can be justified for large projects where the soil profile is relatively uniform over the site.

*Sensitivity.* The remolded strength is shown to be less than the undisturbed strength in Figure 3.51. A quantitative measure of the strength loss on remolding is the sensitivity, which is the ratio of the undisturbed strength to the remolded strength at the same void ratio. The symbol for this parameter is $S_t$. The classification of the sensitivity of clays, as proposed by Skempton and Northey (1952) and modified by Rosenqvist (1953), is shown in Table 3.5.

Bjerrum (1954) has reported sensitivities as high as 1000 in some of the Norwegian clays. Because the undisturbed strengths of the Norwegian clays are low, such high sensitivities mean that the remolded clays turn into viscous fluids. If such clays are disturbed in situ, landslides may result in which the clay flows away like a viscous fluid. Many landslides of this type have taken place in Norway, in Sweden, and along the St. Lawrence River Valley in Canada. Bjerrum (1954) has shown that the sensitivity of Norwegian clays can be correlated with the liquidity index (Figure 3.53). This correlation is useful because it warns the engineer to use special precautions with deposits where the natural water content is equal to the liquid limit or higher. Apparently, special sampling techniques are required when such soils are encountered. Otherwise, the shear strengths measured in the laboratory may be only a small fraction of the strengths in the field.

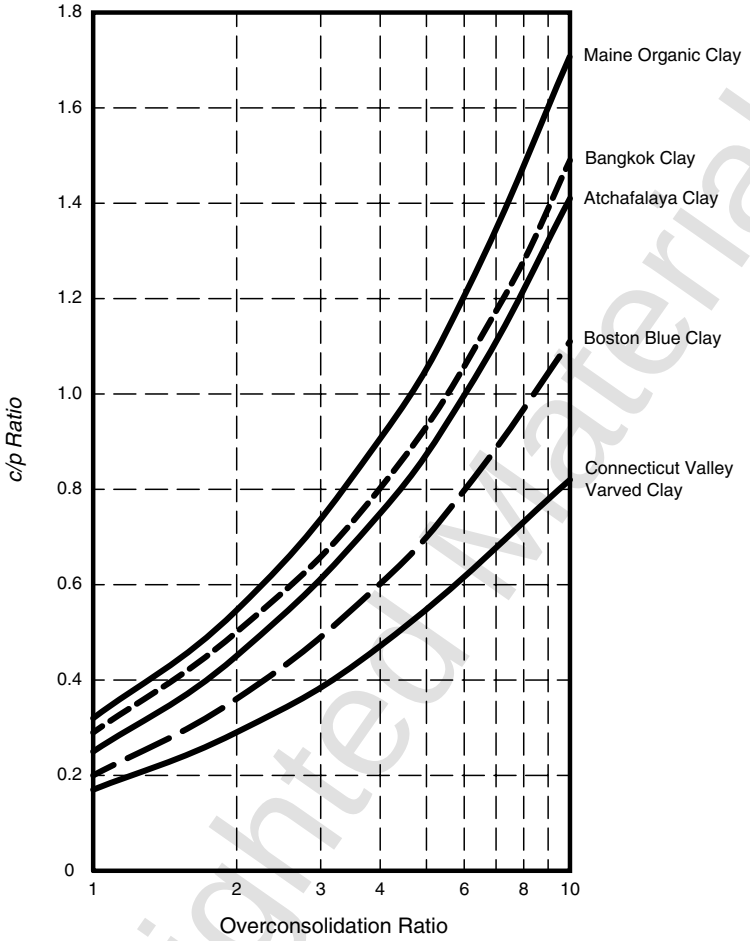


**Figure 3.52** The $c/p$ ratio versus the logarithm of the overconsolidation ratio (from Ladd and Foott, 1974).

**TABLE 3.5 Classification of Sensitivity**

| Sensitivity | Classification |
|---|---|
| 1 | Insensitive |
| 1–2 | Slightly sensitive |
| 2–4 | Medium sensitive |
| 4–8 | Very sensitive |
| 8–16 | Slightly quick |
| 16–32 | Medium quick |
| 32–64 | Very quick |
| 64–∞ | Extra quick |

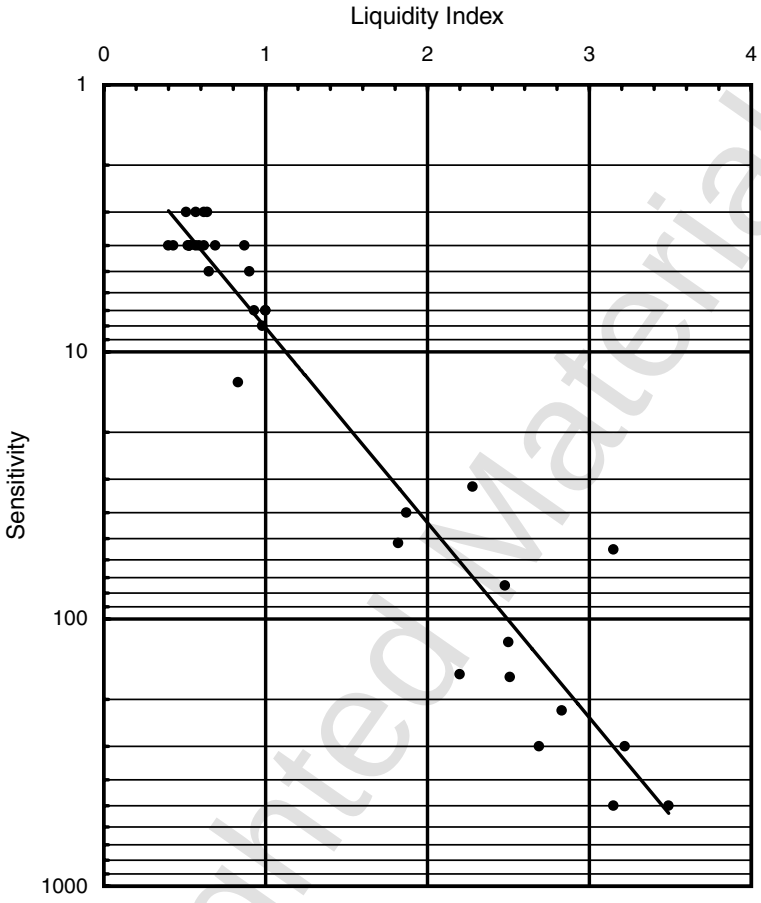


**Figure 3.53** Sensitivity of marine clay from Norway (from Bjerrum, 1954).

*Thixotropy.* If a series of identical specimens of clay are remolded and then allowed to rest at a constant void ratio for varying periods of time before shearing, the strength of the remolded clay will be found to increase with time. The strength increase with time is reversible; that is, a specimen can be allowed to "set up" for some period of time and then remolded again, and the remolded strength will be same as the strength when the soil was originally remolded. Thus, cyclically allowing the specimen to set up, remolding it, and then letting it set up again, will result in strength changes such as those shown in Figure 3.54.

Some of the experimental results obtained by Skempton and Northey (1952) in an early investigation of thixotropy are shown in Figure 3.55. These results are typical of those obtained when specimens are remolded at water contents near the liquid limit.

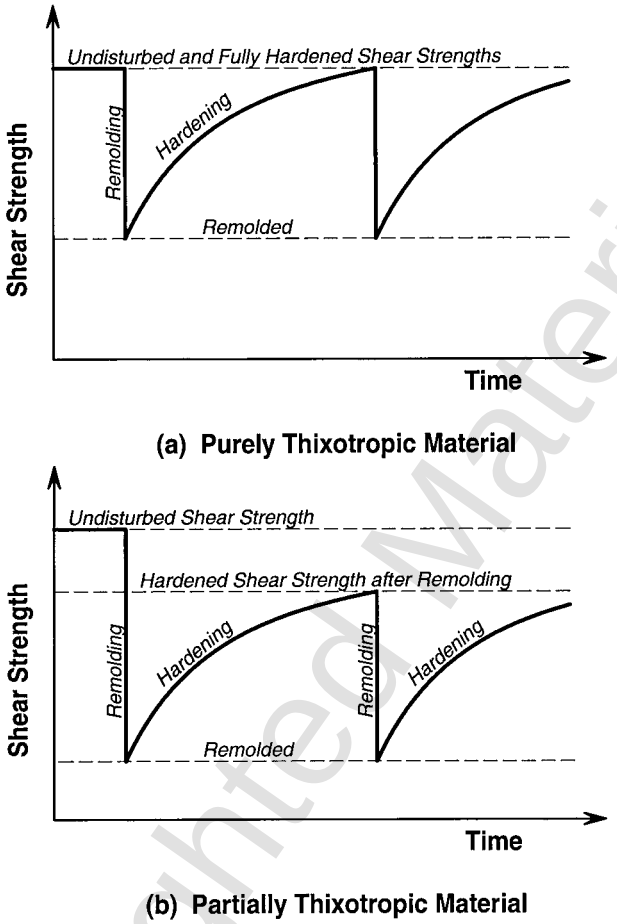


**Figure 3.54** Full and partial thixotropic regain (from Skempton and Northey, 1952).

Specimens remolded at low water contents usually have only a small thixotropic increase in strength. Clay suspensions often undergo thixotropic effects that are many times greater than the effects shown here.

Apparently, clay can develop sensitivity as a result of thixotropic strength increases. However, for quick clays, like those found in Norway, thixotropy accounts for only a small part of the total sensitivity.

*Relationship Between Shear Strength and Water Content for Normally Consolidated Clays.* As discussed previously, if a series of *R*-type triaxial compression tests are performed on identical specimens of clay that have been sedimented from suspensions and normally consolidated, the *R*-envelope is often nearly a straight line, which passes through the origin. In such a case, the shear strength of the soil can be shown to be a constant percentage of the consolidation pressure given by

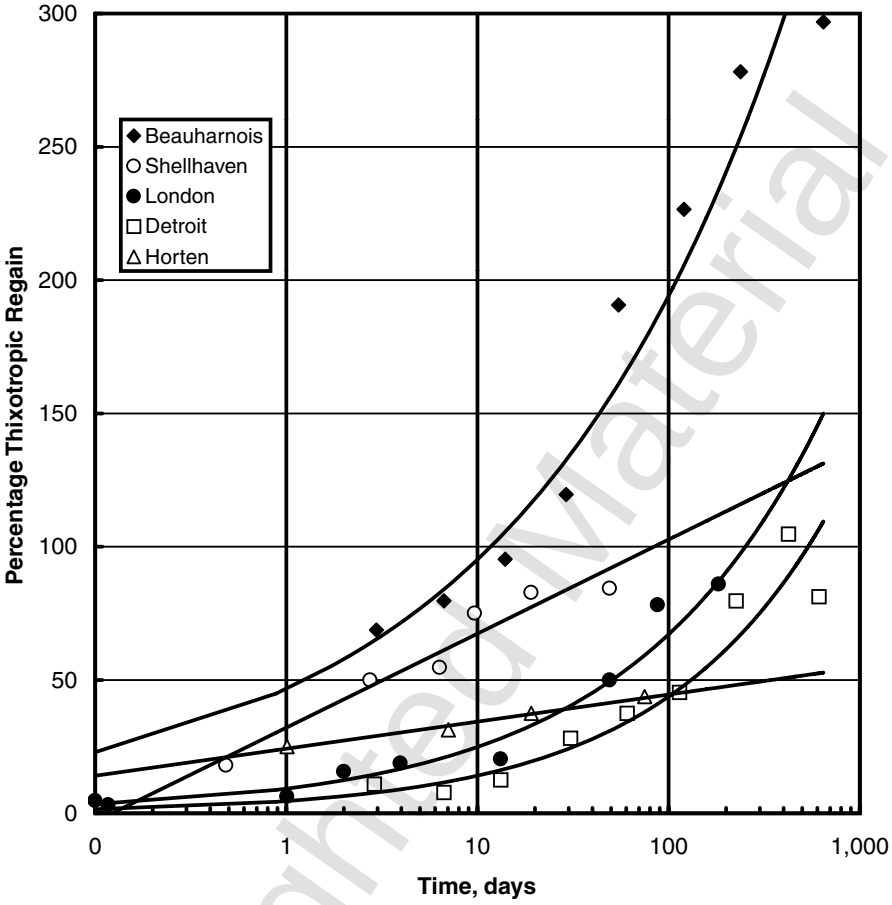


**Figure 3.55** Thixotropic regain in some typical clays (from Skempton and Northey, 1952).

$$\frac{\tau}{\sigma_{3c}} = \frac{\sin \phi_R \cos \phi_R}{1 - \sin \phi_R} \tag{3.95}$$

If the undrained shear strength and consolidation pressure are both plotted against water content (for saturated clay only; if clay is not saturated, use the void ratio), the two curves will be parallel. One such relationship is shown in Figure 3.55. If a specimen is consolidated to Point *a* and subjected to undrained shearing, the strength is given by Point *b*.

The type of relationship shown in Figure 3.55 is useful for many practical problems. The slope of the virgin consolidation curve can be obtained from one-dimensional consolidation tests. If the shear strength of the samples is determined using either unconfined compression tests or *Q*-type triaxial tests, the data can often be conveniently plotted on a diagram such as the one shown

in Figure 3.55. The assumption is made, for example, that 50 unconfined compression tests are performed on samples from a particular stratum. Plotting 50 Mohr's circles for the 50 unconfined compression tests on a Mohr-Coulomb diagram would produce an indecipherable tangle of lines, all passing though the origin, and meaningful interpretation of the data would probably not be possible. Alternatively, 50 values of unconfined compressive strength could be plotted versus water content in a diagram similar to Figure 3.55, and meaningful results might be obtained. The strengths could also be plotted versus depth (see Figure 3.50). The geotechnical engineer usually tries several methods of plotting the data and chooses the method that yields the most meaningful results for the particular problem under investigation.

If the sensitivity of the clay is independent of the consolidation pressure within the range of consolidation pressures encountered at the site, then the curve of remolded strength versus water content will have the same slope as the virgin curve and undisturbed strength curve. However, the sensitivity usually decreases as the consolidation pressure increases, so the remolded-strength curve is expected to be slightly flatter than the other two curves. If the undisturbed and remolded strength curves can be defined accurately, then the degree of disturbance of partially disturbed samples can be defined in terms of the relative position of the strength of the partially disturbed sample with respect to the curves of undisturbed and remolded strength.

***Overconsolidated Saturated Clays*** The previous discussion of clays applies to normally consolidated clays. In nature, most soil deposits vary from slightly to heavily overconsolidated. Lightly overconsolidated sediments are usually treated as if they were normally consolidated. However, the properties of heavily overconsolidated clays are quite different from those of normally consolidated clays, and engineering problems of a different nature are encountered.

*Stress-Strain Properties and Pore Water Pressures.* In the same way that the properties of normally consolidated clays are comparable to those of loose sands, the properties of overconsolidated clays are comparable to those of dense sands. If a specimen of clay is consolidated under a high pressure and then allowed to swell under a much lower pressure, the clay will be considerably more dense than a normally consolidated specimen at the same final consolidation pressure; that is, a specimen consolidated to 1000 psi and then allowed to swell under 10 psi is far denser than a normally consolidated specimen at 10 psi. As a result of its more dense structure, heavily overconsolidated clay tends to expand in volume (i.e., dilate) during shear in a manner similar to that of dense sand during shear. Figure 3.56a shows the results of a drained triaxial compression test on a specimen of kaolinite that had been sedimented from a dilute suspension, consolidated to 120 psi, and then rebounded to 10 psi before shear. Just like the dense sands, the soil appears to decrease in volume at small strains and then to expand throughout the re-

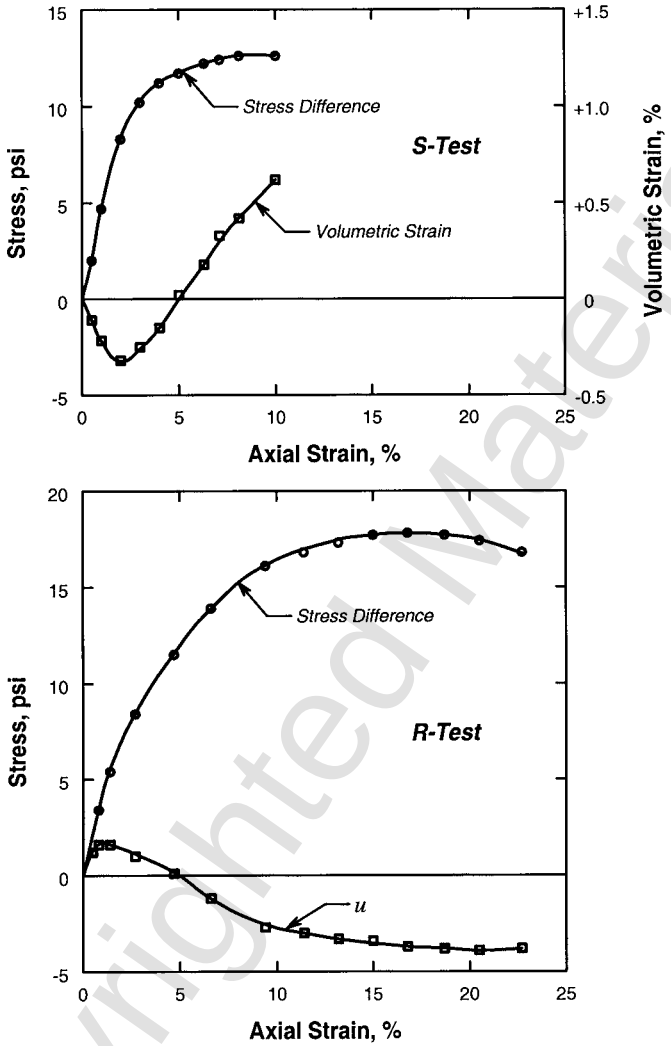


**Figure 3.56** Stress-strain curves for overconsolidated kaolinite (from Olson, 1974).

mainder of the test. As for dense sands, the first application of compressive stress results in a small densification, and larger shearing deformations cause the particles to ride up over each other and the specimen to dilate.

The stress-strain curves for an identical specimen of kaolinite are shown in Figure 3.56b. This specimen was consolidated to 120 psi, rebounded to 10 psi, and then sheared under undrained conditions with pore pressure measurements. In the early part of the stress-strain curve where the soil tends to compress, the porewater pressures are positive but they become negative when the soil tends to expand. Comparison of the failure strains for the two spec-

imens is of interest. In the drained test, the expansion of the soil has a weakening effect because water is drawn into the specimen. Thus, the greater the strain, the weaker the specimen. Failure occurs at about 10% strain. In the undrained test, the development of porewater pressures has a strengthening effect due to an increase in the effective confining pressure, and the specimen became stronger as strain increases. Thus, failure occurs at a strain of 18%, 8% above the strain at which the specimen fails during drained shear.

In considering the effect of overconsolidation on the properties of clays, having a parameter that expresses the degree to which a specimen has been overconsolidated is convenient. For this purpose, the *overconsolidation ratio* (OCR) is defined as the ratio of the maximum consolidation pressure to which a specimen has been subjected to the consolidation pressure just before shear. Thus, the overconsolidation ratio of the specimens is $120/10 = 12$.

The assignment of parameters to the porewater pressures is also convenient. For this purpose, it is convenient to use Skempton's (1954) equation, which describes the changes in porewater pressure due to changes in the state of stress:

$$u = B[\Delta\sigma_3 + A(\Delta\sigma_1 - \Delta\sigma_3)] \tag{3.96}$$

where

$u$ = porewater pressure resulting from the application of stresses,
$\Delta\sigma_1$ = change in major principal total stress,
$\Delta\sigma_3$ = change in minor principal total stress,
$A$ = $A$-coefficient, and
$B$ = $B$-coefficient.

If a saturated specimen of clay is subjected to a change in hydrostatic stress, then the porewater pressure changes by $B$ times the change in hydrostatic stress. However, it has already been concluded that the change in porewater pressure is equal to the change in hydrostatic pressure if the soil is saturated, and that the compressibility of the water is much less than that of the soil structure; thus, $B = 1$ for a saturated clay.

The $A$-coefficient expresses the influence of shearing stress on the porewater pressure. The $A$-coefficient at the point of failure is defined as $A_f$. The range in values of $A_f$ for typical clays as a function of the OCR is shown in Figure 3.57. For normally consolidated clays, $A_f$ is usually between 0.7 and 1.5, with the higher values found for the more sensitive clays.

In Figure 3.58, $\sigma'$ indicates that Mohr's circle is plotted in terms of effective stress at failure, and $\sigma$ indicates that the circle is plotted with $\sigma_3 = \sigma_{3i}$; the first case is used for $R'$-envelopes and the second for $R$-envelopes. The positions of the $R'$-circles for various values of $A_f$ are shown. Because both the $R$- and $R'$-envelopes have positive slopes, the $R'$-envelope will be above

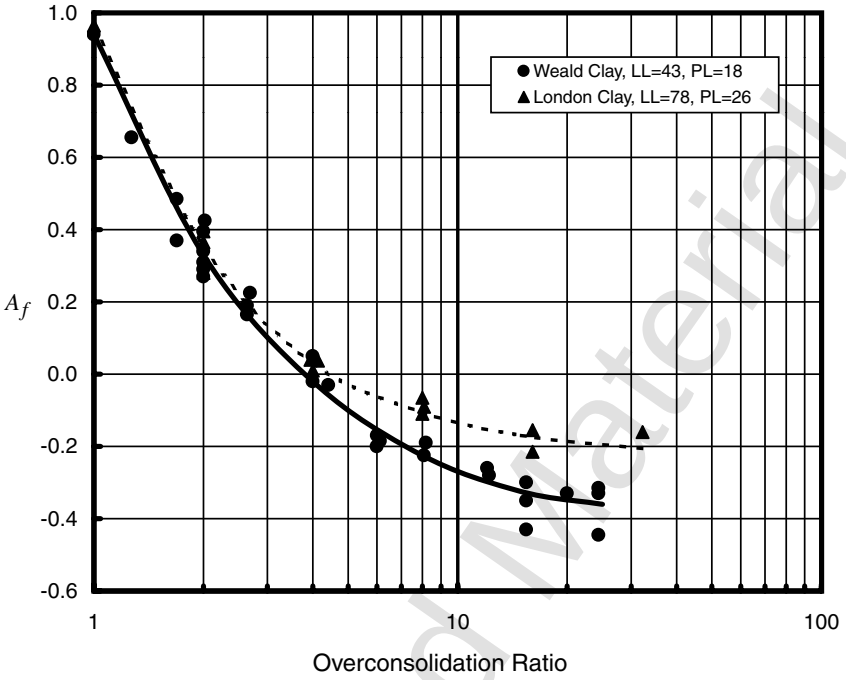


**Figure 3.57** Variation in $A_f$ with OCR for weald clay (from Henkel, 1956).

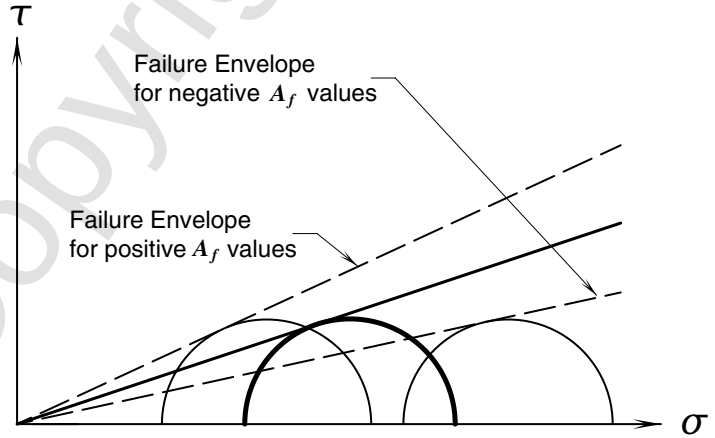


**Figure 3.58** Mohr's circles for *R*-bar triaxial tests.

the $R$-envelope when $A_f$ is significantly greater than zero and will be below the $R$-envelope when the $A_f$-coefficient is zero or negative.

At this stage of the discussion, a rather bothersome problem arises in plotting the Mohr-Coulomb diagrams. When only the results of normally consolidated tests or overconsolidated tests are plotted on a single failure diagram, there is not much difficulty in distinguishing the circles, though even in these cases, it is difficult to determine visually the scatter of the circles from the failure envelope if more than about 10 circles are plotted on a single diagram. However, when circles representing tests on both normally consolidated and overconsolidated specimens are plotted on the same diagram, or when $R'$- and $S$-circles are plotted together, or when many circles are plotted, the diagram becomes a maze of lines and rational interpretation is very difficult. Hence, it is now convenient to define a *modified Mohr-Coulomb diagram* where this problem will be eliminated.

A Mohr's circle tangent to a failure envelope is shown in Figure 3.59. The relationship between the principal stresses derived from the geometry of the circle and the failure envelope are

$$\cos \phi = \frac{\frac{1}{2}(\sigma_1 - \sigma_3)}{\frac{1}{2}(\sigma_1 + \sigma_3)\tan \phi + c}$$

Rearranging,

$$\frac{1}{2}(\sigma_1 - \sigma_3) = c \cos \phi + \frac{1}{2}(\sigma_1 + \sigma_3)\sin \phi \tag{3.97}$$

If, instead of plotting Mohr's circles on a diagram of $\tau$ versus $\sigma$, points are plotted on a plot of $\frac{1}{2}(\sigma_1 - \sigma_3)$ versus $\frac{1}{2}(\sigma_1 + \sigma_3)$, then a failure envelope

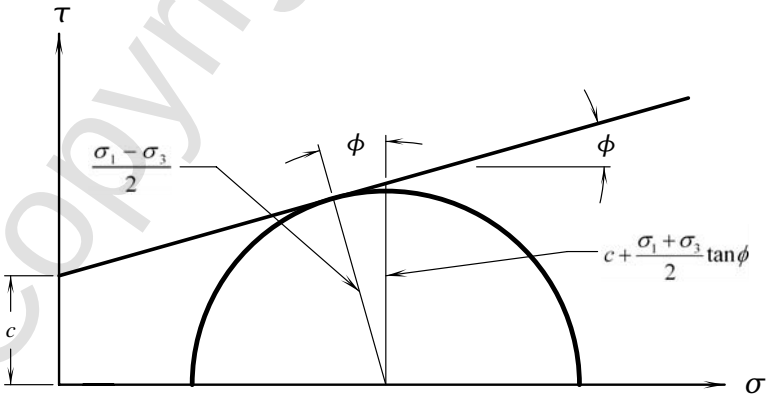


**Figure 3.59** Geometry of Mohr's circle.

is obtained with an intercept equal to $c\cos(\phi)$ and a slope equal to $\sin(\phi)$. If the intercept is designated as $d$ and the slope as $\psi$, Eq. 3.97 would be written in the form

$$\tfrac{1}{2}(\sigma_1 - \sigma_3) = d + \tfrac{1}{2}(\sigma_1 + \sigma_3)\tan\psi \tag{3.98}$$

The standard Mohr-Coulomb shearing parameters are obtained from

$$\sin\phi = \tan\psi \tag{3.99}$$

$$c = \frac{d}{\cos\phi} \tag{3.100}$$

Probably the largest advantage of using a modified Mohr-Coulomb diagram is that each test is represented by a single point rather that a circle. Thus, different types of tests can be plotted on the same diagram and clearly differentiated from each other by using different symbols. Furthermore, when the envelopes are straight lines, linear regression analysis can easily be used to determine the parameters of the failure envelope best fitting the experimental points.

*Overconsolidation by Desiccation and Weathering.* The strength profile of a soil deposit in Norway reported by Moum and Rosenqvist (1957) is shown in Figure 3.60. The increased strength of the upper part of the deposit could not have resulted from consolidation under the existing overburden pressure or from any previous overburden pressure that was eroded away. The increased strength of the upper part of this deposit and of many deposits around the world is the result of desiccation (drying) and chemical alteration (weathering).

Desiccation causes a reduction in the void ratio of the soil. According to the principle of effective stress, the void ratio can be reduced only if the effective stress is increased. Because the total stress at any given depth near the surface is small, the reduction in void ratio and the increase in effective stress must result from the development of negative porewater pressures. In highly plastic clays, this negative porewater pressure would have to be more than 100,000 psf to explain the strength of desiccated crusts.

Strengthened crusts may also result from chemical changes brought on by weathering. These changes may involve simple cation exchange reactions, such as weathering of feldspar to release potassium, which then replaces the adsorbed sodium cations to convert the sodium clay to potassium clay. In other cases, weathering causes the precipitation of cement at the point of contact between the particles. Such cements are commonly calcium carbonate or ferric oxide.

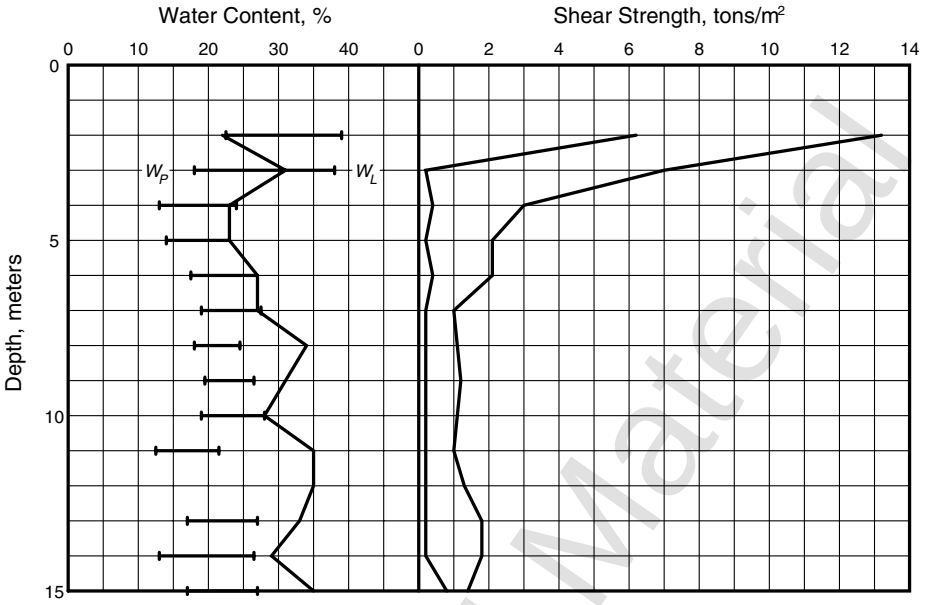


**Figure 3.60** Strength profile showing gain in shear strength due to desiccation (from Moum and Rosenqvist, 1957).

*Fissured Clays.* In a natural soil deposit, the soil may be consolidated under conditions of approximately zero lateral strain. In such a case, the lateral stress is equal to the vertical stress times $K_0$, the coefficient of earth pressure at rest, which may be about 0.5 for a normally consolidated soil. If an element of soil is buried so deeply that the overburden pressure is 1000 psi, then the lateral stress is about 500 psi. At this stage, the soil is normally consolidated. If erosion begins to remove the overburden, the vertical pressure is reduced and approaches zero as a limit. The lateral stress is also released, but does not reduce by as much as the overburden pressure. Thus, a stage is eventually reached where the lateral and vertical stresses are nearly equal. Further erosion may reduce the vertical stress to such a low level that the large lateral stresses can cause shearing deformations to occur. For example, if $\phi' = 30°$ and there is a zero cohesion intercept, the soil will undergo a shearing failure when the lateral stress ($\sigma_1'$) is three times the vertical stress ($\sigma_3'$). The shearing deformations result in the formation of a series of shearing planes. If significant deformations occur along these planes during unloading, planes of weakness will occur in the resultant soil deposit. The formation of such fissures is more likely to occur if the lateral stress is relieved by erosion of river valleys at some distance horizontally from the element of soil under consideration.

Fissures in the soil can also form as a result of tensile stresses developed during desiccation. Such fissures are approximately vertical and tend to have a hexagonal configuration when viewed from above.

The *intact* part of the fissured soil, that is, the part between fissures, may be relatively strong. Some deposits are subjected to cementation during the geologic times involved in the formation of the soil deposit, and the intact part of the soil becomes very strong indeed. The strength of the deposit as a whole is then determined by the strength along the fissures. Often an unconfined specimen of soil in the laboratory will fall apart within a few minutes after the stresses are relieved. Thus, the unconfined compression strength is zero. The field strength is well above zero, as proved by stable slopes in the field. Thus, the unconfined compression strength is too conservative as a measure of the shear strength in the field.

If a confining pressure is applied, the fissures are held closed and the strength is increased significantly over that of unconfined specimens. Triaxial shear testing of some fissured clays reveals an apparently anomalous behavior where the failure envelope has a finite slope, a condition in direct violation of the $\phi = 0$ condition. Examination of such test specimens after shear usually finds that fissures had been partially open at the confining pressures used in testing. This caused soil-to-soil contact to occur over only part of the total area of the shear planes. As the level of confining pressure is increased in the testing series, the area of soil-to-soil contact also increases with increasing confining pressure, thereby causing the measured strength of the soil to increase. If confining pressures are used that are large enough to keep any fissures closed throughout the test, then the $\phi = 0$ condition will be attained.

Fissured clays pose a serious problem to the engineer who relies on laboratory data for field design. Laboratory technicians may discard samples that break apart during attempts to prepare specimens for shear and test only intact specimens. If the fissures are far enough apart so that intact specimens can be obtained, the laboratory strengths will be those of the intact material, while failure in the field will take place along the fissures. Thus, the laboratory strengths are in error in the unconservative direction. If fissured specimens are tested, their strength is found to depend greatly on the orientation and position of the fissures in the specimens, and erratic test results are obtained. Since the strength in the field also depends on the orientation of the fissures, a rational field design is also made very difficult, if possible at all. Meaningful laboratory tests can be obtained only if the specimens are large compared with the spacing of the fissures. Samples of this size are seldom available, and the required equipment is generally not available.

Fissured clays have been selected as one example of the types of problems encountered in testing real soils as opposed to the artificially prepared specimens usually used for research. Each type of natural soil deposit has its own particular idiosyncrasies, and both the testing method (if any useful tests can be performed) and the interpretation of the test data must be adapted to fit the deposit and the requirements of the particular job. Useful laboratory shear strength tests on soil cannot consist of the standard performance and routine interpretation of tests in the same way many laboratories perform tests on asphalt, concrete, and steel.

*Orientation of Failure Planes.* According to Mohr's theory of stresses, the angle $\theta$ between the plane on which the maximum principal stress acts and the failure plane is half of the central angle in the Mohr diagram shown in Figure 3.44. Hence, the failure planes should be oriented as shown in Figure 3.61. It would appear, therefore, that the position of the failure planes could be used as a measure of $\phi'$.

However, the previous discussion has shown that the failure envelope can have a wide range of slopes, depending on whether total or effective stresses are used and on whether the soil is normally consolidated or overconsolidated. The question arises as to which $\phi'$ correlates with the position of the failure planes and, therefore, which $\phi'$ can be called the true angle of internal friction.

The orientation of the failure planes in triaxial specimens has been measured for hundreds of specimens by several qualified researchers, but no simple, definite conclusion can be drawn from their data. The orientation of the planes may be altered considerably by anisotropy resulting from either the method of preparation of the soil specimens or the type of deformation allowed during consolidation. Measurements also show that the orientation of the shear planes changes with increased deformation. Thus, the orientation must be measured at the moment of failure with all the stresses in place, a very difficult procedure when the specimen is encased in a nearly opaque rubber membrane inside a triaxial cell. In addition, some specimens fail by uniform bulging, and either shear planes do not form or else they form at strains much greater than the failure strain. Other specimens fail by splitting down the middle. For these and various other reasons, the orientation of the failure planes cannot be used as a measure of soil behavior. As a necessary

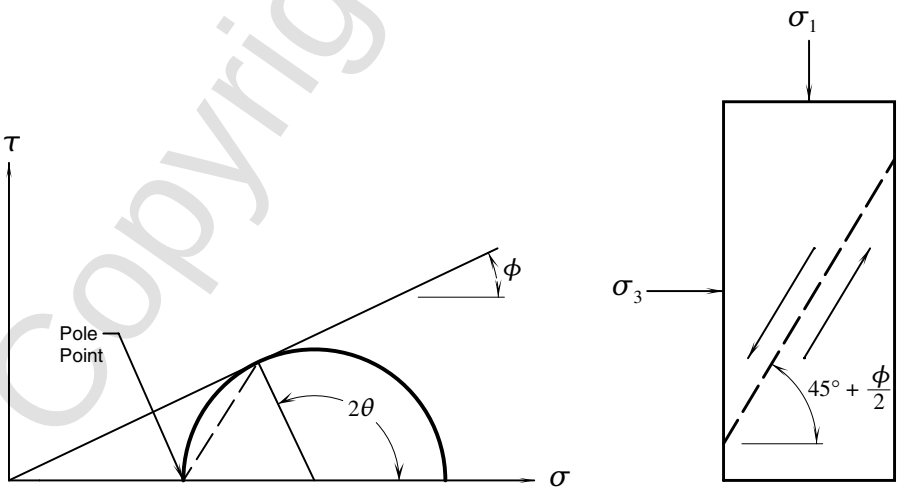


**Figure 3.61** Orientation of shearing planes in a soil deposit.

corollary of this observation, the determination of the position of failure planes in the field is also not possible.

***Influence of Intermediate Principal Stress on Strength*** In triaxial compression tests the intermediate principal stress is equal to the minor principal stress, while in triaxial extension tests the intermediate principal stress is equal to the major principal stress. In slope stability problems in the field, the intermediate principal stress actually has an intermediate value. In such problems, it may be better to define the intermediate principal stress as the stress required to maintain a condition of zero strain parallel to the slope. Naturally, the question arises about the influence of the intermediate principal stress on the shear strength of the soil.

The difficulty of obtaining precise answers to this question is an experimental one: because the construction of an apparatus that allows independent control of the three principal stresses and strains for a material as compressible as soil is very difficult. In fact, a generally satisfactory device has never been constructed, though some notable attempts have been made. (As the versatility of the apparatus approaches the desired value, both the size of the apparatus and its cost approach infinity.)

Available information suggests that the angle of internal friction in plane strain may be several degrees higher than the angle measured in triaxial tests. Because this error is on the safe side, and because experimental data from natural deposits usually scatter considerably, the influence of the intermediate principal stress is usually ignored.

*Unsaturated Soils.* The shear strength of unsaturated soil is a function of the type of soil and its degree of saturation. Soils with low degrees of saturation often behave as frictional materials under undrained shearing conditions. In contrast, soil with a high degree of saturation often behaves as if the degree of saturation is 100%.

The type of laboratory testing necessary to define the shearing characteristics of unsaturated soils is often beyond the capabilities of many soil testing facilities. Readers are referred to the work of Fredlund and Rahardjo (1993) for further information about the mechanics and shearing properties of unsaturated soils.

### 3.6.7 The SHANSEP Method

Between the 1950s and 1970s, geotechnical engineers recognized that the undrained shear strength of many soils followed a characteristic pattern. Initially, many engineers utilized this knowledge through their local experience but did not formalize their thinking in any particular manner. Eventually, several well-known geotechnical engineers began to present graphs of the shear strength that became popular. Foremost among these engineers were Professor Alan W. Bishop of the Imperial College of Science and Technology

in London and Professor Charles C. Ladd of the Massachusetts Institute of Technology. In 1974, Professor Ladd formalized a system to present and characterize the undrained shear strength of soils. This system is known as the SHANSEP (Stress History And Normalized Soil Engineering Properties) system. This system is probably the most widely used system for characterizing the shear strength of soils for engineering in practice in the English-speaking world. The following is a brief presentation of the SHANSEP system.

The SHANSEP system is based on the observation that the shear strength of many soils can be normalized with respect to the vertical consolidation pressure. One example of normalized behavior is illustrated in Figure 3.62. Here, two stress-strain curves measured in consolidated-undrained (CU) tri-

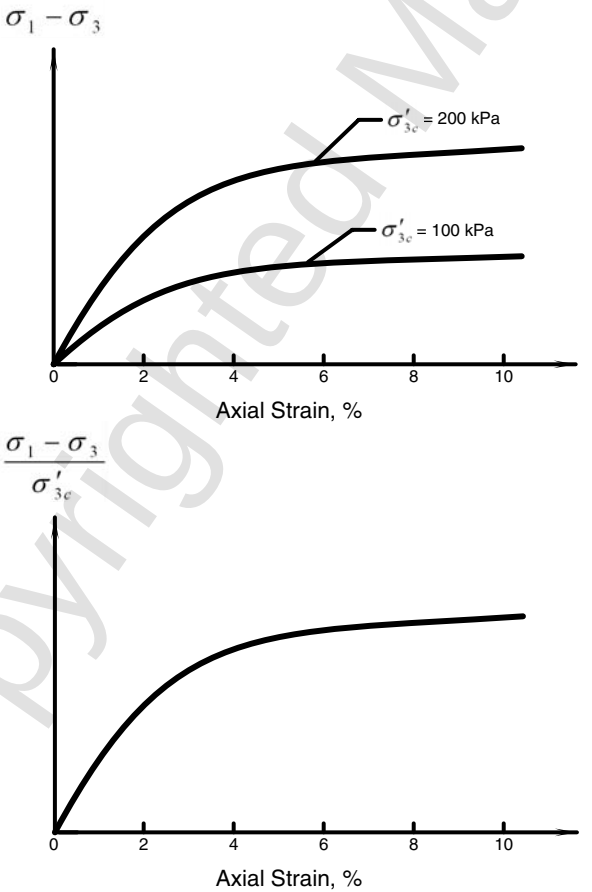


**Figure 3.62** Example of normalized stress-strain behavior in idealized triaxial tests on homogeneous clays (from Ladd and Foott, 1974).

axial tests are plotted. In the upper half of the figure, the unnormalized stress-strain curves are plotted. In the lower half of the figure, the normalized stress-strain curve is plotted. In the normalized plot, the strain axis is unchanged and the stress axis is normalized by dividing the axial stress difference by the vertical consolidation pressure.

When normalized plots are made using CU triaxial data, unique curves are obtained for each value of the OCR. As the overconsolidation ratio increases from 1 to higher values, the strain at peak stress decreases and the normalized stress-strain curves plots higher on the figure.

If a soil exhibits normalized behavior, a figure of strength ratio versus log OCR can be plotted. The strength ratio is defined as the undrained shear strength $c$ divided by the vertical effective stress. Traditionally, the most commonly used symbol for strength ratio is $c/p'$. Other symbols are also used.

The SHANSEP procedure is as follows:

1. A soil investigation is conducted, and a sufficient number of samples are obtained from the soil strata of interest.
2. A series of one-dimensional consolidation tests are run on samples from various depths to define the overconsolidation ratio versus depth in the soil profile.
3. A series of CU test series are performed at confining pressures corresponding to OCR values of 1, 1.5, 2, 4, and 6. Often, this testing program requires that the test specimens be consolidated to stresses well above those found in the field and then rebounded to lower levels of effective stress to obtain the desired OCRs.
4. Figures similar to those shown above are plotted using the test data.
5. The SHANSEP figures can be used to estimate undrained shear strengths in many situations. The general procedure used to determine undrained shear strength is presented in Steps 6 to 9.
6. The effective stress at the depth of interest is computed.
7. The OCR is computed using the known value of maximum past consolidation pressure. (If the new effective stress exceeds the maximum past consolidation pressure, then the soil becomes normally consolidated and OCR = 1.0.)
8. The OCR is then used to obtain the strength ratio from the chart of strength ratio versus OCR logarithm.
9. The undrained shear strength is computed by multiplying by the vertical effective stress by the strength ratio.

When soil is to be placed on or excavated from the site, it is often necessary to estimate the changes in undrained shear strength resulting from consolidation or rebound due to changes in levels of effective stress. If this is the case, the effective stress computed for Step 1 may be computed both prior to

and at the end of consolidation or rebound. The change in undrained shear strength is then the difference in the two values of computed strength.

If the stress-strain behavior is of interest, the OCR can be used to estimate the stress-strain curve.

Noted that if one is interested in the undrained shear strength under a foundation, one must compute the vertical distribution of stresses due to the foundation. A similar situation exists for stresses under an embankment.

### 3.6.8 Other Types of Shear Testing for Soils

Several other types of tests for measuring the shearing properties of soils have been developed in addition to the direct shear and triaxial shear tests. Short descriptions of several of these tests follow.

One type of test is the direct simple shear test. In this test, the soil specimen is distorted by rotation of the sides of the shear box. Rotation of the specimen is accomplished by confining the test specimen in a wire-reinforced membrane, an articulated shear box, or a stack of thin rings that can slide. In each of these configurations, the soil specimen is distorted to develop shear strain within it. This type of test has had limited use by consultants and is usually used in conjunction with triaxial shear tests and consolidation tests to develop constitutive parameters for advanced models of material behavior.

Another type of shear test is the ring shear test, in which the shear box is composed of two horizontal rings. The soil properties measured in this test are the same as those measured in the direct shear test. However, the ring shear test is not limited in its range of deformations because one ring is driven in shear using a worm gear system. Ring shear devices are very useful in measuring the residual shearing resistance on well-formed shear planes, such as those that might develop in a slope failure. These devices are commercially available, but have the limitation that a large-diameter soil sample must be used for testing undisturbed soils.

Other types of tests that are used to measure the dynamic shearing properties of soils are the cyclic triaxial test and the resonant column test. The results of these tests are used to solve problems in earthquake engineering or mechanical vibration for which dynamic soil properties are important.

In the cyclic triaxial test, the soil sample is prepared in the same manner as for a conventional triaxial test but is sheared using various levels of cyclic loading. The main property of interest measured in the cyclic triaxial test is the number of cycles of loading needed to cause the soil specimen to fail.

In the resonant column test, a cylindrical soil specimen is placed under a confining stress and permitted to consolidate. After consolidation is complete, the specimen is vibrated in torsion. The resonant frequency of the specimen is measured as a function of the shearing strain amplitude developed in the specimen, and after vibration ceases, the decay of vibrations is measured. The principal measurements made using the resonant column test are shear wave velocity, shear modulus, and material damping ratio.

Lastly, the performance of stress-path triaxial tests is possible. In this type of test, computer-controlled feedback testing is used to force the stress in the test specimen to follow a prescribed path. A stress path is the trajectory or path of stress states on a Mohr-Coulomb diagram. Stress-path triaxial testing is available at only a few commercial testing laboratories and is usually used only for major projects for which benefits might be realized. Modern computer-controlled triaxial equipment like that shown in Figure 3.63 is capable of performing stress-path testing. However, the foundation engineer must first perform advanced modeling of a problem to determine the desired stress path to be followed.

### 3.6.9 Selection of the Appropriate Testing Method

The foundation engineer must tell the testing laboratory how to test the soil so that the necessary soil properties are measured for the problem at hand. Often the engineer must select soil tests while considering how much money is available for testing. Additionally, the engineer must recognize that meaningful testing can be accomplished only on soil samples of good quality and


**Figure 3.63** Computer-controlled triaxial testing equipment (photograph courtesy of Trautwein Geotac).

that testing of disturbed soil samples may obtain results that are not representative of field conditions.

In light of these considerations, the foundation engineer understands the following limitations and capabilities of the consolidation test, direct shear test, and triaxial test:

1. The consolidation test measures the consolidation properties of the soil needed for calculations of total settlement and time rate of settlement.
2. The direct shear test can be used economically to measure the angle of internal friction of sand. The shortcoming of this test is that it is not possible to measure a stress-strain curve for sand.
3. The direct shear test on clayey soils can be used to measure the drained friction angle of clays more economically than *S*-type triaxial tests. Again, as with direct shear tests on sand, the shortcoming of this test is that it is not possible to measure a stress-strain curve for the soil.
4. *UU*-type triaxial tests are the best tests to measure the undrained shear strength of cohesive soils. While these tests can also be used to test sands, this requires that a specimen be built for testing. This usually involves more work to set up the specimen for testing than for a specimen of cohesive soil. One limitation of the *UU*-type triaxial test is that the effects of consolidation or rebound of vertical stress cannot be adjusted for in the test because the soil specimen is not subjected to consolidation pressures. If the effects of consolidation are important, a shearing test that permits consolidation must be used.
5. The *CD* triaxial test is the best and most expensive test used to measure the fully drained shearing properties of soils. The test results include the consolidation properties of the soil, the angle of friction under fully drained conditions, and the stress-strain curve. Unfortunately, time and budget constraints often eliminate the use of *CD* triaxial test on many projects. If only the fully drained angle of friction is required, a drained direct shear test is a practical alternative.
6. The *CU* triaxial test without measurement of porewater pressures during shear is used when undrained shear strength values are needed for soils that are subject to consolidation in the field.
7. The *CU* triaxial test with measurement of porewater pressures during shear can be used to measure the effective stress shearing parameters of cohesive soils more economically than the *CD* triaxial test.

## PROBLEMS

### Problem Set 1

**P3.1.** Settlements of saturated clays are often modeled with a piston and spring, as shown below. If the load *P* is suddenly increased, describe

the model's reaction at time zero, with the passage of time, and at infinite time.

**P3.2.** The piston shown in Problem P3.1 weighs 128 lb. The spring constant is 400 lb per foot of compression. The spring-piston assembly is initially in equilibrium (no change in the system as a function of time so long as no loads are applied to or removed from the piston), with the valve open and with the dimensions shown. The force $P$ is suddenly increased from zero to 100 lb.

**a.** What was the reading on the pressure gage just before the 100-lb load was added? Use units of psf. The gage reads the pressure at the center of the gage, and the line to the gage is full of water.

**b.** What will the reading on the pressure gage be immediately after applying the 100 lb?

**c.** When enough fluid has leaked out so the piston has settled 0.1 ft, what will the gage read?

**d.** When equilibrium is reestablished, what will the gage reading be and how much will the piston have settled relative to its position when the 100-lb load was added?

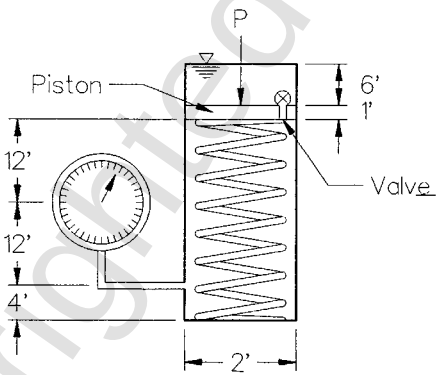


ALL DIMENSIONS IN FEET

### Problem Set 2

**P3.3.** The wet and dry weights of a lump of soil are 86.0 and 61.2 g, respectively. Calculate the water content (in percent).

**P3.4.** A wet soil sample weighs 110.0 g. Its water content ($w$) is 16.7%. Calculate the dry weight in grams.

**P3.5.** The total weight of a chunk of moist soil is 330 lb. Its volume is 3 $ft^3$. The water content was found to be 27%. Find $e$, $\gamma$, $\gamma_d$, and $S$. State any assumptions made.

**P3.6.** A specimen of saturated clay has a water content of 46.5% and a specific gravity of solids ($G_s$) of 2.7. Calculate (a) the total unit weight in pcf and kN/m$^3$ and (b) the dry unit weight in pcf and kN/m$^3$

**P3.7.** For a particular soil, $\gamma = 126.0$ pcf and $\gamma_d = 102.3$ pcf. Calculate the water content ($w$).

**P3.8.** A sand has a dry density of 101.0 pcf and $G_s = 2.67$. What water content is required to obtain 85% saturation?

**P.8.9.** A sample of dry clay weighing 485 g is sealed with 10 g of paraffin (the density of paraffin is 0.90 g/cc). The volume of the soil and paraffin, found by immersion in water, is 310 cc. The density of solids is 2.65 g/cc. What is the void ratio of the soil?

### Problem Set 3

A soil boring has the following profile:

0 to 40 ft sand, dry density = 105 pcf, $S_r = 100\%$, $G_s = 2.72$

40 to 60 ft silt, $w = 35\%$, $S_r = 100\%$ $G_s = 2.80$

The water table is at the surface. Calculate the total stress, the porewater pressure, and the effective stress at the top of the silt layer and then at the bottom of the silt layer. Enter your answers in the following table.

| Location | Total Stress | Porewater Pressure | Effective Stress |
|---|---|---|---|
| top | _____psf | _____psf | _____psf |
| bottom | _____psf | _____psf | _____psf |

**P3.10.** Draw total effective and pore pressure diagrams.

**P3.11.** A steel mold that weighs 4.10 lb and has an inside volume of 1/30 of a cubic foot is filled with a compacted clay. The weight of the mold full of clay is 8.41 lb. The water content is 14.1%, and $G_s = 2.75$. Calculate the void ratio and the degree of saturation.

**P3.12.** Calculate the effective stress at a depth of 40 ft in a submerged clay deposit using a single direct calculation; that is, do not calculate either the total stress or the porewater pressure. The water content of the submerged clay is 70%, and $G_s$ is assumed to be 2.65.

**P3.13.** Calculate the change in total stress at a depth of 30 ft in a clay layer if the water table is dropped from the surface to a depth of 10 ft. The clay has a water content of 40%, $S_r = 100\%$, and $G_s = 2.80$. No change in degree of saturation or water content occurs when the water table is changed.

### Problem Set 4

A soil profile consists of 19 ft of sand (submerged unit weight of 60 pcf) on top of 20 ft of normally consolidated clayey silt on top of an impervious rock. A 15-ft-thick layer of sand fill (total unit weight of 110 pcf) is placed on top of this soil profile. For simplicity, we take the water table at the ground surface (prior to placement of the fill), and we assume that the water table remains at the interface between the sand and the fill during settlement, so no submergence correction needs to be made. The average water content of the clayey silt is 70% and $G_s$ is 2.65.

A one-dimensional consolidation test was performed on the clayey silt, and the following stress-strain data were obtained:

| Effective Stress, psf | Strain | Effective Stress, psf | Strain |
|---|---|---|---|
| 100 | 0.000 | 4,000 | 0.090 |
| 250 | 0.008 | 8,000 | 0.137 |
| 500 | 0.015 | 16,000 | 0.190 |
| 1,000 | 0.030 | 32,000 | 0.246 |
| 2,000 | 0.055 | 64,000 | 0.305 |

**P3.14.** Compute the changes in the void ratio in the consolidation test and plot the $e$ versus log $\sigma'$ curve on three-cycle semi-logarithmic paper.

**P3.15.** Compute the compression index $C_c$ (the slope of the virgin curve).

**P3.16.** Calculate the total settlement of the embankment using single drainage. Subdivide the soil into four layers. Assume that the settlement caused by the compression of the sand layers is negligible. Calculate the settlement of the clayey silt layer by computing average stresses at the center of the layers. The curve you have plotted is not the same as the true field curve because the soil structure was disturbed by the boring and sampling operation. In calculating the settlement in the field, use the field consolidation curve. To estimate the location of the curve, draw a line from the point $e = e_0$, $\sigma' = \sigma'_0$, tangent to the laboratory virgin curve and use this line as the field curve.

**P3.17.** The one-dimensional consolidation apparatus used in the laboratory for this test allows water to drain out at both the top and bottom of the specimen, whereas the bottom of the clayey silt layer in the field is impervious. Does this difference in drainage conditions cause the design engineer to predict higher settlement, the same settlement, or less settlement than will occur in the field? Explain.

### Problem Set 5

A corrected (field) consolidation curve is defined at the following points:

| Effective Stress, psf | Void Ratio | Effective Stress, psf | Void Ratio |
|---|---|---|---|
| 250 | 0.755 | 4,000 | 0.740 |
| 500 | 0.754 | 8,000 | 0.724 |
| 1,000 | 0.753 | 16,000 | 0.704 |
| 2,000 | 0.750 | 32,000 | 0.684 |

**P3.18.** Plot the curve of effective stress versus void ratio using three-cycle semi-logarithmic paper.

**P3.19.** Compute the compression index $C_c$.

**P3.20.** If the soil stratum in the field is 8 ft thick and the initial effective stress at the center of the layer is 1400 psf, how much additional stress can the stratum support before 0.75 in. of settlement occurs? Remember that the curve you plotted in Problem P3.18 is already the correct field curve.

### Problem Set 6

A soil profile consists of 5 ft of sand overlying 40 ft of normally consolidated clay underlain by an incompressible sand, gravel, and then bedrock. The properties of the upper sand are not known, but we estimate that it has a dry density of 95 pcf and a $G_s$ of 2.72. Tests on the clay indicate that it has the following average properties: water content = 40%, $G_s$ = 2.85, and compression index = 0.35. The water table is at the surface.

A wide embankment 20 ft thick is placed at the surface. The dry density of the fill averages 115 pcf, with a water content of 14%.

Calculate the settlement of the surface:

**P3.21.** By dividing the clay layer into two sublayers, each 20 ft thick.

**P3.22.** By using the entire clay layer as a single layer and calculating average stresses at the mid-depth.

### Problem Set 7

A light industrial building is designed using a reinforced concrete slab resting directly on a 10-ft-thick underlying clay layer. We lack adequate funds for a comprehensive soils investigation, but we do collect the following data: water content of the soil prior to construction averages 25%, liquid limit about 75%, plastic limit about 25%, shrinkage limit about 13%, and water content of a sample allowed to soak under a low applied stress about 45%. We assume that the soil is saturated prior to construction.

**P3.23.** How much would the building settle if the clay became air-dried and we assume that all shrinkage is in the vertical direction (no cracking)?

**P3.24.** How much would the building be lifted if the natural clay became soaked instead of being dried?

### Problem Set 8

A soil deposit consists of 10 ft of miscellaneous ''old fill'' over 30 ft of normally consolidated clay over sand and, finally, bedrock. The clay has fully consolidated under the old fill. The water table is at the interface of the fill and clay. The total unit weight of the fill is 122 pcf. The water content of the clay is 49%, the degree of saturation is 100%, and $G_s$ is 2.70. Assume that the fill and lower sand are freely draining. From experience with this saturated clay, the compression index is assumed to be 0.35 and the coefficient of consolidation 0.10 $ft^2$/day. Sixteen feet of additional fill, at a total unit weight of 125 pcf, are placed on the surface.

**P3.25.** Calculate the settlement caused by compression of the clay layer. Use two layers for analysis of the clay.

**P3.26.** Calculate the time required to achieve half of the ultimate settlement.

### Problem Set 9

A mud flat next to a bay is to be developed for industrial purposes. Sand will be sucked up from out in the bay and pumped as a slurry to the site, where it will be dumped and allowed to drain. This is called a *hydraulic fill.* The soils at the site are tolerably uniform and consist of about 30 feet of very soft, slightly organic mud (clay) overlying sand and pervious bedrock. Sufficient fill must be pumped in so that the top of the fill will be 5 ft above the original ground surface after settlement has ceased. The water table is at the original ground surface at the start of filling and stays at the same elevation throughout the settlement time, so that some of the fill becomes immersed as settlement progresses (in which case it loads the subsoil with its submerged unit weight instead of its total unit weight).

Calculate the total thickness of fill that must be pumped onto the site.

Calculate (as best you can) the time-settlement curve of the ground surface and present it in a plot. Show any assumptions made in the analysis.

The soil properties to be used in the analysis include:

*Very soft clay*—water content = 70%, $G_s$ = 2.65 normally consolidated, compression index = 0.54, coefficient of consolidation = 0.05 $ft^2$/day.

*Fill*—$G_s$ = 2.70, dry density = 95 pcf; assume that the degree of saturation is 100% when the sand is below the water table and 30% when it is above the water table.

### Problem Set 10

Many borings were made in San Francisco Bay during the design of the Bay Area Rapid Transit (BART) tunnel. The data you will be given came from a one-dimensional consolidation test on a sample from boring DH-21. The samples were taken using a Swedish foil sampler. The soil profile at the site was as follows:

| | |
|---|---|
| 0–21 ft | Water |
| 21–32 ft | Clay: silty, black organic, very soft, many sand lenses |
| 32–37.6 ft | Clay: silty, blue gray, soft, some organic matter, many lenses of clayey fine to medium sand |
| 37.6–38.3 ft | Shells: silty, sandy, gray, loose |
| 38.3–52 ft | Sand: silty, blue gray, loose, many lenses of soft silty clay 1/8 to 1/2 in. thick, some shell fragments |
| 52–53.3 ft | Clay: very sandy, silty, blue gray, soft, numerous sand lenses |
| 53.3–55.4 ft | Clay: silty, blue-gray, soft, many lenses of silty sand 1/4 to 1/2 in. thick |
| 55.4–56.4 ft | Sand: silty, some silty clay layers |
| 56.4–145 ft | Clay: silty, blue-gray, soft, many lenses of fine to medium sand, occasional lenses of shells (struck oil at 107.3 ft) |
| 145–169 ft | Clay: silty, soft to stiff, greenish-gray, some fine gravel |

A sample from a depth of 62 ft was used. The overburden effective stress at this depth is estimated to be 1850 psf. The soil was trimmed into a small ring (1.768-in. diameter) and loaded up to a peak pressure of 128,000 psf. The relevant data are summarized on the attached data forms. The recorded total settlements are the final settlements under each load, not $S_{100}$.

In addition, the time-settlement data for consolidation under the 4000-psf load are given.

Calculate void rations at each pressure.

**P3.27.** Plot void ratio versus effective stress (log scale) using five-cycle paper.

**P3.28.** Estimate the position of the field curve. Is the deposit normally consolidated or overconsolidated?

**P3.29.** Plot settlement versus time (log scale) using five-cycle paper. Determine $S_0$, $S_{100}$, $S_{50}$, and $t_{50}$. Calculate $c_v$ (use units of $in^2/min$ to match the units used in the plot).

**P3.30.** Plot the theoretical curve of settlement versus time on top of the experimental curve of Problem P3.29.

**P3.31.** Repeat Problems P3.27 to P3.29 using strain versus a log $p$ plot and compare the results.

### Problem Set 11

**P3.32.** Samples of compacted, clean, dry sand were tested in a large direct shear machine with a box 254 by 254 mm in area. The following results were obtained:

| | Test 1 | Test 2 | Test 3 |
|---|---|---|---|
| Normal load (kg) | 500 | 1,000 | 1,500 |
| Peak shear load (kN) | 4.92 | 9.80 | 14.62 |
| Residual shear load (kN) | 3.04 | 6.23 | 9.36 |

Determine the angle of shearing resistance ø for the compacted state (dense) and for the loose state (large displacement or residual).

**P3.33.** Three specimens of nearly (not totally) saturated clay were tested in a direct shear machine. Shear loading was started immediately after the application of the normal load, and testing was completed within 10 minutes of the start of the test. The following results were obtained:

| | Test 1 | Test 2 | Test 3 |
|---|---|---|---|
| Normal stress (psi) | 145 | 241 | 337 |
| Shear stress at failure (psi) | 103 | 117 | 132 |

What are the values for the apparent cohesion and angle of internal friction for the clay? What cohesion value would be obtained from an unconfined compression test of the same soil?

**P3.34.** The following results were obtained from undrained triaxial compression tests on three identical specimens of saturated soil:

| | Test 1 | Test 2 | Test 3 |
|---|---|---|---|
| Confining pressure (psi) | 70 | 140 | 210 |
| $\sigma_1$ at failure (psi) | 217 | 294 | 357 |
| Angle between failure plane and $\sigma_1$-plane (deg.) | 51° | 53° | 52° |

Determine $c_u$ and $\phi_u$ for the soil. Estimate the drained (or effective stress) friction angle. From what type of soil would results such as these be expected?

**P3.35.** The following results were obtained from tests on a saturated clay soil:

**a.** Undrained triaxial tests:

| | Test 1 | Test 2 | Test 3 |
|---|---|---|---|
| Cell pressure (psi) | 100 | 170 | 240 |
| $(\sigma_1 - \sigma_3)$ at failure (psi) | 136 | 142 | 134 |

**b.** Direct shear tests in which the soil was allowed to consolidate fully under the influence of both normal and shear loads:

| | Test 1 | Test 2 | Test 3 |
|---|---|---|---|
| Normal stress (psi) | 62 | 123 | 185 |
| Shear stress at failure (psi) | 73 | 99 | 128 |

Determine values of apparent cohesion and ø for both undrained (total stress) shear strength and drained (effective stress) shear strength.

**P3.36.** A cohesive soil has an undrained friction angle of 15° and an undrained cohesion of 30 psi. If a specimen of this soil is subjected to an undrained triaxial compression test, find the value of confining pressure required for failure to occur at a $\sigma_1$ value of 200 psi.

**P3.37.** The results of undrained triaxial tests with pore water pressure measurements on a saturated soil at failure are as follows:

| | Test 1 | Test 2 |
|---|---|---|
| Confining pressure (psi) | 70 | 350 |
| $\sigma_1$ at failure (psi) | 304 | 895 |
| Pore water pressure at failure (psi) | −30 | +95 |

Determine the cohesion and friction angle for failure with respect to both total and effective stresses.

**P3.38.** Consolidated-undrained triaxial tests with pore water pressure measurements were performed on specimens of a saturated clay. Test results are given below. Plot the Mohr circles at failure and determine the $c$ and $\phi$ values with respect to both total and effective stresses.

| | Test 1 | Test 2 | Test 3 |
|---|---|---|---|
| Cell pressure (psi) | 200 | 400 | 600 |
| Max. prin. stress dif. (psi) | 120 | 230 | 356 |
| Pore pressure at failure (psi) | 102 | 200 | 299 |

**P3.39.** A sample of saturated clay has a pore water pressure of −800 psf when unconfined. A total stress equal to 1000 psf is then applied to all surfaces of the sample, and no drainage is allowed to occur. What is the effective stress in the sample? Fully explain your answer.

**P3.40.** For a saturated clay, $q_u = 2$ tsf. A confining pressure of 100 psi is added under undrained conditions, and a $Q$-type triaxial compression test is performed. What will $c_Q$ be? Fully explain your answer.

**P3.41.** A sample of clay was consolidated to a cell pressure of 20 psi. If $c' = 0$, and $\phi' = 22°$, what will the principal stress difference be at failure in a fully drained test?